COPPE UFRJ
Instituto Alberto Luiz Coimbra de Pós-Graduação e Pesquisa de Engenharia

BIOENERGY AND CARBON CAPTURE AND STORAGE SPATIALLY EXPLICIT MODELLING IN BRAZIL

Isabela Schmidt Tagomori

Tese de Doutorado apresentada ao Programa de Pós-graduação em Planejamento Energético, COPPE, da Universidade Federal do Rio de Janeiro, como parte dos requisitos necessários à obtenção do título de Doutor em Planejamento Energético.

Orientadores: Alexandre Salem Szklo
Pedro Rua Rodriguez Rochedo
Vassilis Daioglou

Rio de Janeiro
Fevereiro de 2022

BIOENERGY AND CARBON CAPTURE AND STORAGE SPATIALLY EXPLICIT MODELLING IN BRAZIL

Isabela Schmidt Tagomori

TESE SUBMETIDA AO CORPO DOCENTE DO INSTITUTO ALBERTO LUIZ COIMBRA DE PÓS-GRADUAÇÃO E PESQUISA DE ENGENHARIA DA UNIVERSIDADE FEDERAL DO RIO DE JANEIRO COMO PARTE DOS REQUISITOS NECESSÁRIOS PARA A OBTENÇÃO DO GRAU DE DOUTOR EM CIÊNCIAS EM PLANEJAMENTO ENERGÉTICO.

Orientadores: Prof. Dr. Alexandre Salem Szklo, D.Sc.

Prof. Dr. Pedro Rua Rodriguez Rochedo, D.Sc.

Dr. Vassilis Daioglou, Ph.D.

Aprovada por: Prof. Dr. Joana Portugal-Pereira, Ph.D.

Prof. Dr. Detlef van Vuuren, Ph.D.

Dr. Walter Rossi Cervi, Ph.D.

RIO DE JANEIRO, RJ – BRASIL

FEVEREIRO DE 2022

Tagomori, Isabela Schmidt

(Bioenergy and carbon capture and storage spatially explicit modelling in Brazil) / Isabela Schmidt Tagomori. – Rio de Janeiro: UFRJ/COPPE, 2022.

XVII, 142 p.: il.; 29,7 cm.

Orientador (es): Alexandre Salem Szklo

Pedro Rua Rodriguez Rochedo

Vassilis Daioglou

Tese (Doutorado) – UFRJ/COPPE/Programa de Planejamento Energético, 2022.

Referências Bibliográficas: p. 113-120.

1. Bioenergia. 2. Captura de Carbono. 3. BECCS. 4. Modelagem Espaço-Explícita. I. Szklo, Alexandre Salem *et al*. II. Universidade Federal do Rio de Janeiro, COPPE, Programa de Planejamento Energético. III. Título.

To my favorite person in the world: my brother, Matheus.

May the Force be with you, always.

“Don’t panic!”

- Douglas Adams

“We must use this opportunity to create a more equal world.

And our motivation should not be fear, but hope.”

- Sir David Attenborough, COP26

Glasgow, 2021

ACKNOWLEDGMENTS

First of all, I would like to thank my supervisors Prof. Dr. Alexandre Szklo, Prof. Dr. Pedro Rochedo and Dr. Vassilis Daioglou. This thesis would not have come to life without you. My most sincere gratitude for the incomparable guidance and for believing in this work. I could not have asked for better partners in this journey.

I would also like to thank Prof. Dr. Detlef van Vuuren, Prof. Dr. Joana Portugal-Pereira and Dr. Walter Cervi for accepting my invitation to be part of the evaluation committee for this thesis. Your contribution is most valuable, and we all appreciate it immensely.

I would like to thank all the professors who have shared their knowledge and enriched the challenge of diving into climate, energy and environmental sciences. Most especially Prof. Dr. Roberto Schaeffer and Prof. Dr. André Lucena, who brilliantly lead the CENERGIA team.

To my colleagues at CENERGIA, for the great privilege of working among such sharp minds but also for simply sharing a cup of coffee and blowing off steam together. Not to mention our “Among Us” sessions, which made coping with social distancing in corona times a million times easier.

To my colleagues at PBL/UU, for being such an amazing team and for making me feel welcome not only in the work environment but also in this lovely rainy land they call Nederland. I must admit that my wish to stay when the opportunity came is definitely partly your fault. My immense gratitude to Detlef van Vuuren, who brilliantly lead the IMAGE team, welcoming me first as a guest and now as a researcher. Hartelijk bedankt!

To all my friends in Brazil, and most especially to the ones that closely shared this journey with me, neurosis included: Cindy, Paula, Fabio, Vinicius, Murilo, Gabriela. Eu amo vocês! And most especially to Luiz Bernardo, thank you for running the BLUES scenarios for me and for always replying to my desperate texts – you are the best!

To all my friends in Nederland, and most especially to the ones that I now consider my international family: Nicole, Lotte, Hsing-Hsuan, Heleen, Mariësse, Ioannis. Thank you for welcoming me into your lives and for making me feel at home. May we share many more adventures (or e-adventures!) in the future. I love you!

I would like to thank my family – my dear, large, loud, full of life family. For always having my back and for being the most amazing, diverse, incredible human beings. For family reunions, road trips, weekend lunches, long hugs and endless support. I am blessed to be among you. I love you!

Finally, to my loving parents and my eternally little brother, Ingrind and Milton and Matheus, who never ever gave me the impression I could not be anything I wanted to be – even a scientist! Thank you! I love you more than I could ever explain in words. I am deeply proud of you and my biggest ambition in life is to know that, in the end, I made you proud of me.

Resumo da Tese apresentada à COPPE/UFRJ como parte dos requisitos necessários para a obtenção do grau de Doutor em Ciências (D.Sc.)

MODELAGEM ESPACIALMENTE EXPLICITA DA BIOENERGIA COM CAPTURA E ARMAZENAMENTO DE CARBONO NO BRASIL

Isabela Schmidt Tagomori

Fevereiro/2022

Orientadores: Alexandre Salem Szklo
Pedro Rua Rodriguez Rochedo
Vassilis Daioglou

Programa: Planejamento Energético

Espera-se que a bioenergia tenha importante papel na descarbonização dos sistemas energéticos, especialmente em cenários que tenham como objetivo manter o aumento da temperatura global abaixo de 2°C. No entanto, a expansão em larga escala da bioenergia, com ou sem captura e armazenamento de carbono, é um tema complexo que deve ser considerado de forma cuidadosa. Esta tese tem por objetivo desenvolver um modelo espacialmente explícito para avaliar diferentes rotas para a produção de bioenergia, levando em consideração variadas dimensões que influenciam o seu desevolvimento. O modelo foi conectado ao *Brazilian Land Use and Energy Systems Model* (BLUES) e aplicado ao contexto brasileiro, com o intuito de investigar maneiras custo-efetivas de atender às projeções futuras de oferta de bioenergia para diversos cenários, com diferentes metas climáticas e níveis de ambição, de forma sustentável e competitiva. Uma importante contribuição desta tese consiste em sua análise sistêmica e na espacialização dos resultados, evidenciando os conflitos entre a alocação de culturas, o uso da terra e as dinâmicas logísticas entre produção, conversão e os centros de demanda e, em alguns casos, as emissões negativas e o armazenamento de carbono, trazendo valiosas informações para o desenvolvimento de políticas climáticas regionais e para o mapeamento de cadeias de valor da bioenergia.

Abstract of Thesis presented to COPPE/UFRJ as a partial fulfillment of the requirements for the degree of Doctor of Science (D.Sc.)

BIOENERGY AND CARBON CAPTURE AND STORAGE SPATIALLY EXPLICIT MODELLING IN BRAZIL

Isabela Schmidt Tagomori

February/2022

Advisors: Alexandre Salem Szklo
Pedro Rua Rodriguez Rochedo
Vassilis Daioglou

Department: Energy Planning

Bioenergy is expected to play a key role in decarbonizing the energy system, especially in scenarios aiming at maintaining global temperature increases below 2°C. However, the large-scale deployment of bioenergy, with and without carbon capture and storage, is a complex subject that should be taken under careful consideration. This thesis aims at developing a spatially explicit model to assess different bioenergy pathways while encompassing various dimensions that influence their optimal deployment. The model was coupled with the Brazilian Land Use and Energy Systems Model (BLUES) and applied to the Brazilian context, in order to investigate the most cost-effective ways of attending the bioenergy supply future projections for different scenarios, with different climate targets and different levels of ambition, in a sustainable and competitive manner. A major contribution of this thesis lies on its systemic approach and the spatial results it provides, highlighting the trade-offs between crop allocation, land use and the logistics dynamics between production, conversion, demand and, in some cases, negative emissions and carbon storage, providing valuable insights for regional and national climate policy design, making this a useful tool for mapping bioenergy value chain pathways.

SUMMARY

LIST OF FIGURES

LIST OF TABLES

LIST OF ACRONYMS

AIM – Asia-Pacific Integrated Modeling

ANP – Agência Nacional de Petróleo, Gás Natural e Biocombustíveis

BDS – Biodiesel

BECCS – Bioenergy and Carbon Capture and Storage

BJT – Biojet (Fischer-Tropsch)

BLOEM – Bioenergy and Land Optimization Spatially Explicit Model

BVCM – Biomass Value Chain Model

CGE – Computable General Equilibrium

COFFEE – Computable Framework for Energy and the Environment

CurPol – Current Policies

DFT – Green Diesel (Fischer-Tropsch)

DFTC – Green Diesel (Fischer-Tropsch) with CCS

E1G – Ethanol 1st Generation

E1GC – Ethanol 1st Generation with CCS

E2G – Ethanol 2nd Generation

EOR – Enhanced Oil Recovery

EPE – Empresa de Pesquisa Energética

FT-BTL – Biomass to Liquids via Síntese de Fischer-Tropsch

FT-BTL-CC – Biomass to Liquids via Síntese de Fischer-Tropsch c/ Captura Carbono

GCAM – Global Change Analysis Model

GLOBIOM – Global Biosphere Management Model

GPP – Good Practice Policies

LPG – Liquefied Petroleum Gas

IAM – Integrated Assessment Model

IAMC – Integrated Assessment Modeling Consortium

IBGE – Instituto Brasileiro de Geografia e Estatística

IECM – Integrated Environmental Control Model

IMAGE – Integrated Model to Assess the Global Environment

IPCC – Intergovernmental Panel on Climate Change

MAgPIE – Model of Agricultural Production and its Impact on the Environment

MCTIC – Ministério da Ciência, Tecnologia, Inovação e Comunicações

MESSAGEix – Model for Energy Supply Strategy Alternatives and their General Environmental Impacts

MONET – Modelling and Optimization of Negative Emissions Technologies

NDC – Nationally Determined Contribution

NETs – Negative Emissions Technologies

NP-50 – National Policies -50%

NP-100 – National Policies -100%

PLUC – PCRaster Land Use Change

REMIND – Regional Model of Investment and Development

SDGs – Sustainable Development Goals

TEA – Total Economy Assessment

UNFCCC – United Nations Framework Convention on Climate Change

WGS – Water-Gas Shift

1. Introduction

1.1 Context

Low carbon scenarios, especially scenarios aiming at maintaining global temperature increases below 2°C, have been heavily relying on carbon dioxide removal to comply with the estimated carbon budget, particularly in the second half of the century. Carbon dioxide removal (CDR) technologies can be defined as technologies that remove carbon dioxide (CO_2) from the atmosphere (Kemper, 2015; Minx et al., 2018). Over the last years, such technologies have gained prominence amidst the discussions regarding climate change, especially due to the limited carbon budget[1] and the ambitious targets estimated for the stabilization of global temperatures (Minx et al., 2018; Fuss et al., 2018; Nemet et al., 2018; Fajardy et al., 2018). Two main reasons are pointed out for the need of negative emissions: first, the need to deal with emissions that surpass the given carbon budget leading to so-called "overshoot" scenarios (Kriegler et al., 2013; van Vuuren et al., 2013; Clarke et al., 2014; Fuss et al., 2018), and second, the need to compensate emissions from sectors where mitigation is more complex and incurs high abatement costs, such as the transport, industry, and agriculture sectors (Gough and Upham, 2011; Fuss et al., 2018).

Bioenergy and carbon capture and storage (BECCS) systems are the CDR options with greatest prominence (Kriegler et al., 2013; Clarke et al., 2014; Rogelj et al., 2016; Minx et al., 2018; Fuss et al., 2018). The concept of BECCS is based on the assumption that bioenergy can be provided with neutral carbon emissions, since the CO_2 sequestrated during the biomass growth cycle compensates the CO_2 released in the biomass energy conversion process. Therefore, the system is regarded as capable of removing CO_2 from the atmosphere when coupled with carbon capture and storage, resulting in negative emissions, already figuring in many integrated assessment models (IAMs) results and their corresponding portfolios (Smith et al., 2014; Kemper, 2015; Creutzig 2016; Fuss et al., 2018; Gough et al., 2018, Rogelj et al., 2018; Daioglou et al., 2020; Hanssen et al., 2020).

[1] Carbon budget can be defined as the cumulative amount of net CO_2 emissions that can be released to the atmosphere in order to limit global warming to a given temperature, with a specific minimum probability (Rogelj et al., 2016; Fuss et al., 2018).

Brazil figures among the world's most important bioenergy producers and consumers. In light of the Paris Agreement, Brazil's updated Nationally Determined Contribution (NDC) to the United Nations Framework Convention on Climate Change (UNFCCC) pledges to reduce GHG emissions by 37% in 2025 and by 43% in 2030, when compared to 2005 (Brasil, 2021). Increasing the participation of bioenergy and biofuels in the national energy mix is crucial to achieve this target. In fact, Rochedo et al. (2018) indicate an extensive expansion of cellulosic biofuels production in Brazil, especially when dealing with climate stringent targets and scenarios.

However, bioenergy is a complex and, at times, controversial topic. The large-scale deployment of BECCS faces many risks and challenges, including biophysical, technological, economic, social and institutional issues. Restrictions are related to the global potential of bioenergy, food security, fertilizers use, land-use and land-use change impacts, water requirements, interaction with biodiversity, and the global capacity of CO_2 storage (Smith et al., 2016; Garcia et al., 2018; Jia et al., 2019; Stenzel et al., 2020; Calvin et al., 2021). If developed in an adequate manner, bioenergy systems have the potential to significantly contribute to climate change mitigation. However, if inappropriately expanded, they can negatively impact the climate and the ecosystems conservation, generating conflicts and inducing direct and indirect land-use changes, causing damages to biodiversity and water bodies, and reducing food security (Kemper, 2015; Samsatli et al., 2015; Fuss et al., 2018; Humpenöder et al., 2018).

Most of the aforementioned challenges are not well represented and/or are not fully incorporated by most Integrated Assessment Models[2] (IAMs). Such issues involve land allocation, accounting for both the spatial and temporal variations of biomass yield and land availability, transport and storage of resources, including the need for pretreatment of biomass for suitable storage options, seasonality, imports and exports, scale of the conversion units, staged investments and retirement of technologies, co-product and end-product values and their respective logistics, and carbon capture, transportation and sequestration, including detailed sequestration site information.

[2] Integrated Assessment Models (IAMs) describe the key processes in the human and the earth systems, and their interactions, aiming at providing relevant insights regarding climate, energy and environmental assessments, global environmental change and sustainable development, as well as support for climate policy and policymakers.

Considering this is as crucial gap in the current literature on mitigation pathways, Koberle et al. (2021) highlight the need for comprehensive and flexible modelling tools that can translate aggregate global projections of IAMs into more robust spatially explicit local projections, giving valuable and actionable regional insights in the process. Moreover, better representation of agricultural and land-use dynamics, along with bioenergy development strategies, and how they are affected by regional characteristics, as well as by the economic, social and political drivers, improves their appropriateness for regional assessments and policy design. According to Koberle et al. (2021), linking global IAMs and regional models could provide the complementary interaction between global mitigation pathways, since bioenergy as a climate mitigation option cannot be fully interpreted without the global context, and regional strategies and aspects that influence potentials, costs, logistics, and system expansion.

In the literature, there are various examples of models focused on biomass supply chain modelling, most of which break the supply chain in multiple blocks, usually including harvesting, storage and conversion, with transport flows among the blocks (Samsatli et al., 2015). Some of the models are limited to a particular purpose, focusing on specific feedstocks or final products, such as You et al. (2012), Akgul et al. (2011), Marvin et al. (2012) and Lin et al. (2014) and Khatiwada et al. (2016), which focus on ethanol production, and Zhang et al. (2020), which focuses on power generation. Most of them are not spatially explicit, not incorporating land area and assuming biomass availability as a fixed parameter. More comprehensive models, such as Samsatli et al. (2015) are spatially explicit, take into account land and biomass availability, as well as capacities allocation and retirement, but do not address land use change and land use change emissions, direct or indirect. Moreover, none of the mentioned models are linked to an IAM.

1.2 Objectives

The main objective of this thesis is to develop a spatially explicit model to assess different bioenergy pathways while encompassing various dimensions that influence their optimal deployment and to apply it to the Brazilian context, investigating the most efficient and cost-effective ways of providing the growing bioenergy demand in future projections while complying with climate targets in a sustainable and competitive manner. By validating the model through its application to the Brazilian context, this

study aims to investigate the role of bioenergy (with and without carbon capture and storage) in the Brazilian climate mitigation strategies and its interactions with the land system and the existing bioenergy value chain.

The model should be capable of:

- Identifying and quantifying main costs of bioenergy pathways,
- Identifying which feedstocks to grow and where to grow them,
- Identifying the optimal location for biomass conversion units,
- Identifying logistics constraints and system expansion projections, taking into account existing bioenergy value chain and accounting for capacities retirement,
- Identifying opportunities and constraints for the deployment of carbon capture, transportation and storage from biogenic sources,
- Determine the emission implications of bioenergy pathway (e.g., direct land use change emissions, biomass production emissions, among others),
- Providing contributions to long-term climate policy design, given the opportunity of competitive advantages (for Brazil or other countries or regions, depending on the context the model is applied to) in low carbon scenarios.

As previously stated, most IAMs do not fully incorporate the regional specificities that influence bioenergy production. Furthermore, sectoral models developed to evaluate bioenergy value chains do not consistently address the various dimensions of the bioenergy systems. Therefore, the originality of the model here proposed lies on its intended ability to be easily soft-linked with IAMs. This allows for a spatially explicit representation of pathways projected by IAMs, while encompassing a variety of feedstocks and technologies (selected based on current use, regional context and expected future trends), incorporating logistics of solids and liquids, integrating carbon transportation and storage networks, and addressing direct land use change and direct land use change emissions.

1.3 Thesis Outline

This thesis is divided into five chapters, and is structured as follows: the first chapter, here presented, outlines the context that motivated this work, as well as the

objectives it aims to achieve; the second chapter introduces the main concepts regarding biomass, bioenergy and the integrated assessment and modelling of bioenergy value chains, providing a comprehensive literature review on these topics; the third chapter presents the methodology, including model development and model application, outlining the case study and the scenario choices; the fourth chapter presents the results; and the fifth chapter provides the final remarks, highlighting the overall findings, conclusions and implications of this study, along with a discussion on current limitations and future work.

2. Literature Review

This chapter provides a brief overview of both basic concepts and methodological aspects regarding biomass and bioenergy. First, it presents the broader definitions of biomass and bioenergy, moving on to an overview of global supply and demand of bioenergy, and the role of Brazil in such context. Then, it discusses the expected challenges and risks of bioenergy deployment, including geophysical, technological, social and economic aspects. Finally, this chapter reviews different modelling approaches to bioenergy value chains, outlining the role of bioenergy in low carbon scenarios and the importance of taking into account regional specificities in the process.

2.1 Biomass and Bioenergy

Biomass is defined as renewable organic matter, animal or plant based, including dedicated energy crops, planted forests, agricultural and forestry residues, manure, municipal solid wastes, among others. Typically, biomass is composed of cellulosic and hemicellulosic structures, lignins, lipids, proteins, sugars, water, hydrocarbons and ashes. Components shares depend on the type of biomass. In general, in a dry basis, the carbon content ranges from 30 to 60% (Khan et al., 2009).

Bioenergy is energy derived from any form of biomass (IPCC, 2014), and if the biomass is produced in a renewable manner, bioenergy can in principle be a renewable and low emission energy resource. Biomass can be converted directly into heat and/or into intermediate energy carriers (solid, liquid and gaseous) to subsequent production of heat, power and biofuels, as well as biomaterials and biochemicals, attending different sectors, such as industry, transport, buildings and the power sector. Figure 2.1 provides an overview of various biomass resources and their conversion to attend the different economy sectors.

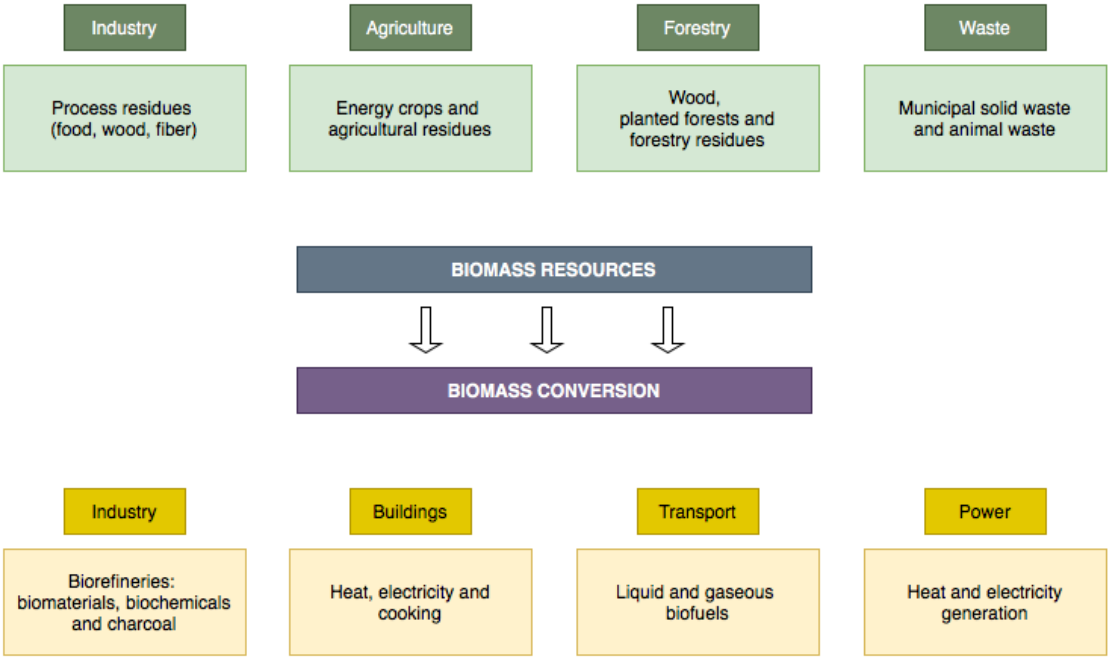

Figure 2.1. Overview of biomass resources and biomass conversion

Biomass use can be categorized into traditional and modern. Traditional uses of biomass encompass the direct combustion of biomass (fuelwood) for cooking, lighting and heating. Such uses have low efficiencies and high pollutants emissions, with significant impacts over human health and local air quality. Modern uses of biomass refer to the conversion of biomass through more efficient technologies to produce heat, power and biofuels (conventional[3] and cellulosic biofuels[4]) (IRENA, 2021). The transition from the traditional uses of biomass to the production of higher quality and more efficient bioenergy is expected to contribute to climate mitigation in the future (IEA Bioenergy, 2021).

[3] Conventional biofuels are market mature and commercially available biofuels, produced from feedstocks consistent of sugars, starches and oils (all of which derived from food crops), as well as animal fats (IEA Bioenergy, 2021).

[4] Cellulosic biofuels are pre-commercial and under development biofuels, produced from lignocellulosic biomass, using feedstocks with low impacts on greenhouse gases emissions and low implications over land use and direct or indirect land use change, such as non-food crops and residues (agricultural residues and forestry residues) (IEA Bioenergy, 2021).

2.2 Bioenergy Supply and Demand

2.2.1 Global Bioenergy Supply and Demand

Biomass is a major source of renewable energy, contributing to approximately 10% of primary energy supply worldwide (IEA, 2020), most of which is directed to cooking and heating in developing regions (IEA, 2020; IPCC, 2014). According to the International Energy Agency (IEA, 2021), the global bioenergy supply reached 65 EJ in 2020. This represents a 22% increase when compared to 2010. Fuelwood still dominates bioenergy supply, with a share of roughly 40%. Interestingly, the share of residues in bioenergy supply increased substantially, going from less than 1 EJ in 2010, to over 6 EJ in 2020.

According to IEA (2021), most (circa 40%) of the produced bioenergy in 2020 was used to attend the traditional uses of biomass, including cooking, lighting and heating. However, this represents a considerable reduction when compared to the 52% share of demand for such uses observed in 2010. Industry and power generation follow the traditional uses of biomass, together accounting for 28% of bioenergy demand worldwide, in 2020. Furthermore, the share of modern bioenergy in total energy supply increased in the past decade, going from 4.6% in 2010 to 6.6% in 2020, making up 53% of total renewable primary energy supply.

Figure 2.2 illustrates the global bioenergy supply and the corresponding shares of main feedstocks, namely bioenergy crops, fuelwood, organic waste, forestry residues, short rotation wood crops and planted forests, for 2010 and 2020 (on top), and the global bioenergy demand, as well as the corresponding sectors, including power generation, industry, buildings and agriculture, transport and the traditional uses of biomass (at the bottom).

Figure 2.2. Global bioenergy supply and demand (2010;2020)

Based on IEA (2021)

Global bioelectricity production reached approximately 590 TWh in 2019, with an expansion in capacity of 8.5 GW when compared to 2018. China accounted for 60% of the expanded capacity (IEA, 2021). Figure 2.3 presents the evolution of biomass production from 2010 to 2019[5].

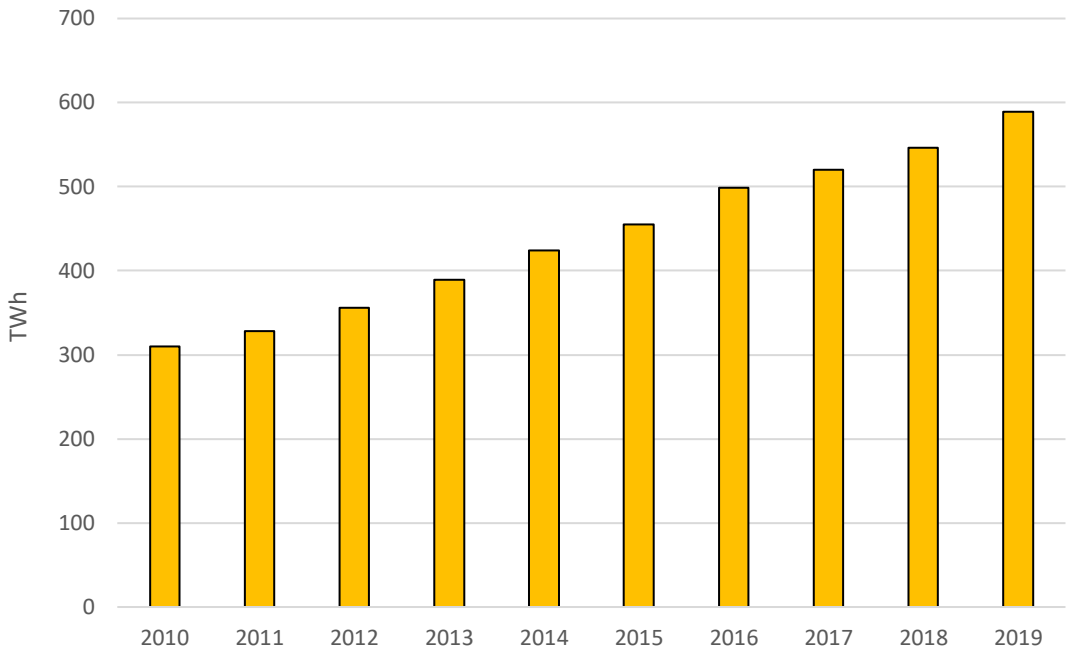

Figure 2.3. Global bioelectricity supply (2010-2019)

Based on IEA (2021)

Global biofuel production reached 96 Mtoe in 2019. While China leads the global bioelectricity production, the United States lead biofuel production worldwide, with a share of 36% of total global production in 2019. Brazil is the second largest biofuel supplier, with a share of 23% of total global production in 2019 (IEA, 2021). Figure 2.4 presents the evolution of global biofuel production from 2010 to 2019, and Figure 2.5 presents the country shares in global biofuel production in 2019.

[5] Bioenergy (bioelectricity and biofuel) production and capacity additions declined in 2020, due to repercussions of the COVID-19 pandemic. Lower demand for transport fuels resulting from the pandemic crisis strongly impacted the biofuel industry (IEA, 2020; IEA, 2021). The official numbers for 2020 are not yet available in the IEA database.

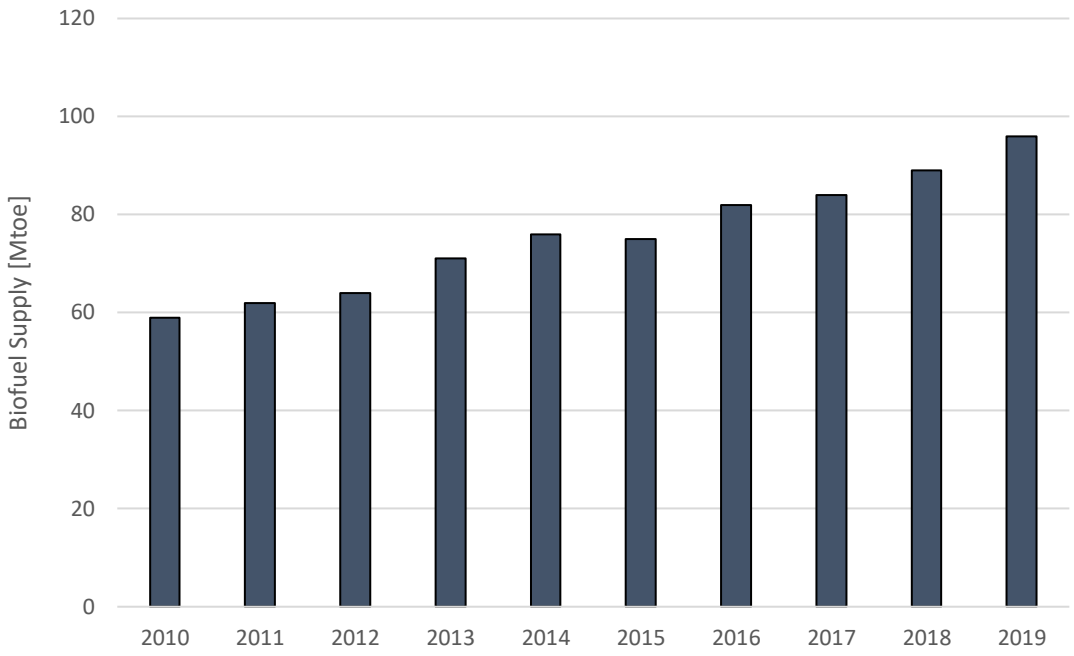

Figure 2.4. Global biofuel supply (2010-2019)

Based on IEA (2021)

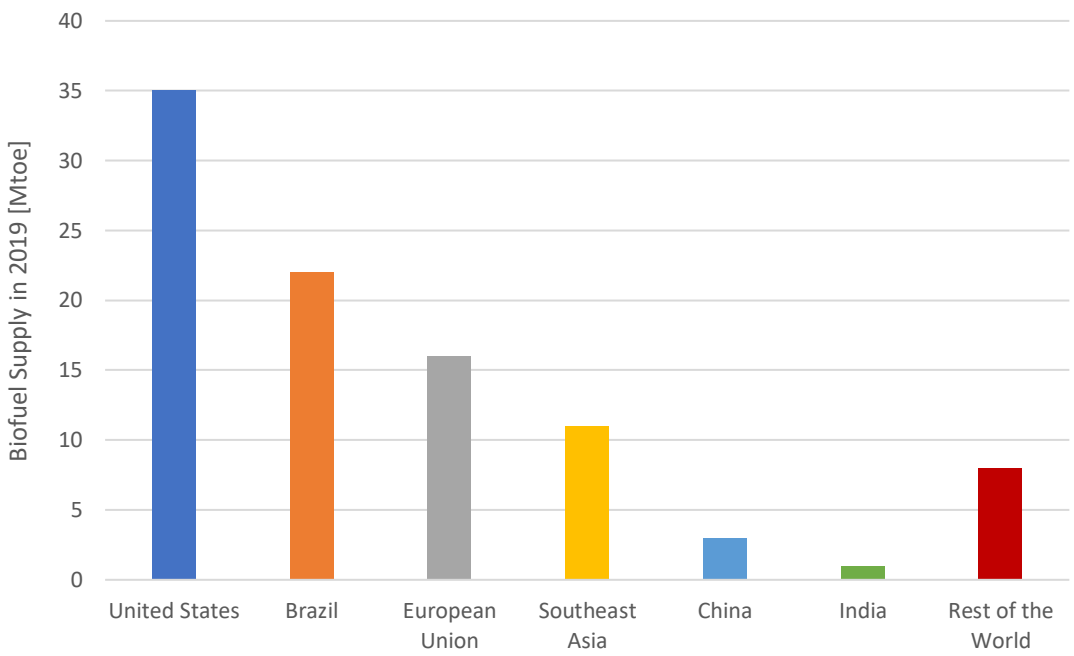

Figure 2.5. Biofuel supply per country in 2019

Based on IEA (2021)

2.2.2 Bioenergy in the Brazilian Energy Matrix

Biomass in an important renewable source in the Brazilian energy matrix, contributing to power supply and the production of biofuels. According to the Energy Research Office (EPE, in its Portuguese acronym[6]), biomass represented over 28% of the total energy supply in 2020 (EPE, 2021a). The two main biomass feedstocks are sugarcane products (19% of total energy supply in 2020) and firewood and charcoal (9% of total energy supply in 2020) (EPE, 2021a). Figure 2.6 illustrates the total energy supply in Brazil, from 2002 to 2020.

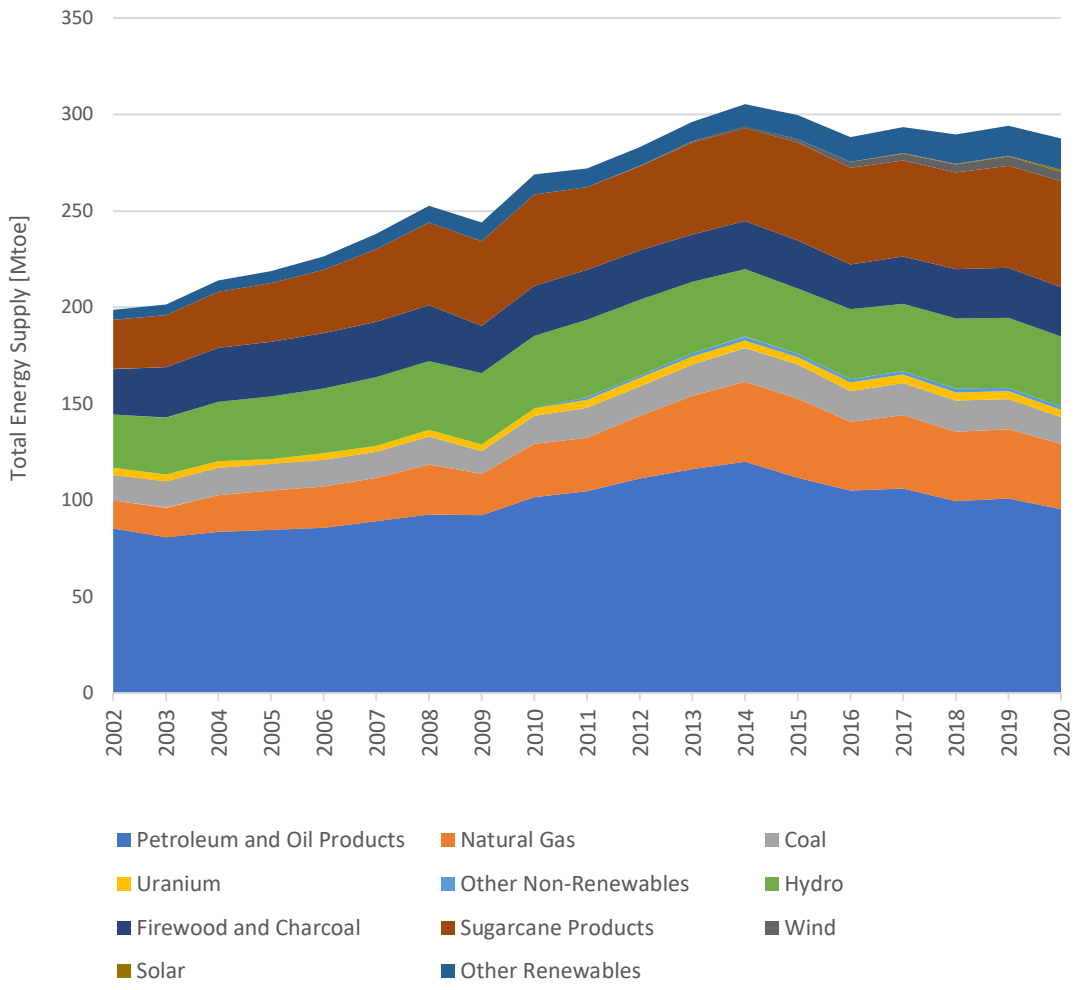

Figure 2.6. Brazilian Historical Total Energy Supply (2002-2020)

Based on EPE (2012;2021a)

[6] Empresa de Pesquisa Energética – EPE.

The Brazilian power sector is largely dominated by hydropower. Biomass is the second most important source for electricity generation (9.1% of total electricity supply in 2020), next to wind and natural gas (8.8% and 8.3% of total electricity supply in 2020, respectively) (EPE, 2021a), as can be seen in Figure 2.7.

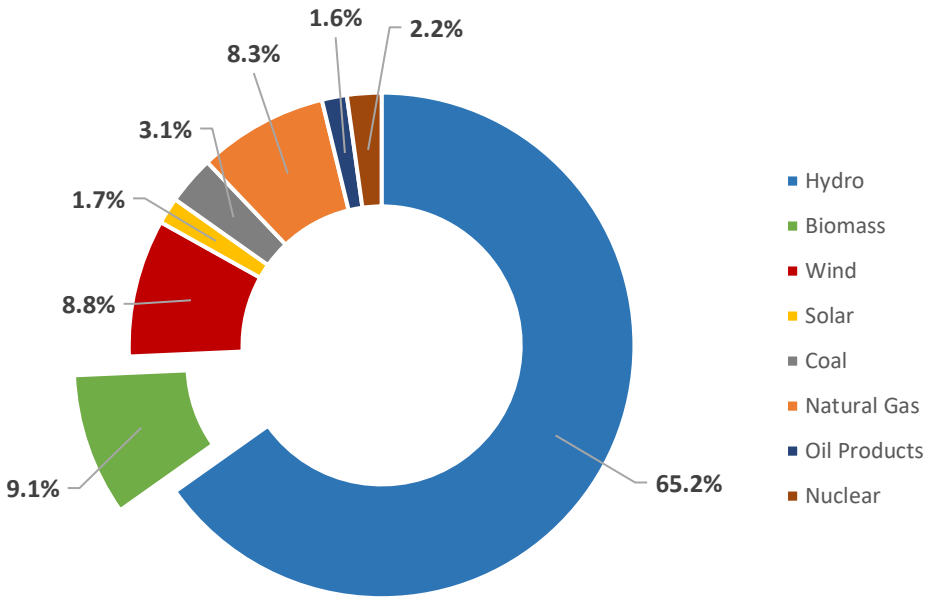

Figure 2.7. Shares of total electricity supply in Brazil, by source, in 2020

Based on EPE (2021a)

The main biomass feedstock used for bioelectricity is sugarcane bagasse. Other important biomass feedstocks are black liquor[7] and fuelwood, from planted forests (mainly eucalyptus and pine) (EPE, 2016). According to the Energy Research Office (EPE), the bioelectricity supply in the country is largely driven by the well-established national sugarcane industry. Since the early 2000s, the supply of bioelectricity has considerably grown due to the expansion of the use of sugarcane bagasse to generate

[7] Black liquor is a by-product of the pulp and paper industry. In terms of composition, black liquor is an aqueous solution of lignin, hemicellulose and the inorganic chemicals used in the processing of wood to produce paper (Speight, 2019).

electricity surplus and the modernization of the cogeneration units, which were previously focused on meeting the energy demands of the units themselves (EPE, 2016).

Current policies to encourage the expansion of biomass in power generation include the reduction in the tariff in the distribution and transmission systems, the distributed generation system, and the energy auctions in the regulated energy market, where the ceiling price corresponds to the maximum bid price allowed to the plants participating in the auction and is an important indication of the practice of incentives to contract alternative energy sources, despite them being more expensive (EPE, 2016; CNPEM, 2017).

Brazil is also a major producer and consumer of biofuels. The two main liquid biofuels that integrate the national energy mix are ethanol and biodiesel. National production of ethanol comes mostly from sugarcane, with a lower participation of maize as feedstock. In 2019, ethanol (anhydrous[8] and hydrated[9]) output reached over 35 million m^3. The production is highly concentrated in the Southeast, which is the largest producing region (58% of national production, in 2019), and the Center-West[10] (31% of national production, in 2019) (ANP, 2020).

Most of the ethanol imported to Brazil comes from the United States. In 2019, Brazil imported a total volume of around 1.5 million m^3 of ethanol, 91% of which from the United States alone. In terms of exports, trading is more diverse, with important markets also in Asia-Pacific. In 2019, Brazil exported a volume of approximately 1.9 million m^3 of ethanol, of which circa 63% to the United States and 30% to Asia-Pacific (most importantly South Korea, accounting for around 26%) (ANP, 2020).

Figure 2.8 presents the annual production of ethanol (anhydrous and hydrated), per Brazilian region, for the period 2010-2019 (on top), and the volumes of imports and exports of ethanol, per global trading regions, for the period 2011-2019 (at the bottom). Note that the net export is positive.

[8] Anhydrous ethanol has > 99.3% alcohol content (ANP, 2020).

[9] Hydrated ethanol has > 92.5 – 96.5% alcohol content (ANP, 2020).

[10] An overview of the Brazilian regions is provided in Annex I.

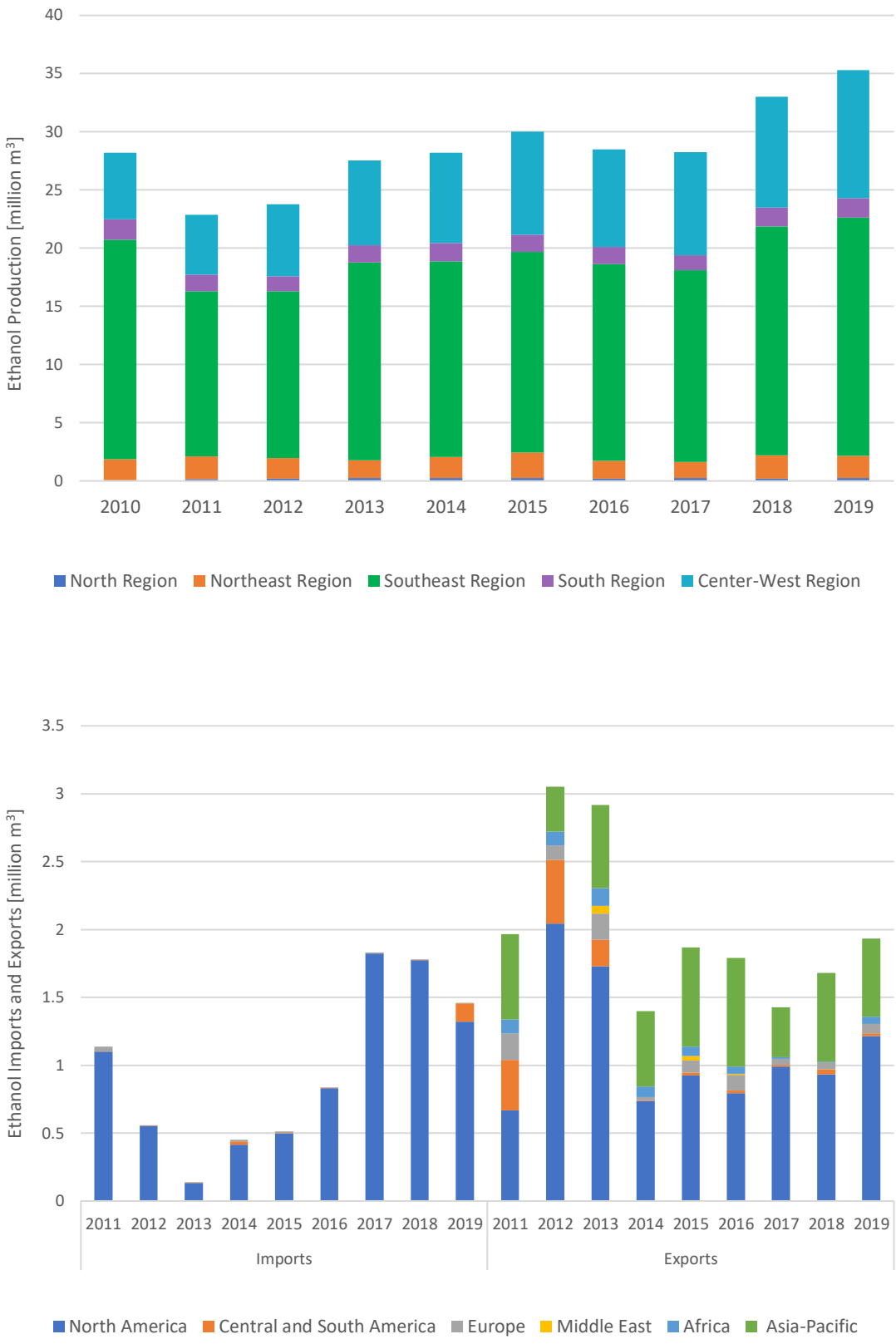

Figure 2.8. Brazilian ethanol (anhydrous and hydrated) production (2010-2019) (top); imports (anhydrous) vs exports (2011-2019) (bottom). Note different scales.

Based on ANP (2020)

Biodiesel production is based on vegetable oils and animal fat. According to the National Petroleum, Natural Gas and Biofuels Agency (ANP), in 2019, 86% of total biodiesel production used vegetable oils as feedstock (68% soybean oil, 18% other oils, such as cotton oil, palm oil, sunflower oil) (ANP, 2020). The production of biodiesel (B100[11]) reached almost 6 million m^3 in 2019. In slight contrast with ethanol production, biodiesel production is highly concentrated in the South and Center-West regions, evenly sharing 82% of total national production (41% each) in 2019 (ANP, 2020). Figure 2.9 presents the annual production of biodiesel, per region, for the period 2010-2019.

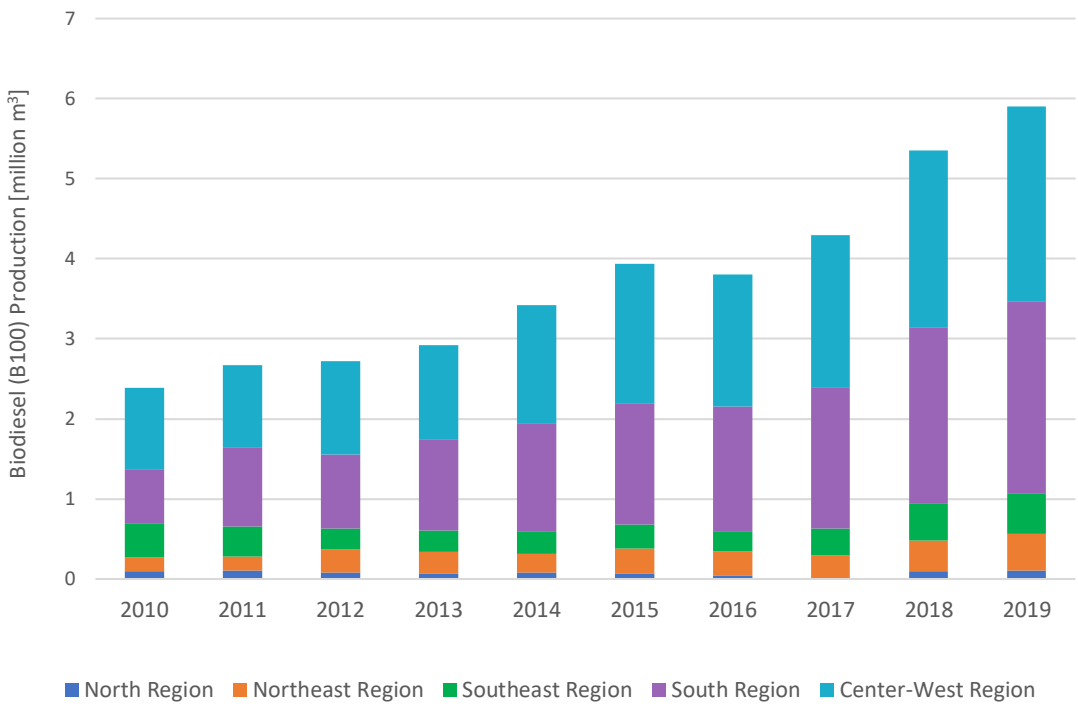

Figure 2.9. Biodiesel (B100) production in Brazil (2010-2019)

Based on ANP (2020)

As can be seen by this overview, biofuels play an important role in the Brazilian energy mix and, according to the country's NDC pledges, are expected to increase their contribution in the future. In terms of policy, as part of the new national directives for

[11] B100 denominates pure biodiesel, i.e., 100% biodiesel.

biofuels, it's worth citing the "RenovaBio" program. "RenovaBio" is a program designed to foster the production of biofuels in Brazil, fomenting their strategic role in the national energy matrix, contributing to climate mitigation and reducing GHG emissions, in light of the Paris Agreement and the Brazilian NDC pledges. By establishing national annual decarbonization goals in the fuels sectors, the program is expected to create a supportive environment for investments in new capacities for biofuel production, inducing energy efficiency gains and reducing emissions throughout the value chain, including production, commercialization and distribution, and consumption (ANP, 2021).

2.3 Uncertainties and Challenges to Bioenergy Production

There are major uncertainties regarding the estimated global and regional bioenergy potentials and the sustainability of its supply (Fuss et al., 2018; Humpenöder et al., 2018). In its Fifth Assessment Report (AR5), published in 2014, the Intergovernmental Panel on Climate Change (IPCC) literature review presented a range of bioenergy potentials from 25 to 675 EJ/year by 2050 (IPCC, 2014). More recently, Fuss et al. (2018) conducted a literature review that resulted in an even wider range, varying from 60 to 1548 EJ/year by 2050. According to the authors, the more optimistic estimates are usually grounded in higher land availability and yields improvements, while the less optimistic ones focus on taking into account biophysical and ecological concerns.

Since then, studies conducted by Daioglou et al. (2019), Wu et al. (2019), Hanssen et al. (2019) and Kalt et al. (2020) show more modest estimates for bioenergy potentials, not surpassing 245 EJ/year by 2050. Overall, the available literature is not consistent, applying different accounting methods, incorporating different types of feedstocks (for example, some studies include residues while others do not), and inconsistently addressing (or not addressing at all) biophysical, technological, economic, institutional, social and ecological dimensions that might constrain and impose challenges to bioenergy supply, especially when coupled with carbon capture, transportation and storage. The main constraints to bioenergy production are outlined below.

2.3.1 Biophysical and ecological constraints

One of the main biophysical constraints to the future deployment of bioenergy lies on the availability of land, given that the large-scale production of bioenergy might lead to competition between energy and food crops, resulting in challenges for land

management and risks to food security. Land use and land use change also involve ecological constraints in terms of biodiversity and ecosystem conservation, as well as water availability. Such constraints directly affect biomass production, being fundamental limiting factors to estimate bioenergy potentials (Fuss et al., 2018; Hasegawa et al., 2020).

Additionally, there are uncertainties regarding the availability of safe storage for the carbon captured. The identification of adequate sites to safely store the captured CO_2 depend on geophysical aspects such as permanence and stability, requiring efforts in assessment and monitoring, in order to avoid leakages and undesirable damages to the integrity of the storage sites (Pinder, 2014). Even though estimates throughout literature claim there is sufficient global geological storage potential, regional storage bottlenecks could limit the deployment of bioenergy when associated with carbon storage (Dooley 2013, Fuss et al., 2018).

2.3.2 Techno-economic constraints

Biomass can fuel dedicated bioenergy systems or co-firing systems, together with conventional fuels (e.g., coal). However, shares of biomass over 20% of the total combustible material reduce the efficiency of the conversion process and increase the energy penalties related to CO_2 capture. Additionally, the particular chemical characteristics of biomass (carbon content, lower heating values, etc.) raise concerns regarding the emission of pollutants (e.g., cadmium and mercury) requiring proper equipment and system adaptations (Akgul et. al, 2014; Kemper, 2015). Given the constraints mentioned above, scaling-up biomass conversion technologies is also a challenge, influencing costs and costs estimates over time.

Costs estimates for bioenergy production associated with carbon capture and storage are highly influenced by the expected future prices of electricity and fuels, the projected availability of biomass, the chosen technological route and the choices for CO_2 transportation (e.g., pipelines, ships, trucks) and storage. Additionally, for some crops (e.g., sugarcane) the seasonal and disperse production imposes economic challenges to carbon transportation and storage, especially related to scale and capital cost recovery (Tagomori et al., 2018; da Silva et al., 2018).

Typically, IAMs use mechanisms such as carbon prices and carbon budgets to evaluate the economic feasibility of climate change mitigation measures, including bioenergy. Furthermore, the choices on discount rates to incorporate investments and

capital costs in the long term influence the performance of capital-intensive technologies. Additionally, there are uncertainties in pricing in potential externalities of biomass and bioenergy production, regarding e.g., land use and land use change and food prices (Humpenöder et al., 2018).

2.3.3 Social and institutional constraints

As previously said, the large-scale deployment of bioenergy and the interactions between energy and food crops could pose threats to food security, raising food prices and driving a number of people to risk of hunger (Humpenöder et al., 2018; Hasegawa et al., 2020). The effects of increasing bioenergy production can alter patterns of food production and consumption, impacting land tenure and creating physical and economic barriers to food access and affordability, as well as raising concerns regarding land property rights, which can, in turn, impact public health and create distributional inequities (Creutzig et al., 2013).

Environmental and societal trade-offs might be unavoidable in what regards large-scale bioenergy production and expansion, even if potential externalities are accounted for and internalized (Rose et al., 2020). In this context, Humpenöder et al. (2018) argue that policy design to regulate such externalities should be comprehensive, assessing such trade-offs between the biophysical, technical, economic, human and ecological dimensions, while encompassing sustainability criteria, in consonance with the sustainable development goals (SDGs) agenda.

2.4 Modelling Bioenergy

Different models apply different approaches to deal with bioenergy systems. IAMs apply broader approaches with global or regional stylized assumptions, while sectoral models are more focused on (and better represent) the local context. Furthermore, throughout the different models, there are various assumptions in terms of feedstocks and final products included, conversion technologies portfolios and their availability across regions and across time, deployment of carbon transportation and storage networks, competition with food, land use change and land use change emissions (direct and indirect), time dimension (decades, years, seasons), and spatial dimension (spatially explicit or not, and at what scale).

COFFEE[12] is a global IAM that applies a non-spatially explicit approach, introducing land cover categories (cropland, crop-veg, forest, for-grass, grassland, flooded and not suited, which includes urban, deserts and permanent ice areas) that aggregate dimensions of land use, soil productivity and travel time. The model is an intertemporal least-cost optimization model, and it works in 5-year time steps from 2010 to 2050 and 10-year time steps from 2050 to 2100. The seasonality of crops is not taken into account. The world is divided in 18 regions, being Brazil one of them. The model includes a large set of technologies for biomass conversion (including the option of carbon capture in the production of electricity, hydrogen and first and second generation biofuels), using various types of feedstocks (including residues from agriculture and forestry) to produce different final products, including solid and liquid biofuels (encompassing a variety of cellulosic fuels options), as well as hydrogen, electricity and heat (IAMC, 2021a; Rochedo, 2016, Daioglou et al., 2020). Logistics aspects are included in the aggregate travel time assumptions, but are not geographic explicitly modelled (Rochedo, 2016).

IMAGE[13] is a global scale modelling framework that approaches land at the grid level, encompassing land cover, land use allocation, forest management, livestock systems, the carbon cycle and natural vegetation (IAMC, 2021b). The model is a recursive dynamic, and it works in yearly time steps, from 1970 to 2100. The seasonality of crops is not taken into account. The model has 26 regions, and Brazil is one individual region. In terms of the technology portfolio, IMAGE includes routes for the conversion of crops and cellulosic biomass into electricity, hydrogen, and solid and liquid biofuels, with the option of capturing carbon in all of them (Daioglou et al., 2020). Agriculture and forestry residues, as well as municipal solid waste, are available for bioenergy production (Koberle et al., 2021). IMAGE applies a food-first principle, so that bioenergy crops do

[12] COFFEE (Computable Framework for Energy and the Environment) is a partial equilibrium model. TEA (Total Economy Assessment) is a computable general equilibrium model. COFFEE-TEA form a multi-regional, multi-sectoral framework, developed by COPPE/UFRJ, Brazil, to assess climate, energy, land and environmental policies (IAMC, 2021a).

[13] IMAGE (Integrated Model to Assess the Global Environment) is a multi-region, multi-sectoral simulation modelling framework, housed at the Netherlands Environmental Assessment Agency (PBL), The Netherlands, to comprehensively investigate the interactions between human development and the natural environment (IAMC, 2021b).

not compete with food crops for land. The model first allocates land for agriculture, pasture and forests, and only remaining lands are available for bioenergy production (Daioglou et al., 2019).

In the MESSAGEix-GLOBIOM[14] modelling framework, GLOBIOM is a recursive dynamic partial-equilibrium model, with a grid-scale bottom-up representation of land-based activities, such as agriculture, forestry and bioenergy production. The framework applies an intertemporal least-cost optimization approach and operates in 10-year time steps, from 2010 to 2100. The model has 11 regions and Brazil is not an individual region, but part of a larger Latin America and the Caribbean region. GLOBIOM is coupled with the Global Forest Model (G4M) to provide spatially explicit projections of forest area, carbon uptake and release, and biomass supply (IAMC, 2021c). In MESSAGEix, the energy component, bioenergy conversion routes represented include the production of electricity, heat, hydrogen, solid, gaseous and cellulosic liquid biofuels (first generation biofuels are not modelled). Carbon capture can be included in electricity, hydrogen and cellulosic biofuels. Food crops and residues are not used as feedstocks, which include only lignocellulosic biomass and managed forests (Daioglou et al., 2020).

The REMIND[15] model is connected with the land model, MAgPIE, via soft-link, to provide the interactions between energy and land through bioenergy demand and supply and their corresponding implications on land, including land use and land use change emissions (IAMC, 2021d). REMIND is an intertemporal optimization model, running from 2005 to 2100 with 5-year time steps until 2060 and 10-year time steps from 2060 to 2100. The model has 11 regions and Brazil is part of the larger Latin America region. REMIND includes in its portfolio biomass conversion routes to produce electricity and heat, hydrogen, solid, gaseous and liquid (first and second generation) biofuels. The production of electricity, hydrogen and cellulosic biofuels can be coupled

[14] MESSAGEix (Model for Energy Supply Strategy Alternatives and their General Environmental Impacts) and GLOBIOM (Global Biosphere Management Model) are the energy and land use models, respectively, that integrate the International Institute for Applied Systems Analysis (IIASA) IAM framework, developed by IIASA, Austria (IAMC, 2021c).

[15] REMIND (Regional Model of Investment and Development) is an energy and economy general equilibrium model and can be soft-linked with MAgPIE (Model of Agricultural Production and its Impact on the Environment), a partial equilibrium model of the agricultural sector, both developed by the Potsdam Institute for Climate Impact Research (PIK), Germany (IAMC, 2021d).

with carbon capture. Feedstocks modelled include cellulosic crops and residues. Bioenergy can compete for agricultural land, pastures and a fraction of forests (a part of forest areas is deemed protected and another part is excluded for wood production for other uses) (Daioglou et al., 2020 Rose et al., 2020).

AIM/CGE[16] applies a land nesting strategy, with nine ecological zones to categorize land, with a land market for each zone where land is allocated according to differences in land rent and the substitutability among land categories. AIM is a recursive dynamic model, running in yearly time steps from 2005 to 2100. The model works with 17 regions, including Brazil as a single region (IAMC, 2021e). AIM includes the use of biomass for the production of electricity, heat and solid and liquid biofuels, all of which have the option of including carbon capture, except for the production of heat (Daioglou et al., 2020). Food crops and lignocellulosic crops can be used as feedstock, as well as residues from agriculture and forestry. Bioenergy production can compete for all types of land (agricultural land, pasture, forests and non-commercial land) (Rose et al., 2020).

GCAM[17] (Global Change Analysis Model) is a recursive dynamic model, running in 5-year time steps, from 2015 to 2100. The macroeconomy and the energy system are represented in 32 regions, including a separate region for Brazil. The land system is divided in 384 regions, which are determined based on the major water basins in each of the 32 macro regions (JGCRI, 2021). GCAM includes the conversion of energy crops (e.g., maize, sugar crops, oil crops), cellulosic biomass and residues (agriculture, forestry and municipal solid waste) into electricity, hydrogen, biogas and biofuels (including solid biofuels and cellulosic liquid biofuels). Land competition encompasses all types of land, including agricultural land, pasture and forests. Model default applies a protection of 90% of natural lands in each region (Rose et al., 2020).

[16] AIM/CGE (The Asia-Pacific Integrated Modeling/Computable General Equilibrium) is a simulation general equilibrium model, integrating the AIM framework, jointly developed by the National Institute for Environmental Studies (NIES) and Kyoto University, Japan, to assess climate mitigation strategies (IAMC, 2021e).

[17] GCAM is stewarded by the Pacific Northwest National Laboratory, Joint Global Change Research Institute (PNNL, JGCRI), United States.

BVCM[18] (Biomass Value Chain Model) is a spatially explicit, intertemporal optimization model. The model works with 10-year time steps, from 2010 to 2050, and includes a seasonal dimension for crop growth and harvest (from one single season to four seasons). BVCM is a sectoral model, and it is currently applied to the United Kingdom (UK). Spatial resolution is 50 length square grid cells, which for the UK results in 157 grid cells. The model has four different levels of land availability. Levels are cumulative: first level includes arable and agricultural areas, second level includes first level and adds herbaceous vegetation and open spaces with little or no vegetation, third level includes second level and adds permanent crop areas and pastures, and fourth level includes third level and adds artificial non-agricultural vegetation areas and forests. Modelled technologies include the conversion of different crops, cellulosic biomass and residues (including agriculture, forestry and municipal solid waste) into electricity, heat, hydrogen, solid, gaseous and liquid biofuels. Carbon capture can be added to power generation and the production of hydrogen and gaseous and/or liquid cellulosic biofuels. Land use and land use change emissions are not accounted for (Samsatli et al., 2015).

BeWhere[19] is a sectoral, spatially explicit optimization model that can be applied to specific regions in order to model renewable energy systems, including bioenergy. BeWhere is a static model. The model allocates conversion facilities based on a given (exogenous) crop allocation (e.g., current geographic information on sugarcane production in Brazil), taking into account the logistics of biomass and biofuel supply. The model focuses on second generation liquid biofuels but can also be used to allocate power and heat units and pellet industries, depending on the local context, including a variety of feedstocks such as agriculture and forestry residues, and lignocellulosic biomass. Carbon capture, transportation and storage options are included in the technologies' portfolio. So far, the model has been applied to Europe, Sweden, Finland, Austria and Brazil (IIASA, 2021; Khatiwada et al., 2016).

MONET[20] (Modelling and Optimization of Negative Emissions Technologies) is a sectoral modelling framework designed to evaluate BECCS value chains, applying

[18] BVCM was commissioned and funded by the Energy Technologies Institute (ETI).

[19] BeWhere was developed by the International Institute for Applied Systems Analysis (IIASA), in Austria, and Luleå University of Technology, in Sweden.

[20] MONET was developed by the Centre for Environmental Policy, Imperial College London, UK.

intertemporal optimization. The model has two different sets of subregions: one subregion where the biomass is imported from and one subregion where the biomass is imported to. Brazil, China, India, the European Union (EU) and the United States comprise the potential regions where the biomass is imported from, all discretized at the state or province level. The UK is the region where the biomass is imported to. Time steps can be either yearly or decadal, from 2030 to 2100. Feedstocks include grassy (e.g., miscanthus, switchgrass) and woody dedicated crops and wheat straw, and are converted to generate power. Land types for biomass growth include agricultural areas, grasslands, forests and marginal lands. Land use change and land use change emissions, direct and indirect, are accounted for (Fajardy, 2020).

PLUC[21] (PCRaster Land Use Change) is a spatiotemporal land-use change model. The framework applies a Monte Carlo analysis approach in order to produce stochastic maps of land availability for bioenergy and the corresponding land use changes (direct and indirect). The model runs in yearly time steps. PLUC is a demand-driven land allocation model and therefore does not have a conversion technologies module. Land dynamics is influenced by suitability factors, including current land use, proximity to water bodies, yields, population density and logistic aspects, such as distance to cities and transport networks (Verstegen et al., 2012). The land use classes, spatial resolution, spatial variability in yields levels and the suitability factors applied are case specific. PLUC has been applied to a number of different regions, including Brazil, Mozambique, East Kalimantan, Southeast of the United States and Ukraine (Verstegen et al., 2012; van der Hilst et al., 2014; Verstegen et al., 2015; Duden et al., 2017; Verstegen et al., 2019).

Table 2.1 summarizes the models described above and their main characteristics.

[21] PLUC was developed by the University of Utrecht, in a collaboration between the Energy and Resources and the Physical Geography departments.

Table 2.1. Modelling of bioenergy value chains: different selected models characteristics

	MODEL				
	COFFEE-TEA	IMAGE	MESSAGEix-GLOBIOM	REMIND-MAgPIE	AIM/CGE
Model Type	IAM	IAM	IAM	IAM	IAM
Modelling Approach	Intertemporal optimization	Recursive dynamic (simulation)	Intertemporal optimization	Intertemporal optimization	Recursive dynamic (CGE)
Spatial Dimension	18 regions	26 regions	11 regions	11 regions	17 regions
Brazil (as region)	Yes	Yes	No	No	Yes
Time Dimension	2010-2100 (5/10-year time steps)	1970-2100 (1-year time steps)	2010-2100 (10-year time steps)	2005-2100 (5/10-year time steps)	2005-2100 (1-year time steps)
Feedstocks	Crops, cellulosic biomass	Crops, cellulosic biomass	Cellulosic biomass	Crops, cellulosic biomass	Crops, cellulosic biomass
Residues	Agricultural and forestry; MSW	Agricultural and forestry; MSW	-	Agricultural and forestry	Agricultural and forestry
Final Products	Electricity*, heat, hydrogen*, 1st* and 2nd* generation biofuels	Electricity*, hydrogen*, 1st* and 2nd* generation biofuels	Electricity*, hydrogen*, biogas, 2nd* generation biofuels	Electricity*, hydrogen*, biogas, 1st and 2nd* generation biofuels	Electricity*, heat, 1st* and 2nd* generation biofuels
Land Availability	Agricultural land, pasture, forests	Remaining lands (food first)	Agricultural land, pasture, forests	Agricultural land, pasture, forests	Agricultural land, pasture, forests
Land Use Change	Yes	Yes	Yes	Yes	Yes

(*) With the option of adding carbon capture and storage.

Table 2.1 (cont.). Modelling of bioenergy value chains: different selected models characteristics

	MODEL				
	GCAM	BVCM	BeWhere	MONET	PLUC
Model Type	IAM	Sectoral	Sectoral	Sectoral	Sectoral (land allocation)
Modelling Approach	Recursive dynamic (simulation)	Intertemporal optimization	Optimization	Intertemporal optimization	Recursive dynamic
Spatial Dimension	32 regions (384 regions for land)	Spatially explicit	Spatially explicit	Spatially explicit	Spatially explicit
Brazil (as region)	Yes	No	Yes	Yes	Yes
Time Dimension	2015-2100 (5-year time steps)	2010-2050 (10-year time steps)	Static	Until 2030/2100 (1/10-year time steps)	(1-year time steps)
Feedstocks	Crops, cellulosic biomass	Crops, cellulosic biomass	Cellulosic biomass	Crops, cellulosic biomass	Crops, cellulosic biomass
Residues	Agricultural and forestry; MSW	Agricultural and forestry; MSW	Agricultural and forestry	Wheat straw	-
Final Products	Electricity*, biogas, hydrogen*, heat, 1st and 2nd* generation biofuels	Electricity*, biogas, hydrogen*, heat, 1st* and 2nd* generation biofuels	Electricity*, heat, 2nd* generation biofuels	Electricity*, heat	-
Land Availability	Agricultural land, pasture, forests	Agricultural land, pasture, forests	-	Agricultural land, pasture, forests	Agricultural land, pasture, forests
Land Use Change	Yes	No	No	Yes	Yes

(*) With the option of adding carbon capture and storage.

The above review highlights the plethora of modelling methods which have been used to assess the role of biomass in decarbonization pathways. However, regardless of the specific modelling approach, bioenergy is only a sustainable energy source if adequately developed. In order to avoid negative impacts on climate and ecosystems conservation, the entire value chain needs to be carefully evaluated, taking into account production, processing, distribution and logistical aspects, as well as existing structures and markets. Therefore, the appropriateness of each deployment strategy depends to a large extent on local and regional circumstances (Koberle et al., 2021).

2.5 Bioenergy in Low Carbon Scenarios

In general, bioenergy deployment is seen in low carbon scenarios as an option for the decarbonization of hard-to-abate sectors and, when coupled with carbon capture and storage, to provide negative emissions (Rogelj et al., 2018; Fuss et al., 2018). Most IAMs include technologies used for producing power, heat and/or fuels (liquid and gaseous) from biomass. While technologies and feedstocks representation and options vary among IAMs, most of them include bioenergy deployment strategies in their results, especially when dealing with stringent climate goals (Kriegler et al., 2017; Rogelj et al., 2018; Daioglou et al., 2020). The bioenergy deployment strategies depend on scenario assumptions and model specificities and characteristics, such as estimated costs, drivers for investment decisions, constraints on capacity expansion and on market share of innovative technologies, learning and scaling-up constraints, as well as other system integration factors (Daioglou et al., 2020).

Figure 2.10 outlines the deployment of bioenergy according to 5 different IAMs, for a scenario with an end-of-century carbon budget of 1000 $GtCO_2$ (NPi_1000[22] scenario). Data was collected from the IAMC (Integrated Assessment Modeling Consortium) 1.5°C Scenario Explorer, hosted by IIASA.

[22] The NPi_1000 scenario assumes currently implemented national policies, with no additional policies in the future, and establishes an end-of-century carbon budget of 1000 $GtCO_2$ (Riahi et al., 2021).

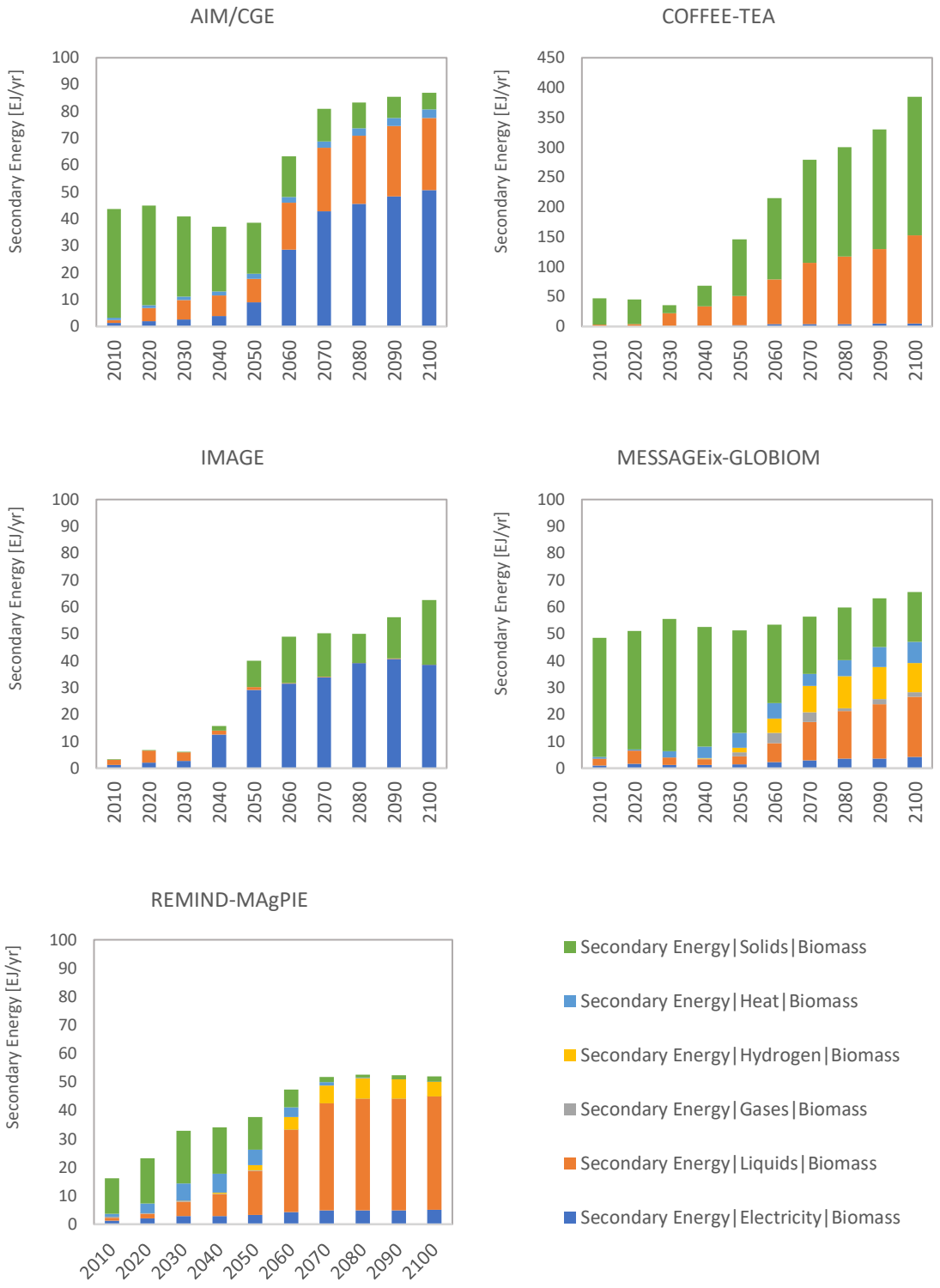

Figure 2.10. Bioenergy output from different IAMs (2010-2100), for the NPi_1000 scenario (Riahi et al., 2021). Note different scale for COFFEE-TEA. AIM/CGE, COFFEE-TEA and MESSAGEix-GLOBIOM include traditional biomass in the category of solids.

AIM/CGE and IMAGE bioenergy outputs are focused on the production of electricity, while COFFEE-TEA shows similar shares of solid and liquid biofuels. MESSAGEix-GLOBIOM and REMIND-MAgPIE spread their outputs in several energy vectors, with REMIND-MAgPIE showing larger shares for liquid biofuels, while MESSAGEix-GLOBIOM shows a growing importance on the production of hydrogen. AIM/CGE, COFFEE-TEA and MESSAGEix-GLOBIOM include traditional biomass in their projections of solids, while IMAGE and REMIND-MAgPIE only account for modern solid biofuels. In this context, the decreases in solid biofuels seen in the results from AIM/CGE and MESSAGEix-GLOBIOM are related to a decrease in the traditional uses of biomass in the future. IMAGE and COFFEE-TEA, on the other hand, see an increase in the production of modern solid biofuels. Overall, most models reach less than 100 EJ/year of bioenergy production in 2100, except for COFFEE-TEA, which is more optimistic, going up to almost 400 EJ/year in 2100.

According to Daioglou et al. (2020), intertemporal optimization[23] (e.g., COFFEE-TEA, MESSAGEix-GLOBIOM, REMIND-MAgPIE) models tend to trigger early investments due to their ability to anticipate barriers to innovative technologies ramp-up, while recursive-dynamic[24] (e.g., IMAGE, AIM/CGE) models find it harder to overcome such barriers. Furthermore, the availability of different technologies, the carbon price profiles and penalties on liquid fossil fuels, as well as the flexibility for technology substitution, such as non-biomass renewables for the decarbonization of the power sector, influence the allocation of biomass between the production of electricity, heat, liquid, gaseous and solid biofuels, as well as other technologies, such as biomass-based hydrogen.

Even though offering a consistent framework on a broader level, most IAMs do not fully incorporate local specificities, making use of stylized assumptions about resource costs and logistical constraints for large regions (Koberle et al., 2021, Daioglou et al., 2020). In this context, this study aims at contributing to literature by proposing in the next chapter the development of a new bioenergy modelling tool, that can be linked

[23] Intertemporal optimization models capture the behavior of the system over a given timeframe.

[24] Recursive-dynamic models capture the behavior of the system one time step at a time.

to IAMs, making use of the interactions between IAMs broader approach and the downscaling to the local context.

3. Methods

This chapter presents the methodological procedure followed by this study, which can be divided into two main steps: first the development of the Bioenergy and Land Optimization spatially Explicit Model (BLOEM), and second the application of the model to a case study of bioenergy targets, defined within broader climate mitigation scenarios for Brazil, coupled through soft-link with the Brazilian Land Use and Energy System (BLUES) model. The overview of the main steps in the methodological procedure is depicted in Figure 3.1.

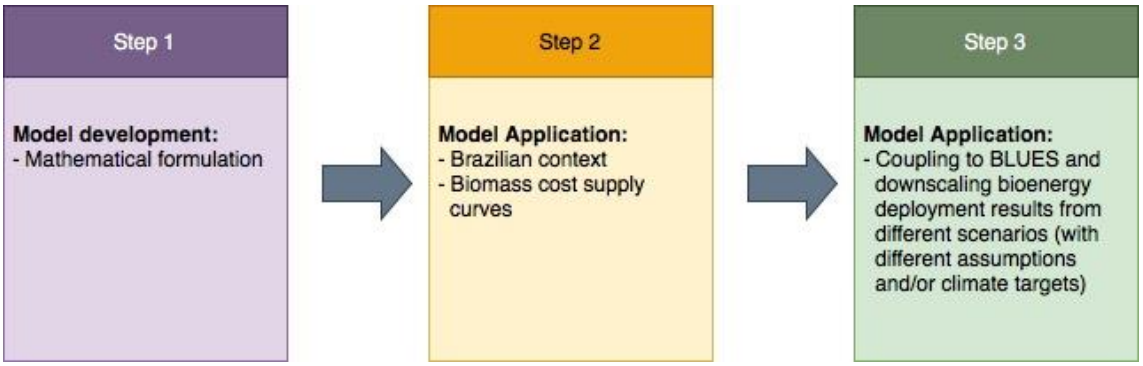

Figure 3.1. Main steps of this thesis methodology

The first section of this chapter describes and documents the development of BLOEM. It provides the structure and mathematical formulation of the model, with all equations and constraints, as well as a list of sets, parameters and variables applied. The second section describes the formulation of the case study and the adaptation of the model to the Brazilian context, including the spatial representation of the country and the collection of data on costs, capital investments, conversion efficiencies, land availability, and all other required parameters, as well as the scenario choices.

3.1 The Bioenergy and Land Optimization Spatially Explicit Model (BLOEM)

The Bioenergy and Land Optimization Spatially Explicit Model (BLOEM) is a perfect foresight, spatially explicit, least-cost optimization model. The model is formulated as a linear programming model, accounting for both total system's costs and GHG emissions, aiming at complying with a given bioenergy production target at minimum cost.

The model formulation can be applied to different regions, spatial resolutions and time frames, according to the availability of required data and computational effort. The model can be used for standalone runs, but it can also be coupled with different levels (global, regional, national) of integrated assessment models (IAMs), through soft-link[25]. The model was developed in the General Algebraic Modeling System (GAMS) modeling platform and is solved using the CPLEX Optimizer. Data preparation and results analysis can be conducted in R, Python, or other programming languages that communicate with GAMS.

3.1.1 Model Structure

BLOEM is a model developed to evaluate pathways for bioenergy deployment. Therefore, BLOEM is structured to:

- Given a bioenergy production target (aggregated or disaggregated across different types of bioenergy vectors);

- Subject to a set of constrains such as costs (production and conversion of biomass, transportation of feedstocks and products, among other costs), biomass yields, land availability, technologies available for the conversion of biomass into bioenergy vectors and logistics constraints;

- Determine what types of feedstocks to grow and where to grow them, which conversion technologies to deploy and where to locate the conversion facilities, indicating system expansion and retirement of capacities,

[25] When two models are soft-linked, they operate together, feedbacking each other in an iterative process. This approach takes advantage of the strength of both models, generally without affecting the structure of either of them (Krook-Riekkola et al., 2017). However, the soft-link requires a convergence rule to stop the iteration between models.

throughout the time frame, transportation and distribution of feedstocks and final products and, if the portfolio of conversion technologies includes carbon capture and storage, where to store the carbon captured, and value chain emissions;

- In order to minimize the total system cost.

An overview of the model's structure is depicted in Figure 3.2.

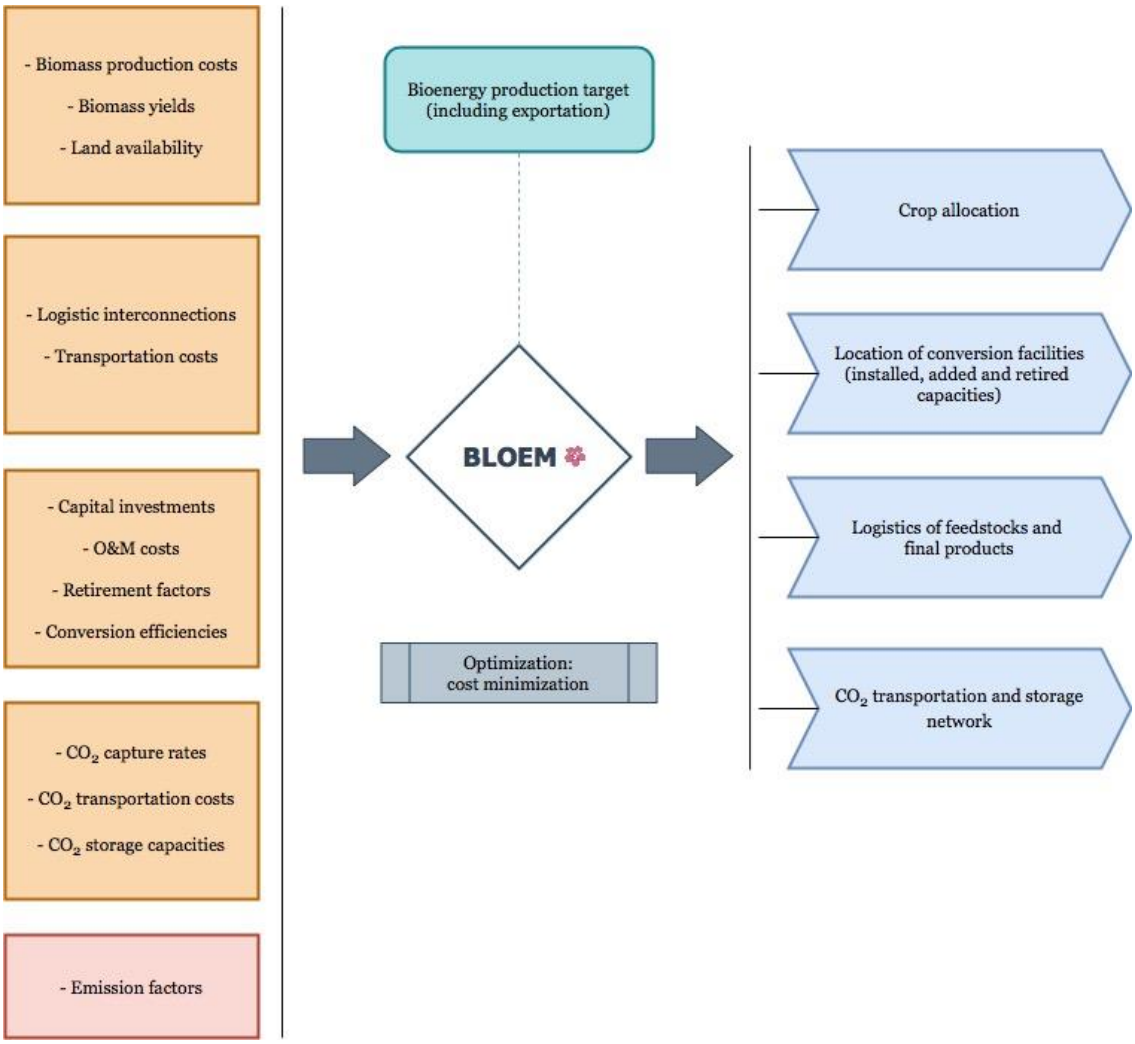

Figure 3.2. Overview of BLOEM's structure

3.1.2 Model Dimensions

3.1.2.1 Time

The time dimension is represented in one level, which can be months, years, decades, or any other level according to the modeler's preferences and objectives. Future developments are expected to include a second level to the time dimension, which would allow for the model to have, for example, a perspective on the seasonable aspects of biomass (accounting for years and seasons, or decades and seasons).

Each time step "t" is an element of the time set "T", so that $t \in T$.

3.1.2.2 Space

The space dimension is represented in one level: the region of interest can be divided into a number of grid cells of any given shape and size. Usually, this choice is guided by the availability of data on a grid perspective and the desired and/or required spatial resolution. All grid cells are geographically located (latitude and longitude dimensions).

Each grid cell "c" is an element of the space set "C", so that $c \in C$.

3.1.2.3 Resources

Resources include bioenergy crops (feedstocks), intermediate products, co-products and final products. Resources can be consumed or produced by a technology and can be transported from one grid cell to another. The user may choose the set of resources according to crop availability and suitability to the region being modeled, as well as the set of technologies available and bioenergy vectors production targets.

Each resource "r" is an element of the resource set "R", so that $r \in R$.

3.1.2.4 Technologies

Technologies are the processes used to convert input resources, such as bioenergy feedstocks and intermediate products, into output resources, such as intermediate products, co-products and final products. All technologies have their own sets of efficiencies, lifetime and retirement rates, overall costs (investments and operation and maintenance) and learning. The portfolio of technologies may vary across time and space.

Each technology "j" is an element of the technologies set "J", so that $j \in J$.

3.1.2.5 Land

Land encompasses different land cover types, according to the region being modeled. Land is space specific such that each grid cell may have fractions of different types of land. Accounting for different land cover types provides scenario specific amounts of land available for bioenergy production and of protected areas, where protected areas are a subset of land.

Each land type "l" is an element of the land set "L", so that $l \in L$.

3.1.2.6 Period

The period dimension represents the projected period related to gradual land use change emissions, which accounts for the differences in carbon stocks between natural vegetation and the growth of energy crops. The projected period is a modeler's choice and depends on the premises and the selected time horizon. For instance, IPCC (2006) uses a 20 years period for its GHG accounting guidelines, whereas Daioglou et al., (2017) chooses an 85 years period. The period dimension varies from q_1 to q_N, where "q_1" is the first and "q_N" is the last time step of the projected period "N".

Each period step "q" is an element of the period set "Q", so that $q \in Q$.

3.1.3 Mathematical Formulation

3.1.3.1 Sets, subsets, parameters and variables

- Sets and subsets

The main sets are time (T), space (C), resources (R), technologies (J), land (L), and period (Q).

All sets and subsets are listed in Table 3.1, below.

Table 3.1. Sets and subsets

Indices, sets and subsets	Description
$t \in T$	Time
$c \in C$	Space (grid cells)
$c \in C^S \in C$	Storage sites (grid cells) for CO_2 storage
$r \in R$	Resources
$r \in R^B \in R$	Bioenergy crops
$r \in R^I \in R$	Intermediate products
$r \in R^C \in R$	Co-products
$r \in R^P \in R$	Final products
$j \in J$	Technologies
$l \in L$	Land cover types
$l \in L^P \in L$	Protected areas (protected land cover types)
$q \in Q$	Period for accounting gradual land use change emissions

- Parameters

A list of all 42 parameters is provided in Annex II, Table AII.1. Units for each parameter can vary according to modeler's preferences (for example, units of costs could be in USD, EUR or any other currency).

- Variables

A list of all 35 variables is provided in Annex III, Table AIII.2. Similar to the parameters, units can be adapted according to modeler's preferences. Biomass consumption and the production of bioenergy, intermediate and co-products are measured in terms of energy per time. Units of capacity are measured in terms of input or output per time, where units of input and output are measured in energy basis.

3.1.3.2 Objective function

The objective function, to be minimized, accounts for the total system costs, as defined by Equation (1). It encompasses impacts of biomass production, biomass transportation, biomass conversion, final products transportation and distribution, CO_2 capture, transportation and storage, and GHG emissions.

$$Z = \sum_{t \in T} (I_t^{BP} + I_t^{BT} + I_t^{BC} + I_t^{ET} + I_t^{CC} + I_t^{TG}) \qquad \forall t \in T \quad (1)$$

Where Z represents the total system cost (to be minimized), in unit of costs; I_t^{BP} represents the impacts of biomass production in time "t"; I_t^{BT} represents the impacts of biomass transportation in time "t"; I_t^{BC} represents the impacts of biomass conversion in time "t"; I_t^{ET} represents the impacts of bioenergy transportation (logistics and distribution) in time "t"; I_t^{CC} represents the impacts of carbon transportation and storage in time "t"; and I_t^{TG} represents the impacts related to greenhouse gases emissions in time "t". All impacts are measured in units of costs.

3.1.3.3 Land availability

The amount of land available for bioenergy crops is an input to the model and can account for different constraints such as excluding protected land areas and factoring agriculture dedicated areas (in a food-first concept, for example), among others. Land availability is grid cell specific and can vary across time. The fraction of a grid cell that is dedicated to produce bioenergy crops (A_{rlct}) is constrained by the amount of land available for bioenergy crop growth ($LdAv_{lct}$), as defined by Equation (2).

$$\sum_{r \in R^B} A_{rlct} \leq LdAv_{lct} \qquad \forall r \in R^B, \forall l \in L, \forall c \in C, \forall t \in T \quad (2)$$

Where A_{rlct} represents the fraction of land cover type "l" in grid cell "c" dedicated to bioenergy crop "r" in time "t"; and $LdAv_{lct}$ represents the fraction of land cover type "l" in grid cell "c" available for bioenergy production in time "t".

3.1.3.4 Biomass production

The impact of biomass production in each time step, as seen in the objective function (I_t^{BP}) is given by Equation (3). The costs of production Co_{rct}^{BP} encompass farmgate costs, transportation costs for biomass collection within the grid cell radius, and land rent. If a carbon tax (k_t^*) is applied, total biomass production costs also incorporate the costs relative to direct land use change emissions[26], for the conversion of natural lands (e.g., forests) into bioenergy crop lands.

$$I_t^{BP} = df_t * \sum_{r \in R^B} \sum_{l \in L} \sum_{c \in C} (Co_{rct}^{BP} + k_t^* * ef_{rlc}) * B_{rlct}$$

$$\forall r \in R^B, \forall l \in L, \forall c \in C, \forall t \in T \quad (3)$$

Where I_t^{BP} represents the impact of biomass production in time "t", in unit of costs; df_t is the discount factor that brings impacts in each time step back to base time "t_1"; Co_{rct}^{BP} represents the cost of production related to bioenergy crop "r" in grid cell "c" in time "t", in unit of cost per unit of output; k_t^* represents the carbon price in time "t", in unit of costs per unit of CO_2 emission; ef_{rlc} represents the emission factor for direct land use change for crop "r" in land cover type "l" in grid cell "c", in unit of CO_2 emission per unit of output; and B_{rlct} represents the production of bioenergy crop "r" in land cover type "l" in grid cell "c" in time "t", in unit of output.

Land use change emission factors are crop, land cover type and grid cell specific. They are calculated as the difference in carbon stocks between the natural vegetation and its substitution for energy crops, accounting for instantaneous emissions. Instantaneous emissions are emissions due to land clearing, in the first time period.

[26] Indirect land use change emissions are currently not accounted for, given that the model only deals with bioenergy crops and does not include other crops, such as food crops, and does not deal with the dynamics of competition for land from, for example, land-based mitigation strategies (e.g., reforestation and afforestation).

Instantaneous land use change emissions are estimated[27] as follows:

$$Glc_t^i = \sum_{r \in R^B} \sum_{l \in L^P} \sum_{c \in C} ef_{rlc}^i * \left(A_{rlct} - A_{rlc,t-1}\big|_{\Delta>0}\right) * Ga_c$$

$$\forall r \in R^B, \forall l \in L^P, \forall c \in C, \forall t \in T \quad (4)$$

Where Glc_t^i represents direct instantaneous land use change emissions in time "t", in unit of CO_2emission; ef_{rlc}^i represents the emission factor for direct instantaneous land use change for crop "r" in land cover type "l" in grid cell "c", in unit of CO_2 emission per unit of area; A_{rlct} represents the fraction of land type "l" in grid cell "c" converted to the production of crop "r" in time "t"; $A_{rlc,t-1}$ represents the fraction of land type "l" in grid cell "c" converted to the production of crop "r" in the previous time step "t-1"; and Ga_c represents the area of grid cell "c", in unit of area. This calculation only applies if the difference in dedicated are to bioenergy is greater than zero ($\Delta > 0$). If bioenergy production is abandoned in a grid cell ($\Delta < 0$), no emissions are accounted for. The same applies to the gradual land use change emissions below.

We also estimate gradual land use change emissions, which account for differences in carbon stocks between natural vegetation and energy crops, for a projected period. For gradual land use change emissions, emissions are spread in a pre-defined projected period, "N" (from "q_1" to "q_N"). They are estimated as follows:

$$Glc^g = \sum_{r \in R^B} \sum_{l \in L^P} \sum_{c \in C} \left(\sum_{q_1}^{q_N} ef_{rlcq}^g \right) * \left(A_{rlct} - A_{rlc,t-1}\big|_{\Delta>0}\right) * Ga_c$$

$$\forall r \in R^B, \forall l \in L^P, \forall c \in C, \forall t \in T \quad (5)$$

[27] Direct land use change emissions (both instantaneous and gradual) are estimated post-optimization, to avoid complex operations within the optimization part of the model, which would result in losses of performance and exceed computational efforts and requirements. This does not significantly affect the model's results, since the extra costs related to direct land use change emissions are already incorporated into the costs of biomass production, following Equation 3.

Where Glc^g represents direct gradual land use change emissions, in unit of CO_2 emission; ef^g_{rlcq} represents the emission factor for direct gradual land use change for crop "r" in land cover type "l" in grid cell "c" in time "t", in unit of CO_2 emission per unit of area; A_{rlct} represents the fraction of land type "l" in grid cell "c" converted to the production of crop "r" in time "t"; $A_{rlc,t-1}$ represents the fraction of land type "l" in grid cell "c" converted to the production of crop "r" in the previous time step "t-1"; and Ga_c represents the area of grid cell "c", in unit of area. The term "q_N" represents the last time step of the projected period "N".

Biomass production (B_{rlct}) is constrained by the amount of land dedicated to crop growth and crop yields, as defined by Equation (6).

$$B_{rlct} \leq Ga_c * A_{rlct} * Y_{rct} \qquad \forall r \in R^B, \forall c \in C, \forall t \in T \quad (6)$$

Where B_{rlct} represents the production of bioenergy crop "r" in land cover type "l" in grid cell "c" in time "t", in unit of output; Ga_c represents the area of grid cell "c", in unit of area; A_{rlct} represents the fraction of land cover type "l" in grid cell "c" dedicated to bioenergy crop "r" in time "t"; and Y_{rct} represents crop yields for bioenergy crop "r" in grid cell "c" in time "t", in unit of output per area.

3.1.4 Biomass conversion

The impact of biomass conversion in each time step, as seen in the objective function (I_t^{BC}) encompasses total investments and O&M costs, as given by Equation (7).

$$I_t^{BC} = I_t^{TCI} + I_t^{TOM} \qquad \forall t \in T \quad (7)$$

Where I_t^{BC} represents the impact of biomass conversion in time "t", in unit of costs; I_t^{TCI} represents the impact of capital investments in time "t", in unit of costs; and I_t^{TOM} represents the impact of operation and maintenance costs in time "t", in unit of costs.

Total capital investments account for equipment purchase, construction, installation and contingency costs, representing the impacts associated with building new capacities of a given technology, as defined in Equation (8).

$$I_t^{TCI} = df_t * \sum_{j \in J} \sum_{c \in C} w_j * TCI_{jct} * CA_{jct} \qquad \forall j \in J, \forall c \in C, \forall t \in T \quad (8)$$

Where I_t^{TCI} represents the impact of capital investments in time "t", in unit of costs; df_t is the discount factor that brings impacts in each time step back to base time "t_1"; w_j is the technology discount factor related to technology "j"; TCI_{jct} represents the total capital investment in technology "j" in grid cell "c" in time "t", in unit of cost per unit of capacity; and CA_{jct} represents the capacity added of technology "j" in grid cell "c" in time "t", in unit of capacity.

The technology discount factor spreads capital investment according to the lifetime of the plant, according to Equation (9).

$$w_j = \frac{v * (1+v)^{lfj}}{(1+v)^{lj} + 1} * \sum_{p=1}^{l_j} (1+v)^{-(p-1)} \qquad \forall j \in J \ (9)$$

Where w_j is the technology discount factor related to technology "j"; *v* is the discount rate; lf_j represents the lifetime of the plant for technology "j", in years; and *p* represents the period, varying from 1 to lf_j.

Operation and maintenance impacts encompass fixed and variable costs and are related to the installed capacities as defined in Equation (10).

$$I_t^{TOM} = dd_t * \sum_{j \in J} \sum_{c \in C} \left(FOM_{jct} * CJ_{jct} + VOM_{jct} * CP_{jct} \right)$$

$$\forall j \in J, \forall c \in C, \forall t \in T \quad (10)$$

Where I_t^{TOM} represents the impact of operation and maintenance costs in time "t", in unit of costs; dd_t is the discount factor that brings impacts in each time step back to base time "t_1"; FOM_{jct} represents the fixed operation and maintenance costs related to technology "j" in grid cell "c" in time "t", in unit of cost per unit of capacity; CJ_{jct} represents the installed capacities of technology "j" in grid cell "c" in time "t", in unit of capacity; VOM_{jct} represents the variable operation and maintenance costs related to

technology “j” in grid cell “c” in time “t”, in unit of cost per unit of capacity per time; and CP_{jct} represents the rate of operation of technology “j” in grid cell “c” in time “t”; in unit of capacity.

The installed capacities in each grid cell in each time step vary according to the dynamics between existing, added and retired capacities, as defined by the balance provided in Equation (11).

$$CJ_{jct} = CE_{jct} + CJ_{jc,t-1} + CA_{jct} - CR_{jct} \qquad \forall j \in J, \forall c \in C, \forall t \in T \quad (11)$$

Where CJ_{jct} represents the installed capacities of technology “j” in grid cell “c” in time “t”, in unit of capacity; CE_{jct} represents the existing capacity of technology “j” in grid cell “c” in “t_1”, in unit of capacity; $CJ_{jc,t-1}$ represents the installed capacity of technology “j” in grid cell “c” in the previous time step “t-1”, in unit of capacity; CA_{jct} represents the capacity added of technology “j” in grid cell “c” in time “t”, in unit of capacity; and CR_{jct} represents the retirement of capacities of technology “j” in grid cell “c” in time “t”; in unit of capacity.

The retirement of capacities includes the retirement of existing capacities (CRE_{jct}), i.e., capacities already in place in time step t_1 (CE_{jct}), and the retirement of capacities added by the optimization (CA_{jct}).

$$CR_{jct} = CRE_{jct} + \sum_{t' \in T} CA_{jct'} * rf_{jt't} \qquad \forall j \in J, \forall c \in C, \forall t, t' \in T \quad (12)$$

Where CR_{jct} represents the retirement of capacities of technology “j” in grid cell “c” in time “t”; in unit of capacity; CRE_{jct} represents the retirement of existing capacities of technology “j” in grid cell “c” in time “t”, in unit of capacity; $CA_{jct'}$ represents the capacities added of technology “j” in grid cell “c” in time “t`”, in unit of capacity; and $rf_{jt't}$ represents the retirement factor of technology “j” installed in time “t`” and retired in time “t”.

The rate of operation of each technology (CP_{jct}) is constrained by the installed capacity (CJ_{jct}) and the respective availability, or capacity factor (cf_{jt}), as defined in Equation (13).

$$CP_{jct} \leq CJ_{jct} * cf_{jt} \qquad \forall j \in J, \forall c \in C, \forall t \in T \quad (13)$$

Where CP_{jct} represents the rate of operation of technology "j" in grid cell "c" in time "t"; in unit of capacity; CJ_{jct} represents the installed capacities of technology "j" in grid cell "c" in time "t", in unit of capacity; and cf_{jt} is the capacity factor, from 0 to 1.

The production[28] of a given bioenergy product $r \in R^P$ is given by Equation (14).

$$E_{rct} = \sum_{j \in J} CP_{jct} * \beta_{rj} \qquad r \in R^P, \forall j \in J, \forall c \in C, \forall t \in T \quad (14)$$

Where E_{rct} represents the production of bioenergy product "r" in grid cell "c" in time "t"; in unit of output per time; CP_{jct} represents the rate of operation of technology "j" in grid cell "c" in time "t", in unit of capacity; and β_{rj} represents the ratio of production of bioenergy product "r" by technology "j". If a resource is being produced by a given technology (e.g., bioenergy products, co-products and intermediates), β_{rj} represents the ratio of production, and therefore $\beta_{rj} > 0$. If a resource is being consumed by a given technology (e.g., bioenergy crops), β_{rj} represents the ratio of consumption, and therefore $\beta_{rj} < 0$.

The production of a given intermediate product $r \in R^I$ is given by Equation (15).

$$I_{rct} = \sum_{j \in J} CP_{jct} * \beta_{rj} \qquad r \in R^I, \forall j \in J, \forall c \in C, \forall t \in T \quad (15)$$

[28] The calculations for the production final products, co-products and intermediates, as well as for the consumption of feedstocks are mathematically similar. They are modelled separately simply to make the results more transparent and easier to read, as well as faster to check after each run.

Where I_{rct} represents the production of intermediate "r" in grid cell "c" in time "t", in unit of output per time; CP_{jct} represents the rate of operation of technology "j" in grid cell "c" in time "t", in unit of capacity; and β_{rj} represents the ratio of production of intermediate "r" by technology "j".

The production of a co-product $r \in R^S$ is given by Equation (16).

$$S_{rct} = \sum_{j \in J} CP_{jct} * \beta_{rj} \qquad r \in R^C, \forall j \in J, \forall c \in C, \forall t \in T \quad (16)$$

Where S_{rct} represents the production of co-product "r" in grid cell "c" in time "t", in unit of output per time; CP_{jct} represents the rate of operation of technology "j" in grid cell "c" in time "t", in unit of capacity; and β_{rj} represents the ratio of production of co-product "r" by technology "j".

The consumption of bioenergy crops $r \in R^B$ is given by Equation (17).

$$HB_{rct} = \sum_{j \in J} CP_{jct} * \beta_{rj} \qquad r \in R^B, \forall j \in J, \forall c \in C, \forall t \in T \quad (17)$$

Where HB_{rct} represents the consumption of bioenergy crop "r" in grid cell "c" in time "t"; in unit of input per time; CP_{jct} represents the rate of operation of technology "j" in grid cell "c" in time "t", in unit of capacity; and β_{rj} represents the ratio of consumption of bioenergy crop "r" by technology "j".

3.1.5 Biomass transportation

Biomass can be transported from one grid cell to another, depending on the location of the conversion facilities. The logistics interconnections for biomass transportation can be constrained by a maximum distance (MaxX), from the centroid of the grid cell where the crop is being grown, to the centroid of the grid cell where the conversion facility is located. For that purpose, a flag can be set to turn off the transportation of biomass between grid cells more than a maximum distance apart, as presented in Equations 18 and 19.

The flows of bioenergy crops between grid cells are modelled according to the resource balance given by Equation (18), in which the consumption of bioenergy crops in a given grid cell (H_{rct}) accounts for crop growth in the grid cell (B_{rct}) and flows into and out of the grid cell.

$$B_{rct} + FlagBT_{c'c} * \sum_{c' \in C} Bn_{rc'ct} + HB_{rct} = FlagBT_{cc'} * \sum_{c' \in C} Bn_{rcc't}$$

$$\forall r \in R^B, \forall c \in C, \forall t \in T \quad (18)$$

Where:

$$FlagBT_{cc'} = \begin{cases} 0, & MX_{cc'} > MaxX \\ 1, & MX_{cc'} \leq MaxX \end{cases} \qquad \forall c, c' \in C$$

And B_{rct} represents the production of bioenergy crop "r" in grid cell "c" in time "t", in unit of output; $Bn_{rc'ct}$ represents the flow of bioenergy crop "r" from grid cell "c`" to grid cell "c" in time "t" (the flow of bioenergy crop "r" into grid cell "c"), in unit of output, e.g., GJ; $HB_{rct}$ represents the consumption of bioenergy crop "r" in grid cell "c", in unit of output; $Bn_{rcc`t}$ represents the flow of bioenergy crop "r" from grid cell "c" to grid cell "c`" in time "t" (the flow of bioenergy crop "r" out of grid cell "c"), in unit of output; $MX_{cc'}$ represents the distance between grid cells "c" and "c`", in unit of distance; and MaxX represents the maximum distance to connect two grid cells, in unit of distance.

The impact of biomass transportation across cells is given by Equation (19). It accounts for transportation costs, the distance between grid cells (corrected by a tortuosity factor) and the amount of biomass being transported.

$$I_t^{BT} = df_t * \sum_{r \in R^C} \sum_{c,c' \in C} TrCo_r * MX_{cc'} * \tau_c * Bn_{rcc't}$$

$$\forall r \in R^B, \forall c \in C, \forall t \in T \quad (19)$$

Where I_t^{BT} represents the impacts of biomass transportation in time "t", in unit of costs; df_t is the discount factor that brings impacts in each time step back to base time

"t_1"; $TrCo_r$ represents the costs of transportation for bioenergy crop "r", in unit of cost per unit of output per unit of distance; $MX_{cc'}$ represents the distance between grid cells "c" and "c`", in unit of distance; $\tau_c$ is the tortuosity factor associated with grid cell "c"; and $Bn_{rcc't}$ represents the flow of bioenergy crop "r" from grid cell "c" to grid cell "c`" in time "t", in unit of output.

3.1.6 Bioenergy transportation

Similar to the flows of bioenergy crops, bioenergy logistics accounts for the flows of bioenergy products from the conversion facilities to geographically explicit local demands. For the logistics of distribution of final products (liquid biofuels) no constraints on grid cell interconnections were added, so that grid cells can communicate with each other regardless of the distance between them.

$$E_{rct} + \sum_{c' \in C} En_{rc'ct} = HE_{rct} + \sum_{c' \in C} En_{rcc't} \qquad \forall r \in R^P, \forall c \in C, \forall t \in T \quad (20)$$

Where E_{rct} represents the production of bioenergy product "r" in grid cell "c" in time "t"; in unit of output per time; $En_{c'ct}$ represents the flow of bioenergy product "r" from grid cell "c`" to grid cell "c" in time "t" (the flow of bioenergy product "r" into grid cell "c"), in unit of output per time; $En_{cc't}$ represents the flow of bioenergy product "r" from grid cell "c" to grid cell "c`" (the flow of bioenergy product "r" out of grid cell "c"), in unit of output per time; and HE_{rct} represents the amount of bioenergy product "r" consumed in grid cell "c" in time "t", in unit of output per time.

The impact of bioenergy transportation across cells is given by Equation (21). Similar to the impact of biomass transportation, it accounts for transportation costs, the corrected distance between grid cells, and the products being transported.

$$I_t^{ET} = df_t * \sum_{r \in R^P} \sum_{c,c' \in C} TrCo_r * MX_{cc'} * \tau_c * BEn_{rcc't}$$

$$\forall r \in R^P, \forall c \in C, \forall t \in T \quad (21)$$

Where I_t^{BT} represents the impacts of biomass transportation in time "t", in e.g., US$; df_t is the discount factor that brings impacts in each time step back to base time

"t_1"; $TrCo_r$ represents the costs of transportation for bioenergy product "r", in unit of cost per unit of output per unit of distance ; $MX_{cc'}$ represents the distance between grid cells "c" and "c`", in unit of distance; $\tau_c$ is the tortuosity factor associated with grid cell "c"; and $BEn_{rcc't}$ represents the flow of bioenergy product "r" from grid cell "c" to grid cell "c`" in time "t", in unit of output.

3.1.7 CO_2 capture, transportation and storage

For all technologies, CO_2 capture is given by Equation (22).

$$Vcap_{ct} = \sum_{j \in J} CP_{jct} * \gamma_j \qquad \forall j \in J, \forall c \in C, \forall t \in T \quad (22)$$

Where $Vcap_{ct}$ represents the amount of CO_2 captured in grid cell "c" in time "t", in t unit of CO_2 emission; CP_{jct} represents the rate of operation of technology "j" in grid cell "c" in time "t", in unit of capacity per time; and γ_j represents the level of CO_2 capture by technology "j", in unit of CO_2 emission per unit of output. If a given technology includes carbon capture, then $\gamma_j > 0$. Otherwise, $\gamma_j = 0$.

CO_2 logistics (transportation and storage dynamics) account for flows of CO_2 from the conversion facilities to the CO_2 storage sites, as shown in Equation 23.

$$Vcap_{ct} + \sum_{c' \in C} Vn_{c'ct} = Vseq_{ct}|_{c \in C^S} + \sum_{c' \in C} Vn_{cc't} \qquad \forall c \in C, \forall t \in T \quad (23)$$

Where $Vcap_{ct}$ represents the amount of CO_2 captured in grid cell "c" in time "t", in unit of CO_2 emission; $Vn_{c'ct}$ represents the flow of CO_2 from grid cell "c`" to grid cell "c" in time "t" (the flow of $CO_2$ into grid cell "c"), in unit of $CO_2$ emission; $Vn_{cc't}$ represents the flow of $CO_2$ from grid cell "c" to grid cell "c`" (the flow of CO_2 out of grid cell "c"), in unit of CO_2 emission; and $Vseq_{ct}$ represents the amount of CO_2 sequestrated in grid cell "c" in time "t", in unit of CO_2 emission.

CO_2 storage is constrained by the cumulative storage capacity of each selected storage site ($c \in C^S$), as seen in Equation 24.

$$\sum_{t \in T} Vseq_{ct} \leq MaxSt_c \qquad \forall c \in C^S, \forall t \in T \quad (24)$$

Where $\mathrm{Vseq_{ct}}$ represents the amount of CO_2 sequestrated in grid cell "c" in time "t", in unit of CO_2 emission; and $\mathrm{MaxSt_c}$ represents the cumulative storage capacity of grid cell "c", in unit of CO_2 emission.

The impact of carbon transportation across cells is given by Equation 25. It includes the costs of carbon transportation both onshore and offshore (if the storage site is an offshore site). The costs for offshore transportation of CO_2 take into account the extra transportation costs (by either pipelines or ships) for the CO_2 to be stored offshore, in e.g., depleted oil or gas fields.

$$I_t^{CC} = df_t * \left(\sum_{c,c' \in C} \sum_{t \in T} OnCo_{cc'} * Vn_{cc't} + \sum_{c \in C} OfCo_c * Vseq_{ct}|_{c \in C^S} \right)$$

$$\forall c \in C, \forall t \in T \quad (25)$$

Where $\mathrm{I_t^{CC}}$ represents the impacts of carbon transportation in time "t", in unit of costs; $\mathrm{df_t}$ is the discount factor that brings impacts in each time step back to base time "$\mathrm{t_1}$"; $\mathrm{OnCo_{cc'}}$ represents the onshore costs of carbon transportation between grid cells "c" and "c'", in unit of costs per unit of CO_2 emission; $\mathrm{Vn_{cc't}}$ represents the flow of CO_2 from grid cell "c" to grid cell "c`" in time "t", in unit of $CO_2$ emission; $\mathrm{OfCo_{cc'}}$ represents the offshore costs of carbon transportation between grid cells "c" and "c`", in in unit of costs per unit of CO_2 emission; and $\mathrm{Vseq_{ct}}$ represents the amount of CO_2 sequestrated in grid cell "c", in unit of CO_2 emission.

3.1.8 GHG emissions

GHG emissions are accounted for as follows: during bioenergy crops growth we include emissions from production, such as farming and fertilizer use; we include emissions related to logistics and transportation, both of biomass feedstocks and bioenergy carriers (e.g., biofuels); and we include negative emissions, from carbon sequestration. Emissions from direct land use change are already accounted for in the spread of biomass production costs (see Section 1.1.5, Equation 3), and therefore are not included here.

The impact of GHG emissions is calculated following Equation 26.

$$I_t^{TG} = k_t^* * GG_t \qquad \forall t \in T, \forall c \in C \quad (26)$$

Where I_t^{TG} represents the impacts related to greenhouse gases emissions in time "t", in unit of costs; k_t^* represents the carbon price in time "t", in unit of costs per equivalent of unit of CO_2 emissions; and GG_t represents gross emissions, in equivalent of unit of CO_2 emissions.

GHG emissions are calculated as follows:

$$GG_t = Gbp_t + Gfr_t + Gbt_t + Gbc_t + Get_t - \sum_{c \in C} Vseq_{ct} \qquad \forall t \in T \quad (27)$$

Where GG_t represents gross emissions, in equivalent of unit of CO_2 emissions; Gbp_t represents biomass production emissions, in equivalent of unit of CO_2 emissions; Gfr_t represents emissions from fertilizers, in equivalent of unit of CO_2 emissions; Gbt_t represents emissions from biomass transportation (from production sites to conversion facilities), in equivalent of unit of CO_2 emissions; Gbc_t represents emissions from the conversion process, in equivalent of unit of CO_2 emissions; Get_t represents emissions from bioenergy (e.g., biofuels) transportation, in equivalent of unit of CO_2 emissions; and $Vseq_{ct}$ represents the amount of CO_2 sequestrated in grid cell "c" in time "t", in equivalent of unit of CO_2 emissions.

Emissions from biomass production are calculated according to Equation 28.

$$Gbp_t = \sum_{r \in R^B} \sum_{l \in L} \sum_{c \in C} fp_r * B_{rlct} * fd \qquad \forall r \in R^B, \forall l \in L, \forall c \in C \quad (28)$$

Where Gbp_t represents biomass production emissions, in equivalent of unit of CO_2 emissions; fp_r represents fuel consumption for biomass production per crop "r", in volume per equivalent of unit of output; B_{rlct} represents the production of bioenergy crop "r" in grid cell "c" in time "t", in unit of output; and fd represents the emission factor of fuel, in equivalent of unit of CO_2 emissions per volume.

Emissions from fertilizer use are calculated according to Equation 29.

$$Gfr_t = \sum_{r \in R^B} \sum_{l \in L} \sum_{c \in C} ff_{rc} * A_{rlct} * Ga_c * nf \qquad \forall r \in R^B, \forall l \in L, \forall c \in C \quad (29)$$

Where Gfr_t represents emissions from fertilizer use for biomass production, in equivalent of unit of CO_2 emissions; ff_{rc} represents the emission factor for fertilizer use per crop "r" in grid cell "c", in unit of N_2O emissions per unit of area; A_{rlct} represents the fraction of land cover type "l" in grid cell "c" dedicated to bioenergy crop "r" in time "t"; and nf represents the conversion factor to unit of CO_2eq.

Emissions from biomass transportation are calculated according to Equation 30.

$$Gbt_t = \sum_{r \in R^B} \sum_{c,c' \in C} ft_r * MX_{cc'} * \tau_c * Bn_{rcc't} \qquad \forall r \in R^B, \forall c \in C \quad (30)$$

Where Gbt_t represents biomass transportation emissions, in equivalent of unit of CO_2 emissions; ft_r represents the emission factors for biomass transportation per crop "r", in equivalent of unit of CO_2 emissions per unit of output per unit of distance; $MX_{cc'}$ represents the distance between grid cells "c" and "c`", in unit of distance; $\tau_c$ is the tortuosity factor associated with grid cell "c"; and $Bn_{rcc't}$ represents the flow of bioenergy crop "r" from grid cell "c" to grid cell "c`" in time "t", in unit of output.

Emissions from biomass conversion are calculated according to Equation 31.

$$Gbc_t = \sum_{r \in R^P} \sum_{c \in C} \sum_{j \in J} fc_{rj} * CP_{jct} * \beta_{rj} \qquad \forall r \in R^P, \forall c \in C, \forall j \in J \quad (31)$$

Where Gbc_t represents biomass conversion emissions, in unit of CO_2eq; fc_{rj} represents the emission factor for biomass conversion per bioenergy product "r" per technology "j", in unit of CO_2eq per unit of output; CP_{jct} represents the rate of operation of technology "j" in grid cell "c" in time "t", in unit of capacity; and β_{rj} represents the ratio of production of bioenergy product "r" by technology "j".

Emissions from final products transportation are calculated according to Equation 32.

$$Get_t = \sum_{r \in R^P} \sum_{c,c' \in C} fw_r * MX_{cc'} * \tau_c * BEn_{rcc't} \qquad \forall r \in R^P, \forall l \in L, \forall c \in C \quad (32)$$

Where Get_t represents final products transportation emissions, in unit of CO_2eq; fw_r represents the emission factors for final products transportation per product "r", in unit of CO_2eq per unit of output; $MX_{cc'}$ represents the distance between grid cells "c" and "c`", in unit of distance; $\tau_c$ is the tortuosity factor associated with grid cell "c"; and $BEn_{rcc't}$ represents the flow of bioenergy product "r" from grid cell "c" to grid cell "c`" in time "t", in unit of output.

3.1.9 Bioenergy production targets

Bioenergy production targets include local demands and export targets, if applicable, and are determined as follows.

$$Pb_{rct} + Ex_{rct} \leq HE_{rct} \qquad \forall r \in R^P, \forall c \in C, \forall t \in T \quad (33)$$

Where Pb_{rct} represents the production target for bioenergy product "r" in grid cell "c" in time "t"; in unit of output per time; Ex_{rct} represents the export target for bioenergy product "r" in grid cell "c" in time "t"; in unit of output per time; and HE_{rct} represents the amount of bioenergy product "r" consumed in grid cell "c" in time "t", in unit of output per time.

3.2 Model Application: Case Study of Bioenergy in the Brazilian Energy Matrix

3.2.1 Spatial Resolution

For the purposes of this study, the model has been configured for Brazil. The Brazilian territory is divided into 2912 square grid cells. The spatial resolution was determined according to the IMAGE[29] (Integrated Model to Assess the Global Environment) spatial distribution (and data availability) in the 30 arcmin frame for the Brazilian region. The processing of data on a grid level was done in R[30]. The distances between each grid cell (in pairs) were determined based on the grid cells centroids using

[29] The IMAGE modelling framework is developed by the IMAGE team, under the authority of PBL Netherlands Environmental Assessment Agency, together with the University of Utrecht (UU). Brazil is one of the 26 regions in IMAGE.

[30] Data processing and results analysis can be done using R, Python, Julia, or other languages, according to the modeler's preferences.

the geographic information system software QGIS[31]. The spatial resolution is depicted in Figure 3.3.

Figure 3.3. Spatial resolution for Brazil, 30arcmin

[31] QGIS is an open-source Geographic Information System (GIS) software, licensed under the GNU General Public License. QGIS is an official project of the Open Source Geospatial Foundation (OSGeo) (QGIS).

3.2.2 Time Frame

The time frame was divided in decadal steps, from 2020 to 2050.

Model calibration had 2020 as base year, where the production matched current levels for sugarcane and oil crops, and their corresponding main products, namely ethanol (first generation) and biodiesel.

3.2.3 Resources

3.2.3.1 Bioenergy crops

A total of 5 different bioenergy crops was selected: sugarcane, oil crops, woody biomass, grassy biomass, and maize. Sugarcane, oil crops and woody biomass were selected based on recent results from BLUES and their corresponding portfolios, showing a significant participation of first and second-generation ethanol, biodiesel and cellulosic biofuels from woody biomass. Grassy biomass and maize were included only in the estimation of the cost supply curves, due to the expectations of further relevance of these crops for the region in the future (Daioglou et al., 2019). They were not included in the model runs for land allocation and bioenergy deployment, since they did not figure in the selected scenarios from BLUES 1.0.

3.2.3.2 Intermediate products

Intermediate products included sugarcane juice, which goes into the fermentation process to produce ethanol, and sugarcane bagasse, which can either be directed to bioelectricity production or to second-generation ethanol production. Syngas from the gasification of biomass is not included in the subset of intermediate products because the gasification process is coupled to the Fischer-Tropsch synthesis in one technology[32]. The same applies to the oils from oil crops crushing.

3.2.3.3 Final bioenergy products

The selected final products are ethanol (both first and second generation), biodiesel, green diesel, biojet, and bioelectricity. First generation ethanol, bioelectricity from bagasse and biodiesel are already vastly deployed in Brazil and are important to the

[32] This includes the cleaning of the raw syngas and its adjustment via WGS (water-gas shift) reactions.

country's energy mix (EPE, 2021a). Green diesel and biojet figure in many projected scenarios in different global and national IAMs results (Rochedo et al., 2018; Daioglou et al., 2020) and have a core participation in BLUES (Rochedo et al., 2018).

3.2.3.4 Co-products

Main co-products from the production of cellulosic biofuels are bio-naphtha and bioliquid petroleum gas, which can be used to produce biomaterials, such as ethylene, propylene and butadiene, and to compose the pool of petrol and LPG (liquefied petroleum gas) (Oliveira, 2020).

3.2.4 Technologies Portfolio

The term "technology" encompasses all conversion plants used to process either bioenergy crops or intermediate products, and produce intermediate products, final products and/or co-products. For the purposes of this study, the selected technologies portfolio is based on the BLUES model database and recent results, which can be found in further detail in Rochedo et al. (2018).

Capital investments and operation and maintenance costs, lifetime, efficiencies of conversion and rates of carbon capture, when applicable, were collected from the database in the BLUES model (Angelkorte, 2019; Rochedo et al., 2018; Tagomori et al., 2018). Data on existing capacities (location and installed capacities) for 2020 was collected from WEBMAP EPE (EPE, 2021b).

Figure 3.4 depicts the overview of the portfolio of technologies, while Table 3.2 and Table 3.3 present the main input data and parameters related to the technologies portfolio.

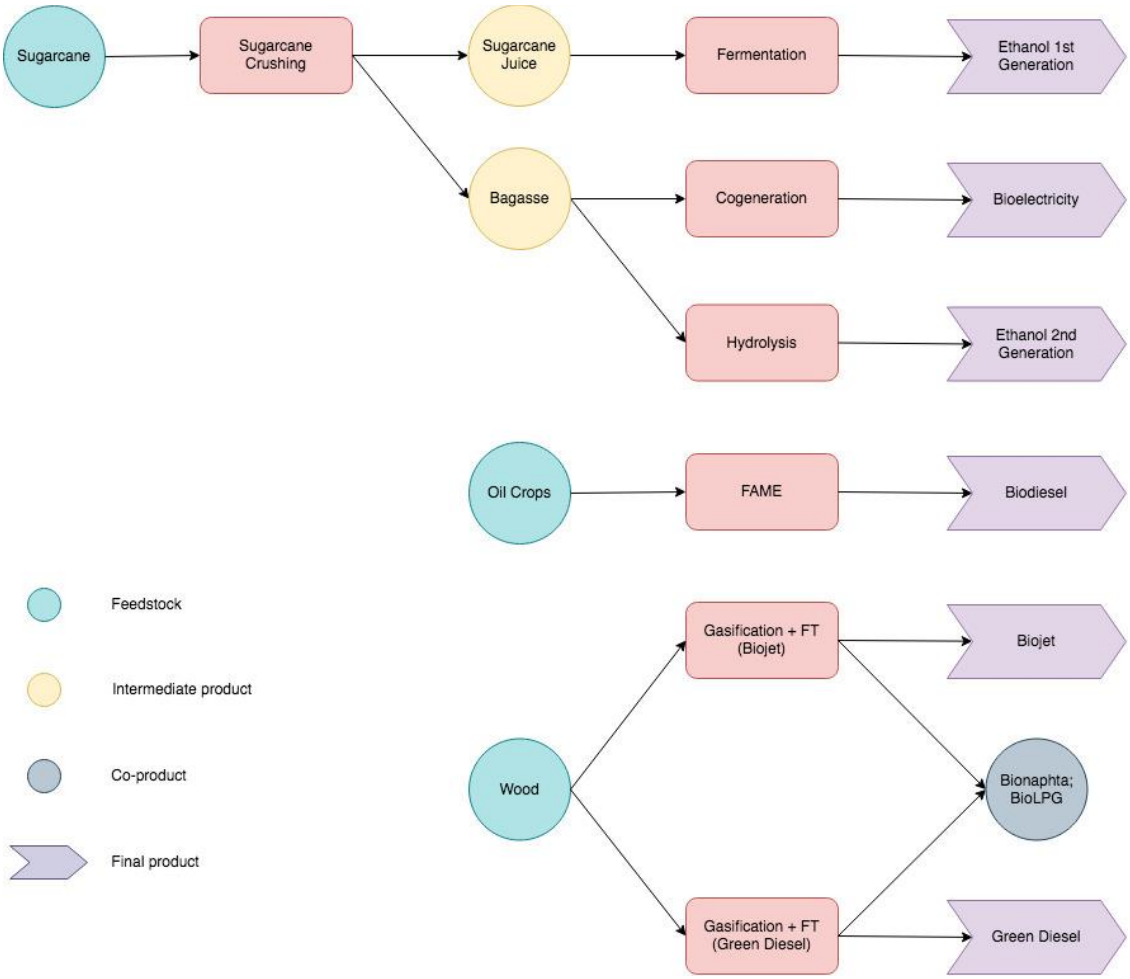

Figure 3.4.Portfolio of considered technologies[33]

[33] For this study, the portfolio of considered technologies is limited by the results from BLUES for the selected scenarios, which are presented in Section 3.3. Other technological routes (e.g., the production of green diesel or biojet via hydroprocessing of vegetable oils, or via oligomerization of alcohols) can be easily included in the portfolio in order to attend different scenarios outputs.

Table 3.2. Technologies parameters: investments, costs and lifetime

Technology	Tech Code	Capital Investment [US$/kW]	Fixed O&M [US$/kW]	Variable O&M [US$/kWy]	Lifetime of Plant [y]
Sugarcane Crushing	SGC	1	0	1	30
Ethanol 1G from Sugars Fermentation	E1G	647	10	0	30
Bagasse Cogeneration	COG	1,304	24	0	30
Ethanol 2G from Bagasse Hydrolysis	E2G	1,400	110	50	30
Biodiesel from Oil Crops Processing	BDS	21	8	78	20
Green Diesel from Gasification + FT	DFT	5,350	217	0	25
Biojet from Gasification + FT	BJT	5,528	223	0	25
Ethanol 1G from Sugars Fermentation + CCS	E1GC	650	11	0	30
Green Diesel from Gasification + FT + CCS	DFTC	5,420	220	0	25
Biojet from Gasification + FT + CCS	BJTC	5,600	227	0	25

Note: No learning rate was applied to the above costs, but the model has the possibility of reducing the costs over the years.

Table 3.3. Technologies parameters: conversion efficiencies and rate of CO_2 capture (if applicable)

Technology	Sugarcane	Oil Crops	Wood	Sugarcane Juice	Bagasse	Ethanol 1G	Ethanol 2G	Biodiesel	Green Diesel	Biojet	Electricity	Bionaphtha	Bio-LPG	CO_2
SGC [A]	-1	0	0	0.56	0.18	0	0	0	0	0	0	0	0	0
E1G [A]	0	0	0	-0.45	0	1	0	0	0	0	0	0	0	0
COG [A]	0	0	0	0	-1.15	0	0	0	0	0	1	0	0	0
E2G [A]	0	0	0	0	-2.70	0	1	0	0	0	0	0	0	0
BDS [A]	0	-2.44	0	0	0	0	0	1	0	0	0	0	0	0
DFT [A]	0	0	-3.16	0	0	0	0	0	1	0	0	0.40	0.35	0
BJT [A]	0	0	-3.26	0	0	0	0	0	0	1	0	0.36	0.36	0
E1GC [A,B]	0	0	0	-0.45	0	1	0	0	0	0	0	0	0	0.03
DFTC [A,B]	0	0	-3.16	0	0	0	0	0	1	0	0	0.40	0.35	0.30
BJTC [A,B]	0	0	-3.26	0	0	0	0	0	0	1	0	0.36	0.36	0.30

Notes: [A] Conversion efficiencies in GJ of product/GJ of input.

[B] Level of CO_2 capture in tCO_2/GJ of product.

3.2.5 Discount factor

The discount factor accounts for annual payments within a decade, and discounts them back to the first decade, 2020. In this study, we used a discount rate of 10% per year. The annual discount factor is determined according to Equation 34.

$$df_t^a = \left(\sum_{p=1}^{10}(1+v)^{-(p-1)}\right) * (1+v)^{-(t-t_1)} \qquad \forall t \in T \quad (34)$$

Where df_t^a is the discount factor that brings impacts in each time step back to base time "t_1"; v is the discount rate; p is the period, in this case, years within a decade; t is the time period, and t_1 is the base year (in this case, 2020).

For capital investments, where the payments happen in one year and therefore should not be discounted within the decade, the discount factor only bring investments back to present value, according to Equation 35.

$$df_t^b = (1+v)^{-(t-t_1)} \qquad \forall t \in T \quad (35)$$

Where df_t^b is the discount factor that brings impacts in each time step back to base time "t_1"; v is the discount rate; t is the time period, and t_1 is the base year.

3.2.6 Land Availability for Bioenergy in Brazil

The model accounts for six different types of land: forests, agricultural land, pastures, urban areas, other lands (including savannahs, grasslands and scrublands) and bioenergy land. The dynamics in land expansion, such as the expansion of agricultural areas, are estimated according to the projections from IMAGE-LPJmL[34] (Doelman et al., 2020). A food-first principle is applied, which means that food crops have priority in land

[34] LPJmL is the Lund-Potsdam-Jena managed Land model, developed and maintained by the Potsdam Institute for Climate Impact Research (PIK), built up from a Dynamic Global Vegetation Model (DGVM) to simulate the global terrestrial carbon cycle and the responses of carbon and vegetation patterns under climate change (PIK, 2021). It is incorporated by the IMAGE framework to implement the carbon, vegetation, land and water dynamics.

allocation over bioenergy crops. In order to comply with the food-first principle but also acknowledge that crops such as sugarcane and oil crops are already partly directed to bioenergy production, a factor of the projected agricultural land is directed towards bioenergy production. In order not to cause confusion with land for agriculture, we label this fraction of agricultural land "bioenergy land". This factor was estimated based on current sugarcane for ethanol production of 40-60%, as reported by the Brazilian Sugarcane Industry Association (UNICA) and indicated in biofuel consumption from the International Energy Agency (IEA), as well as on current oil crops for biodiesel production of 10%, as reported by the Brazilian National Petroleum Agency (ANP) and the Food and Agriculture Organization of the United Nations (FAO) oil crops production statistics (UNICA, 2020; IEA, 2020; ANP, 2020; FAO, 2018).

For the purposes of this case study, all forests, pastures, agricultural land and urban areas were considered not available for bioenergy crops. Only IMAGE projected bioenergy land and other land are deemed available for bioenergy crops. For other lands, a cap of 25% was applied to savannahs and 90% to scrublands and/or grasslands. In all cases no more than 75% of a given grid cell can be used for bioenergy crop growth (Daioglou et al., 2019). This is a restrictive assumption, stricter than the current national forest code, but the idea is to test if bioenergy projections can be met without negative impacts on forests and protected areas, as well as to understand the land pressures that they imply. Future studies should further investigate the forest code assumptions and their implications for bioenergy.

The resulting land availability maps are depicted in Annex IV, Figure AIV.1.

3.2.7 Biomass Yields and Potentials

Potential biomass yields at the grid level were obtained from IMAGE-LPJmL, which computes photosynthesis, maintenance and growth respiration. Actual yields were calculated by applying a management factor to potential yields. Such factors represent management and farmer behavior that in turn affect crop yields (Daioglou et al., 2019). All yields were brought to dry basis. For oil crops, a further calibration of the IMAGE yields on a grid level was applied using data from BLUES (regional level differences in yields). This was necessary to better represent the expected behavior for soybeans across different Brazilian regions, based on observed data.

Management factors per crop, per time step, and data on water content per crop can be found in Annex V, Table AV.1. Maps on yields for all crops in all time steps can be found in Annex VI, Figures AVI.1-5.

Biomass supply potentials for each crop individually were determined based on actual yields and land availability, as shown in Equation 34.

$$Po_{rct}^{BP} = Y_{rct} * Ga_c * \sum_{l \in L} LdAv_{lct} \qquad \forall r \in R^B, \forall l \in L, \forall c \in C, \forall t \in T \quad (34)$$

Where Po_{rct}^{BP} represents the supply potential for bioenergy crop "r" in grid cell "c" in time "t", in unit of output, e.g., GJ; Y_{rct} represents crop yields for crop "r" in grid cell "c" in time "t", in unit of output per area, e.g., GJ/km^2; Ga_c represents the area of grid cell "c", in unit of area, e.g., km^2; and $LdAv_{lct}$ represents the fraction of land cover type "l" in grid cell "c" available for bioenergy production in time "t".

3.2.8 Biomass Supply Costs

The supply costs for bioenergy crops include farm gate costs, land rent costs and costs for biomass collection (transportation within a given grid cell) and are determined as follows:

$$Co_{rct}^{BP} = \frac{(FCo_{rct} + LRt_{ct})}{Y_{rct}} + TpCo_r \qquad \forall r \in R^B, \forall c \in C, \forall t \in T \quad (35)$$

Where Co_{rct}^{BP} represents the supply costs for bioenergy crop "r" in grid cell "c" in time "t", in unit of cost per unit of output, e.g., US$/GJ; FCo_{rct} represents the farm gate costs for crop "r" in grid cell "c" in time "t", in unit of cost per area, e.g., US$/km^2; LRt_{rct} represents land rent costs in grid cell "c" in time "t", in unit of cost per area, e.g., US$/km^2; Y_{rct} represents crop yields for crop "r" in grid cell "c" in time "t", in unit of output per area, e.g., GJ/km^2; and $TpCo_r$ represents the costs for biomass collection within a grid cell, for crop "r", in unit of cost per unit of output, e.g., US$/GJ.

Farm gate costs at a regional level[35] were obtained from Angelkorte (2019). Costs for biomass collection within the grid cell were based on Tagomori et al. (2019) and adapted to the different types of feedstocks. Farm gate costs and costs for biomass collection are presented in Annex VII, Table AVII.1. Land rent costs at the grid level were obtained from Doelman et al. (2020). Maps on land rent costs for all time steps are presented in Annex VIII, Figure AVIII.1.

3.2.9 Biomass and Biofuels Transportation

To determine the logistics interconnections between grid cells for biomass transportation, a maximum distance of 300 km was used. As previously noted, no constraints on biofuels transportation were added.

The costs for biomass and biofuels transportation were determined based on Tagomori (2017) and Vera et al. (2020), adapting the load weight according to the feedstock or product being transported. Values are presented in Table 3.4.

Table 3.4. Transportation Costs

Load	Transportation Cost [US$/GJ/km]
Sugarcane	0.0066
Oil crops	0.0022
Wood	0.0032
Grass	0.0052
Maize	0.0023
Ethanol	0.0040
Biodiesel	0.0050
Biojet	0.0050
Green diesel	0.0050

Based on Tagomori (2017) and Vera et al. (2020)

[35] Brazilian regions: North (N), Northeast (NE), Center-West (CO), Southeast (SE) and South (S). See Annex I.

Tortuosity factors in a regional level were collected from Fajardy et al. (2018), which presents road tortuosity factors for several different Brazilian states. To aggregate them to a regional level, we have taken the highest factor in each region (Table 3.5).

Table 3.5. Tortuosity Factors

Region	Tortuosity Factor
North	2.5
Northeast	1.5
Center-West	1.5
Southeast	1.5
South	1.5

Based on Fajardy et al. (2018)

3.2.10 Storage Sites and Carbon Transportation and Storage Costs

For the purposes of this study, we have selected four potential storage sites. Three of the potential storage sites are mature oil and gas fields: 1 onshore and 2 offshore, for which the CO_2 captured would be used for enhanced oil recovery (EOR). The remaining storage capacity (fourth potential storage site) accounts for offshore oil and gas fields in the Southeast region, based on Rochedo (2016). The choice of storage sites was based on data availability and the required experience regarding the geological structure, physical properties, feasibility and safety of the potential sites. We have excluded saline aquifer options due to geological uncertainties and limited seismic data availability.

The maximum capacity of storage for all storage sites, onshore and offshore, where collected from Nogueira (2020), Oliveira et al. (2020) and Rochedo (2016). The costs of CO_2 onshore transportation via pipelines were based on da Silva et al. (2018). The costs of CO_2 offshore transportation were based on Nogueira (2020). For the offshore storage sites, we assume that the CO_2 is first transported via pipelines to the selected ports. Five ports were selected: Açu, Rio de Janeiro, Angra, Santos and Paranaguá. From there, the CO_2 is transported offshore, to be stored, either by pipelines or ships. This approach is based on the work developed by Nogueira (2020). The choice between pipelines and

ships takes into account the least costly option, depending on the distance between the port and the storage site.

The maximum storage capacity and offshore CO_2 transport costs for the offshore storage sites are presented in Table 3.6. The costs for onshore CO_2 transport are presented in Table 3.7. The maximum storage capacity for the onshore storage site is presented in Table 3.8.

Table 3.6. Offshore Storage Sites

Port	Destination	Distance [km]	Offshore CO_2 Transport Cost [US$/t$CO_2$]	Maximum Storage Capacity
Açu	Albacora	105	4.00	169.7 $MtCO_2$
Rio de Janeiro	Marimbá	270	9.20	23.0 $MtCO_2$
Angra	Marimbá	400	13.30	21.7 $MtCO_2$
Santos	Marimbá	600	19.50	19.8 $MtCO_2$
Santos	Other O&G fields	> 800	38.80	26.0 $GtCO_2$ [(A)]
Paranaguá	Marimbá	850	28.80	17.3 $MtCO_2$

[(A)] The remaining storage potential for offshore oil and gas fields in the Southeast region is based on Rochedo (2016), and the transport costs are estimated to be higher due to the absence of the EOR revenue.

Based on Nogueira (2020) and Rochedo (2016)

Table 3.7. Onshore CO_2 Transport Costs

	Distance [km]				
	< 150	**150 – 250**	**250 – 400**	**400 – 600**	**> 600**
Onshore CO_2 Transport Costs [US$/t$CO_2$]	18.60	48.60	94.00	120.00	176.40

Based on da Silva et al. (2018)

Table 3.8. Onshore Storage Site

Site	Maximum Storage Capacity [$MtCO_2$]
Água Grande	53.0

Based on Oliveira et al. (2020)

Figure 3.6 depicts the onshore storage site, the selected ports connected to the offshore storage sites, and the potential storage sites (mature oil and gas fields).

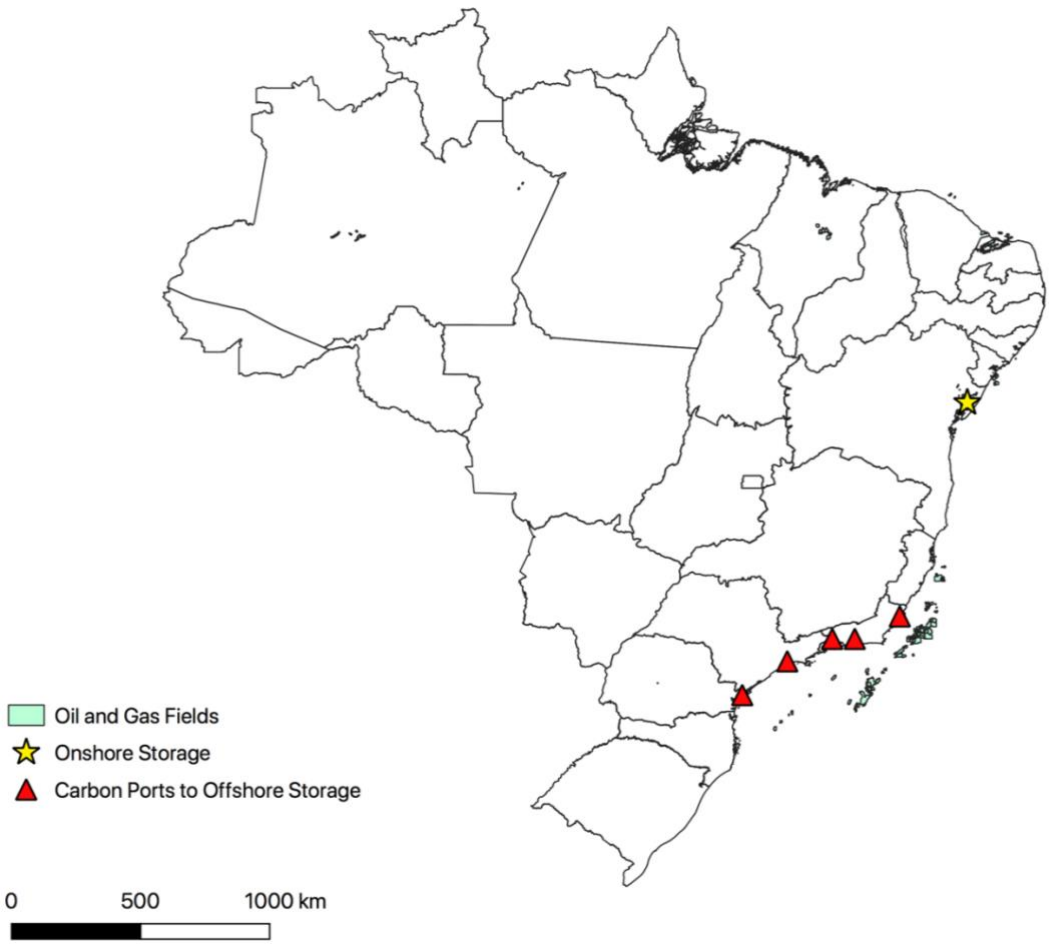

Figure 3.5. Onshore and offshore storage sites and carbon ports

3.2.11 Spatial Distribution of Demand for Bioenergy Products

In order to spatially distribute the demand for bioenergy products, data on population density from the Brazilian Institute of Geography and Statistics (IBGE, *Instituto Brasileiro de Geografia e Estatística*) was used (IBGE, 2020a). Municipalities under 300,000 inhabitants were excluded. The distribution according to population density was crossed and matched with data on states capitals locations, as well as the locations of fuels and biofuels distribution terminals (EPE, 2021b), as displayed in Figure 3.7.

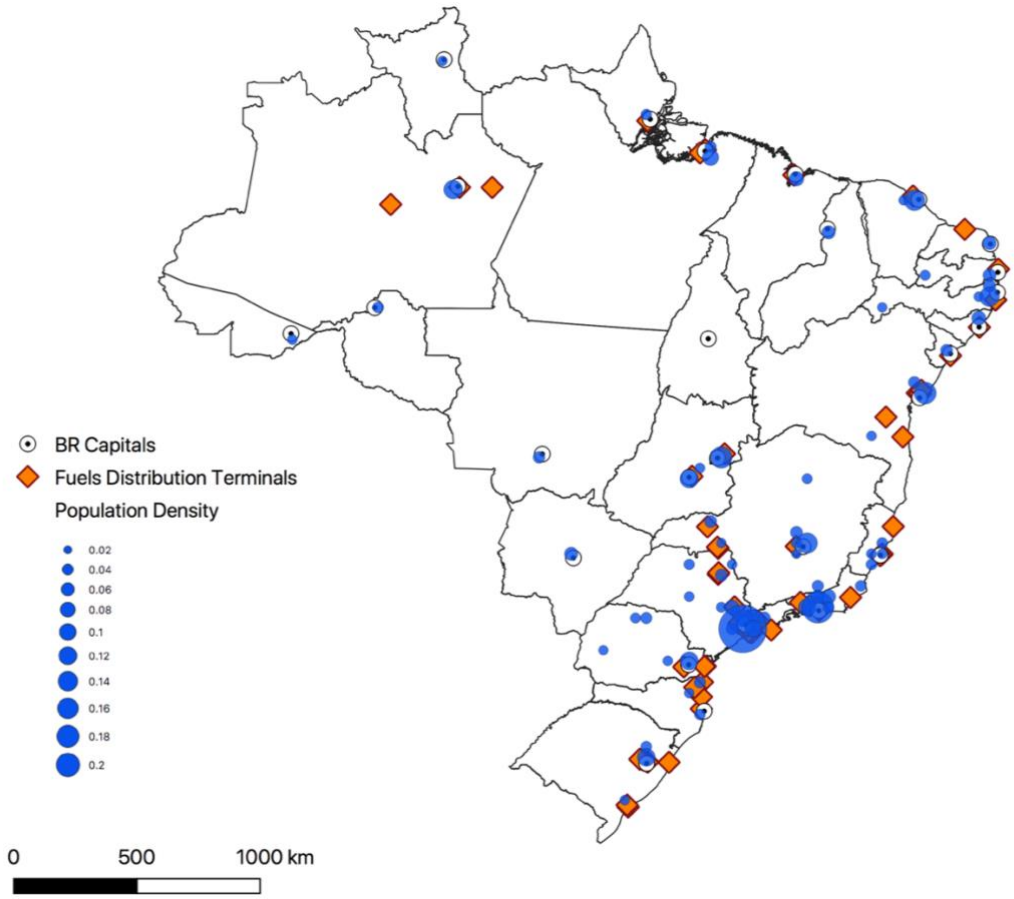

Figure 3.6. Population density and location of distribution terminals for fuels

The bioenergy targets are then spatially distributed, pondered by population density, as in Equation 38.

$$Pb_{rct} = PopDen_c * BioenergyProductionTarget_{rct}$$

$$\forall r \in R^P, \forall c \in C, \forall t \in T \quad (38)$$

Where $\mathrm{Pb_{rct}}$ represents the production target for bioenergy product "r" in grid cell "c" in time "t"; in unit of output per time; $\mathrm{PopDen_c}$ represents the population density in grid cell "c"; and $\mathrm{BioenergyProductionTarget_{rct}}$ represents the production target for bioenergy product "r" in grid cell "c" in time "t", in unit of output per time.

3.2.12 Emission Factors

3.2.12.1 Emissions factors for land use change

The emission factors for direct land use change, for instantaneous emissions, gradual emissions and both combined, on a grid level, were obtained from IMAGE, following the methodology proposed by Daioglou et al. (2017). An amortization period of 30 years was considered. Maps for the emission factors at a grid scale, as well as average instantaneous and gradual emission factors, can be found in Annex IX.

3.2.12.2 Emissions factors for biomass production

For biomass production, a factor of fuel consumption per crop was applied alongside the emission factor for the fuel itself (in this case, conventional diesel fuel). The factor of fuel consumption per crop was obtained from BLUES as proposed by Angelkorte (2019). The emission factor for conventional diesel fuel was obtained from the IPCC Guidelines for National Greenhouse Gases Inventories (IPCC, 2006). All factors used can be found in Table 3.9.

Table 3.9. Fuel consumption for biomass production

Crop	Fuel Consumption for Biomass Production (l-diesel/GJ-prim)
Sugarcane	0.2935
Oil Crops	7.2839
Wood	0.0566
Emission Factor for Fossil Diesel = 0.73 tCO_2/l-diesel	

Based on Angelkorte (2019)

3.2.12.3 Emissions factors for fertilizers

The emission factors related to the use of fertilizers, per crop and per region, were obtained from BLUES as proposed by Angelkorte (2019). Such emission factors refer only to use and do not include emissions related to the upstream production of fertilizers. All factors used can be found in Annex X, Table AX.1.

3.2.12.4 Emissions factors for biomass conversion

The emission factors for biomass conversion, per bioenergy product per technology, were obtained from the database on IMAGE (Daioglou et al., 2019) and are presented on Table 3.10.

Table 3.10. Emission factors for biomass conversion

Bioenergy Product	Conversion Technology	Emission Factor (fc_{rj}) [$kgCO_2eq/GJ$]
Ethanol second generation	E2G	0.7605
Biodiesel	BDS	0.0131
Note: For all other technologies not listed above $fc_{rj} = 0$.		

Based on Daioglou et al. (2019)

3.2.12.5 Emissions factors for biomass and biofuels transportation

The emission factors for biomass and biofuels transportation were determined based on Vera el al. (2020), combining data on fuel consumption, load weight and the emission factor related to the fuel in use (in this case, conventional diesel fuel). The resulting emission factors are presented in Table 3.11.

Table 3.11. Emission factors for biomass and biofuel transportation

Biomass/Biofuel	**Emission Factor** (eft_r or efw_r) **[kgCO$_2$/km/GJ]**	
Sugarcane	0.0040	$eft_{r=sugarcane}$
Oil crops	0.0022	$eft_{r=oilcrops}$
Wood	0.0032	$eft_{r=wood}$
Grass	0.0038	$eft_{r=grass}$
Maize	0.0040	$eft_{r=maize}$
Ethanol 1st generation	0.0021	$efw_{r=ethanol1stgen}$
Ethanol 2nd generation	0.0021	$efw_{r=ethanol2gen}$
Biodiesel	0.0016	$efw_{r=biodiesel}$
Green diesel	0.0014	$efw_{r=greendiesel}$
Biojet fuel	0.0014	$efw_{r=biojet}$

Based on Vera et al. (2020)

3.3 Scenarios Selection and IAMs Bioenergy Production Levels

3.3.1 Base Year

The base year was set at 2020. Current levels of production are estimated according to the Oil, Natural Gas and Biofuels Statistical Yearbook 2020, from the Brazilian National Petroleum Agency (ANP, 2020), and can be found in Table 3.12.

Table 3.12. Base year (2020) level of production for ethanol and biodiesel

Biofuel	Level of Production in 2020	
	10^3 m^3/year	PJ/year
Ethanol (1st generation)	35,307	830
Biodiesel	5,901	210

Based on ANP (2020)

3.3.2 Scenarios Selection

For the purposes of this study, we have chosen five different scenarios from BLUES 1.0: Current Policy (CurPol), NDC PLUS (NDC+), Good Practice Policies (GPP), National Policies -50% (NP-50) and National Policies -100% (NP-100). NDC+ and GPP are scenarios developed for COMMIT[36] (Climate Policy Assessment and Mitigation Modeling to Integrate National and Global Transition Pathways). CurPol, NP-50 and NP-100 (net zero) are scenarios developed for ENGAGE[37] (ENGAGE Feasibility of Climate Pathways). An overview of each scenario as well as the corresponding bioenergy production targets are presented in Figure 3.8.

CurPol is a scenario based on middle of the road socio-economic conditions and the second marker baseline scenario of the Shared Socioeconomic Pathways (SSP2), assuming policies currently ratified will be implemented. No carbon price profile is assigned to this scenario.

[36] COMMIT is a project developed by an international and multidisciplinary consortium of top research groups around the world, aiming at contributing to global stocktake, discussing national and global low-carbon pathways together with project partners and policymakers. COMMIT is funded by Directorate General Climate Action (DG CLIMA) and EuropeAid, under grant agreement No. 21020701/2017/770447/SER/CLIMA.C.1 EuropeAid/138417/DH/SER/MuliOC (COMMIT).

[37] ENGAGE is a project developed by an international and multidisciplinary consortium of top research groups around the world, aiming at designing cost-effective, technologically sound and socially and politically feasible pathways consistent with the Paris Agreement. ENGAGE is funded by the European Union's Horizon 2020 research and innovation programme, under grant agreement No. 821471 (ENGAGE).

NDC+ is a scenario based on the Brazilian Nationally Determined Contributions (NDC), assuming that it will be implemented by 2030, reflecting a continuation of such measures from 2030 on by extrapolating the equivalent carbon price in 2030, using the GDP growth rate up to 2050.

GPP is a scenario built upon current policies, which assumes that good practice policies proven effective in certain countries will be implemented worldwide until 2050. Timing and stringency of policies and targets are adjusted for low/medium income and high-income countries.

NP-50 (consistent with 2DG) and NP-100 (net zero) are stylized scenarios, following a cost-optimal trajectory to meet, respectively, 50% and 100% emission reductions by 2050.

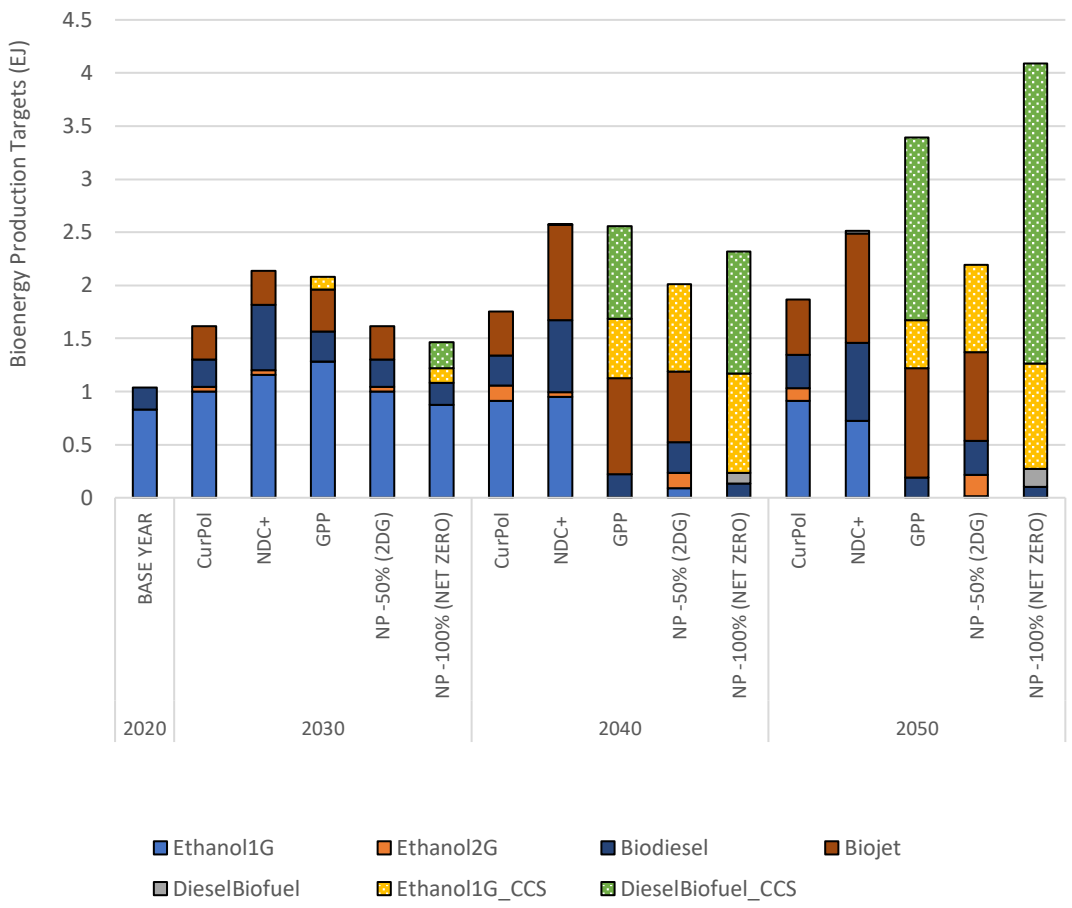

Figure 3.7. BLUES results for bioenergy production in Brazil, in different scenarios

Table 3.13 presents the carbon price trajectories considered for the scenarios that include such projections, namely NDC+, GPP, NP-50 and NP-100. CurPol is the only scenario without carbon price. None of the chosen scenarios includes export of bioenergy products, from Brazil.

Table 3.13. Carbon price trajectory

Scenario	Carbon Price [US$/t$CO_2$]			
	2020	**2030**	**2040**	**2050**
CurPol	0	0	0	0
NDC+	0	1	3	5
GPP	0	25	45	65
NP-50	0	18	40	53
NP-100	0	56	92	234

Note: For the CurPol, NDC+ and GPP scenarios, the carbon price trajectory is exogenous to the model (BLUES). For the NP-50 and NP-100 scenarios, the carbon price trajectory is endogenously estimated by BLUES.

Having the mathematical formulation ready and applied to the Brazilian context, soft-linking it to BLUES, the next chapter presents the results for the case study regarding the role of bioenergy in the Brazilian energy matrix, in the different scenarios outlined above.

4. Results: Case Study of Bioenergy in the Brazilian Energy System

This chapter presents the results of the case study focused on the Brazilian energy system. First, it goes through the results for biomass production costs and potentials, and the resulting biomass cost-supply curves. Then, it presents the results from the BLOEM runs.

4.1 Biomass Production Costs and Potentials

Production potentials and costs ranges for 2030 and 2050, for all five crops, are presented in Figure 4.1. Minimum costs represent the grid cell with the lowest cost and maximum costs represent the grid cell with the highest cost.

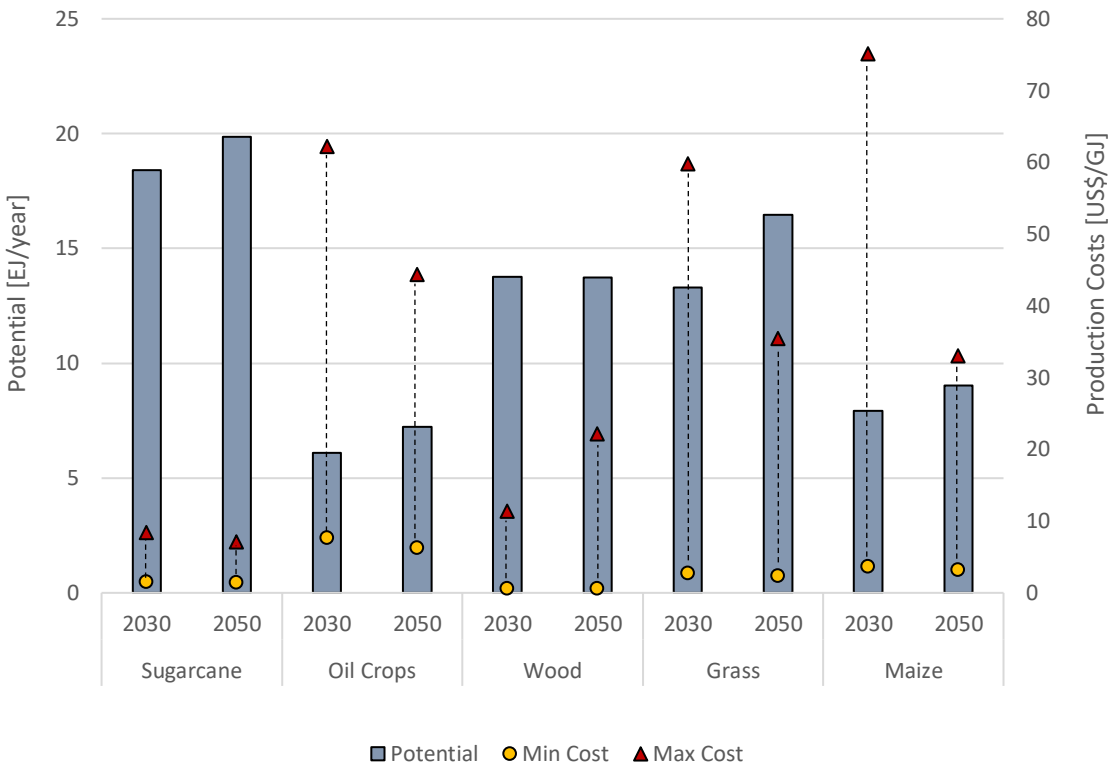

Figure 4.1. Production potentials and cost ranges for 2030 and 2050

Sugarcane production costs reach a maximum of approximately 8 US$/GJ in 2030. Oil crops production costs reach approximately 62 US$/GJ in 2030. Wood production costs reach around 22 US$/GJ by 2050. Grass production costs go up to 60 US$/GJ, while maize costs reach approximately 75 US$/GJ, in 2030. Sugarcane has the highest production potentials, reaching almost 20 EJ/year by 2050. Oil crops have the lowest production potentials, with less than 7 EJ/year by 2050. As land availability is the same for all individual crop cases, production potentials are a direct reflect of different yields per crop across time.

Figures 4.2-4.6 present production costs and potentials[38] for all crops, on a grid basis, in the period from 2030 to 2050. The results indicate that the highest costs are concentrated in the semi-arid region for all crops (driven by lower yields in the region), except for maize, where highest costs can be found in the South. Overall, the production costs reduce with time, except for wood, where highest production costs are achieved by 2050. This is due to the increasing improvements in yields expected for the coming decades.

Production potentials reach a maximum of approximately 60 PJ/year for sugarcane, 30 PJ/year for oil crops, 60 PJ/year for wood, 50 PJ/year for grass and 60 PJ/year for maize, on a grid basis, i.e., in a single grid cell. Such potentials are widespread across the country, going from the Northeast to the South, especially around the Amazon borders for sugarcane, wood and grass, and more focused on other land (savannahs, scrublands) areas for oil crops and maize. Potentials increase through time, due to yield improvements and the expansion of land availability.

[38] For all feedstocks, the grid cells where there is no production potential, e.g., most grid cells in the North region, will also present zero production costs (due to lack of potential).

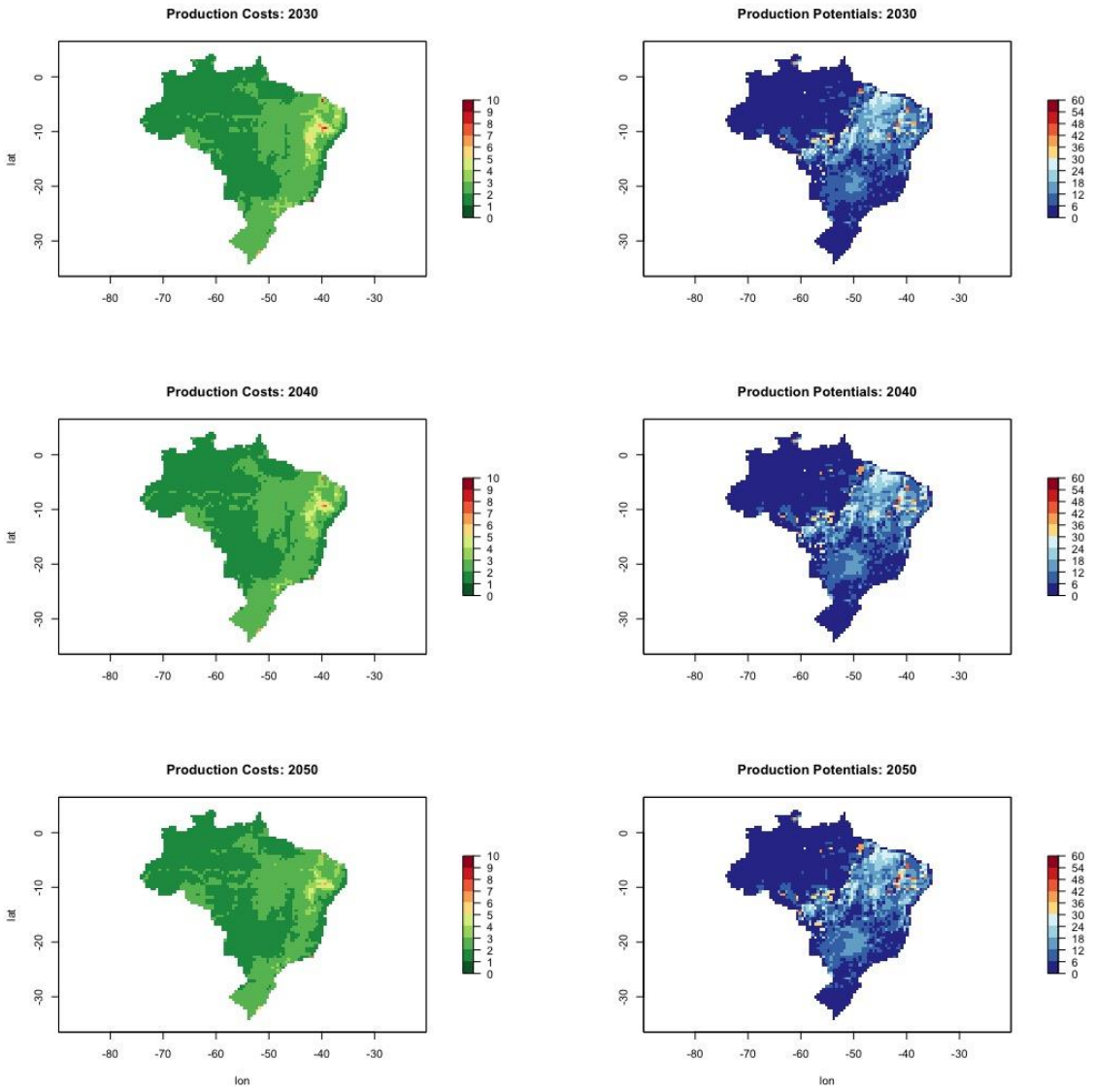

Figure 4.2. Sugarcane production costs (left) and potentials (right) (2030-2050)

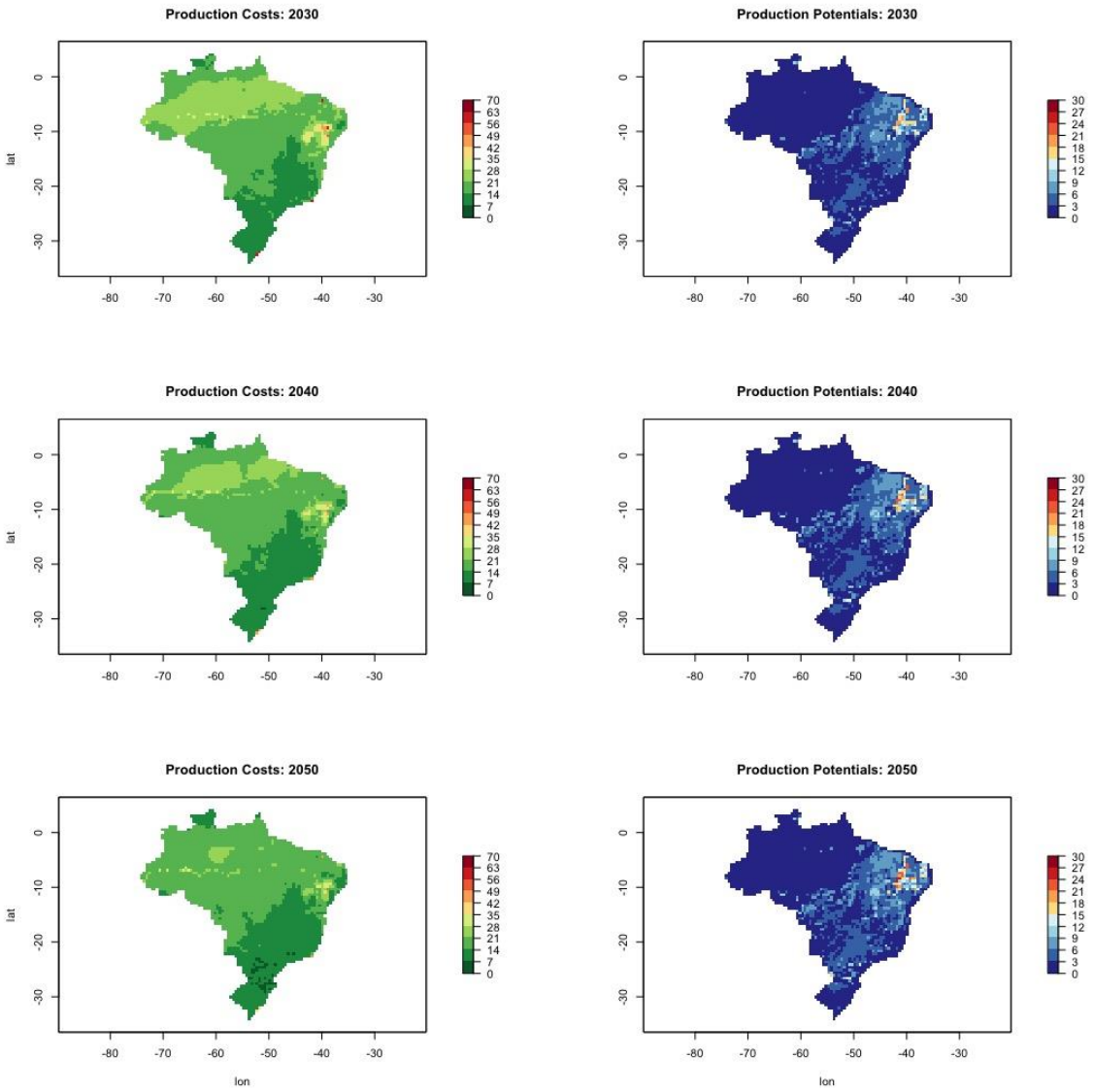

Figure 4.3. Oil crops production costs (left) and potentials (right) (2030-2050)

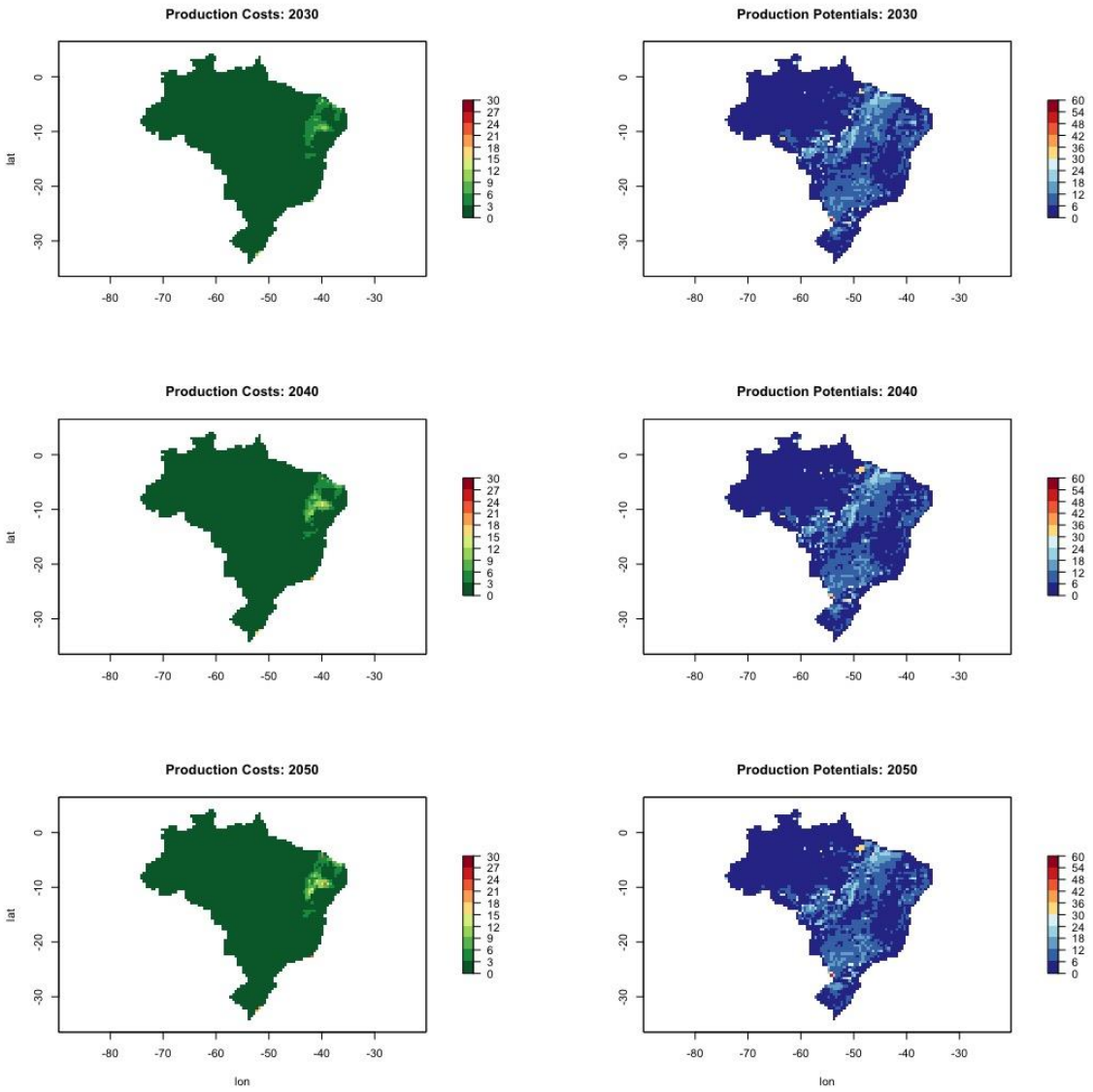

Figure 4.4. Wood production costs (left) and potentials (right) (2030-2050)

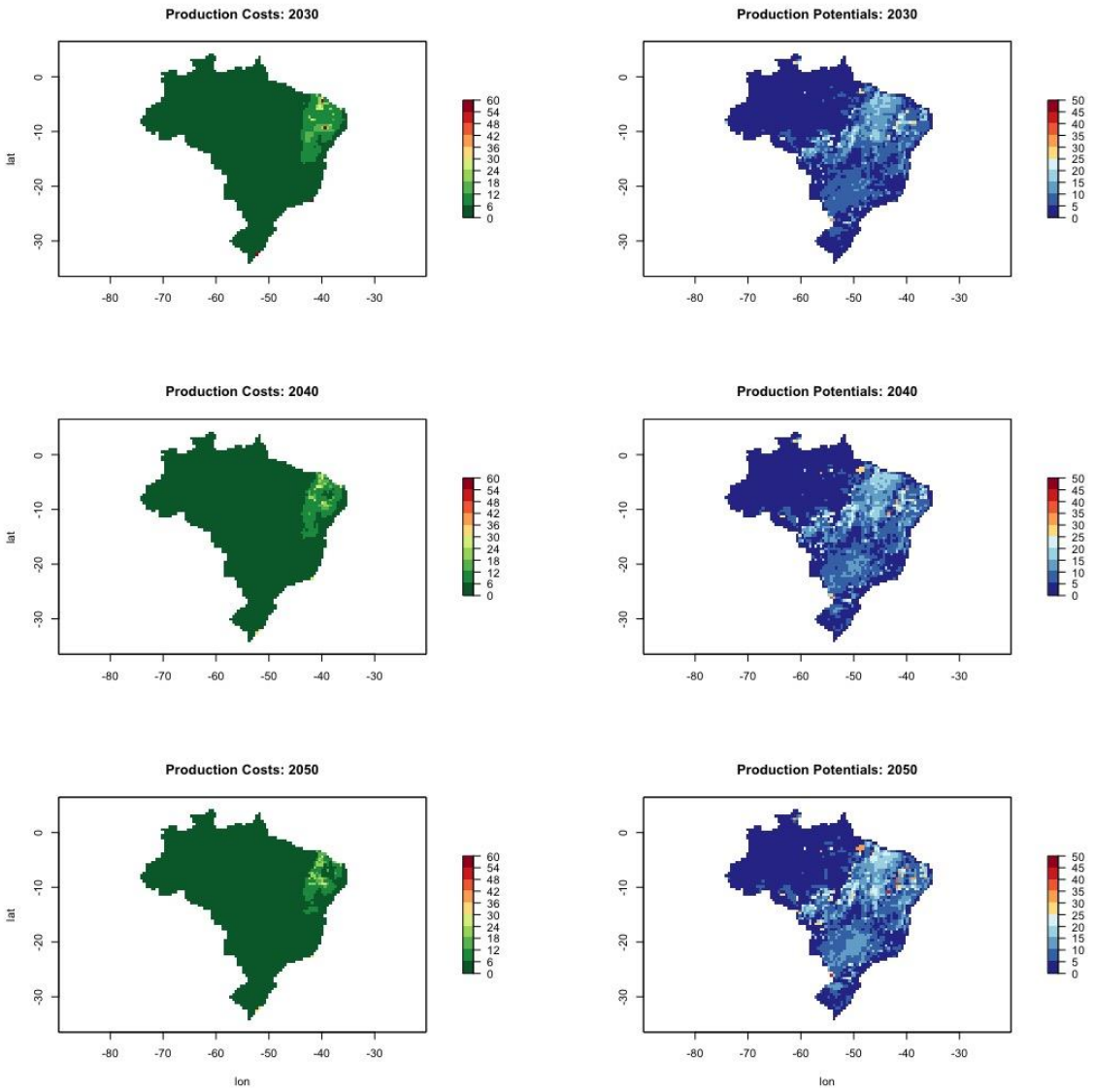

Figure 4.5. Grass production costs (left) and potentials (right) (2030-2050)

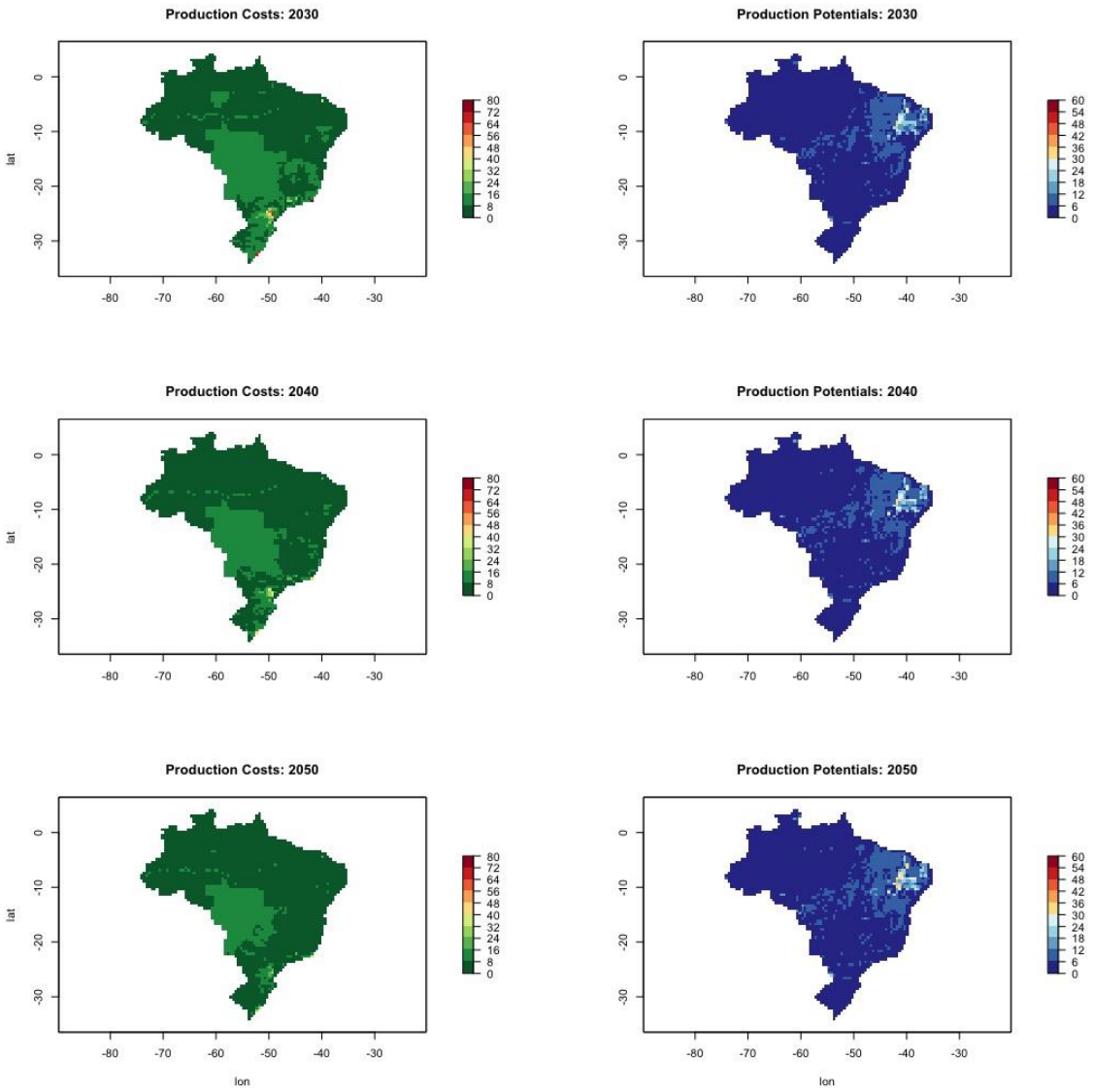

Figure 4.6. Maize production costs (left) and potentials (right) (2030-2050)

4.2 Biomass Cost Supply Curves

Having estimated costs and potentials, on a grid basis, the biomass cost supply curves were drawn for all selected crops. Figure 4.7 displays the cost supply curves for both 2030 and 2050. For most crops, supply potentials increase from 2030 to 2050. Assuming all land available will be dedicated to a single crop, sugarcane has the highest supply potentials reaching 19.8 EJ/year in 2050, followed by 16.4 EJ/year in 2050 for grass, 13.7 EJ/year in 2050 for wood, 9.0 EJ/year in 2050 for maize and 7.2 EJ/year in 2050 for oil crops.

The results show that most of the estimated potentials can be supplied under lower costs. For example, taking the thresholds of 5-10 US$/GJ, approximately 17-18 EJ/year of sugarcane (92-98% of the total potential), 12-13 EJ/year of wood (87-95% of the total potential), 9-12 EJ/year of grass (68-90% of the total potential) and 1-7 EJ/year of maize (13-88% of the total potential) could be supplied in 2030, and circa 18-19 EJ/year of sugarcane (91-96% of the total potential), 13-14 EJ/year of wood (66-87% of the total potential), 14-16 EJ/year of grass (85-97% of the total potential) and 2-8 EJ/year of maize (22-88% of the total potential) could be supplied in 2050. The only exception are the oil crops, for which such thresholds would mean less than 1 EJ/year (less than 14% of the total potential) in 2050.

It is worth noting that the supply curves are partially mutually exclusive. This means that the total potentials for each individual crop cannot be summed up. However, due to the geographic distributions and the allocation of crops per grid cell, at a given threshold the total potential of bioenergy supply (in a mix of different crops) is likely to be higher than the potential of an individual crop.

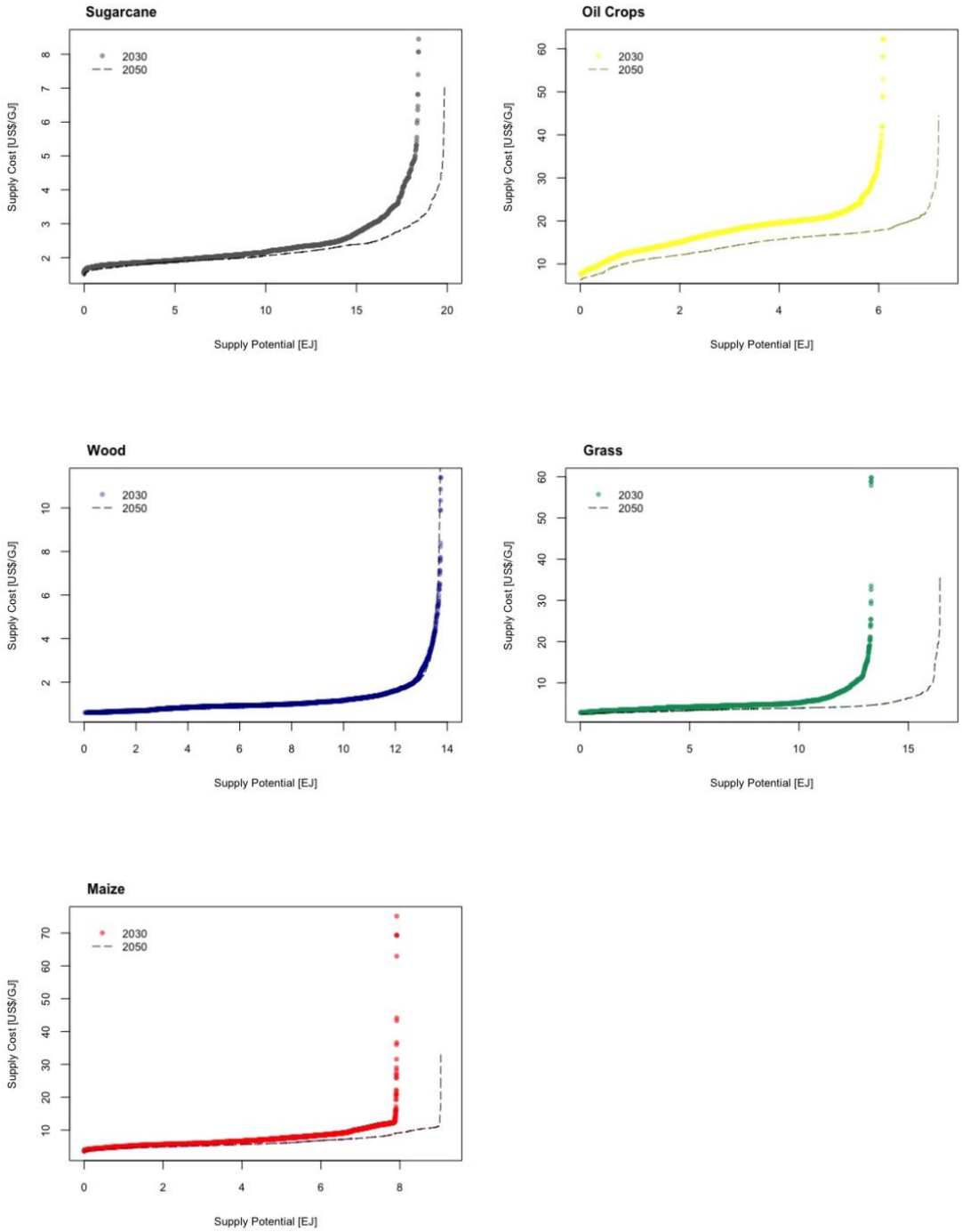

Figure 4.7. Biomass cost supply curves

4.3 Results from BLOEM and the Case Study on the Brazilian Energy Matrix

4.3.1 Base Year (2020)

For the base year of 2020, the installed capacities for biofuel production across the country, according to EPE (2021), are presented in Figure 4.8.

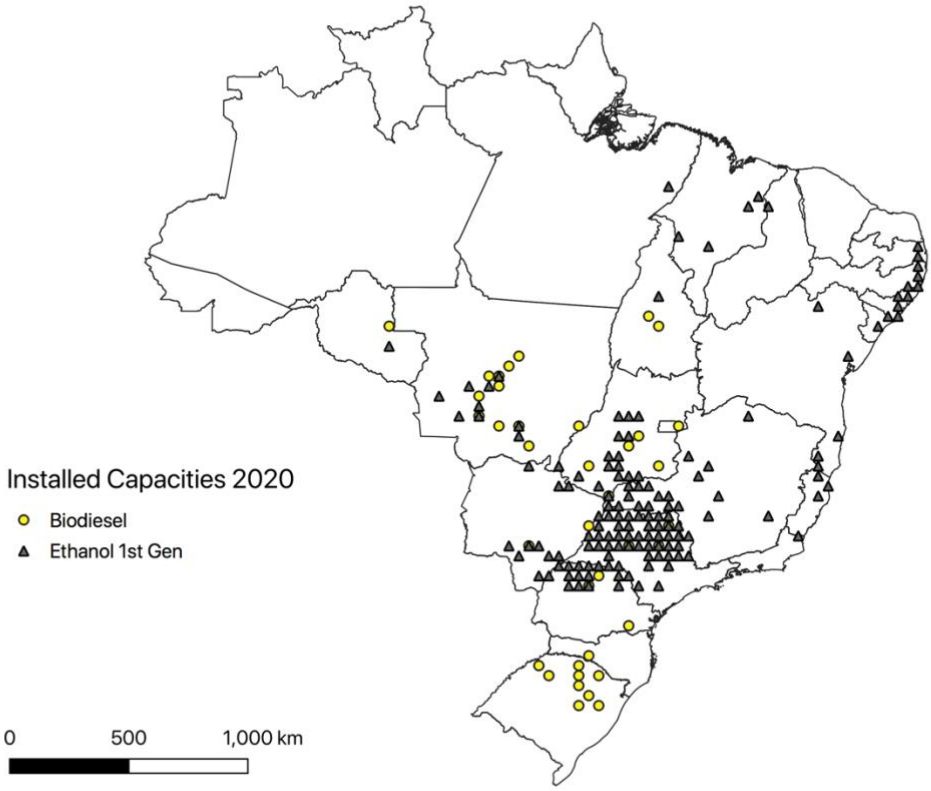

Figure 4.8. Installed capacities in 2020, based on EPE (2021)

Results for land allocation in 2020 (base year, common to all of the scenarios) are presented in Figure 4.9. The results are consistent with current production for both sugarcane and oil crops (mostly soybean), with sugarcane production concentrated in the Center-South, as well as along the Northeast coast, while oil crops appear more concentrated in the South, with local occurrences in the Center-South.

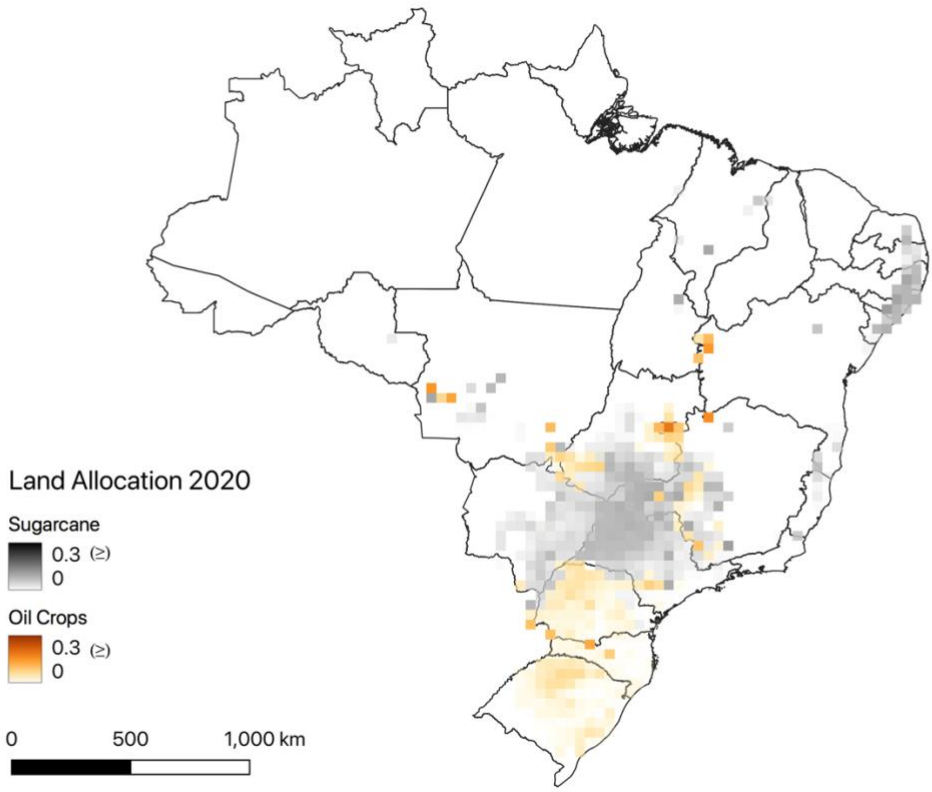

Figure 4.9. Land allocation per crop in 2020

4.3.2 Land Allocation and Land Use Change

The maps for land allocation, for all five scenarios, for 2030 and 2050, are presented in Figures 4.10 and 4.11, respectively. In the few cases where two or more crops are allocated to the same grid cell, the figures show the dominant crop. Additionally, maps for land allocation per individual crop, for all five scenarios, for 2030 and 2050, can be found in Annex XI.

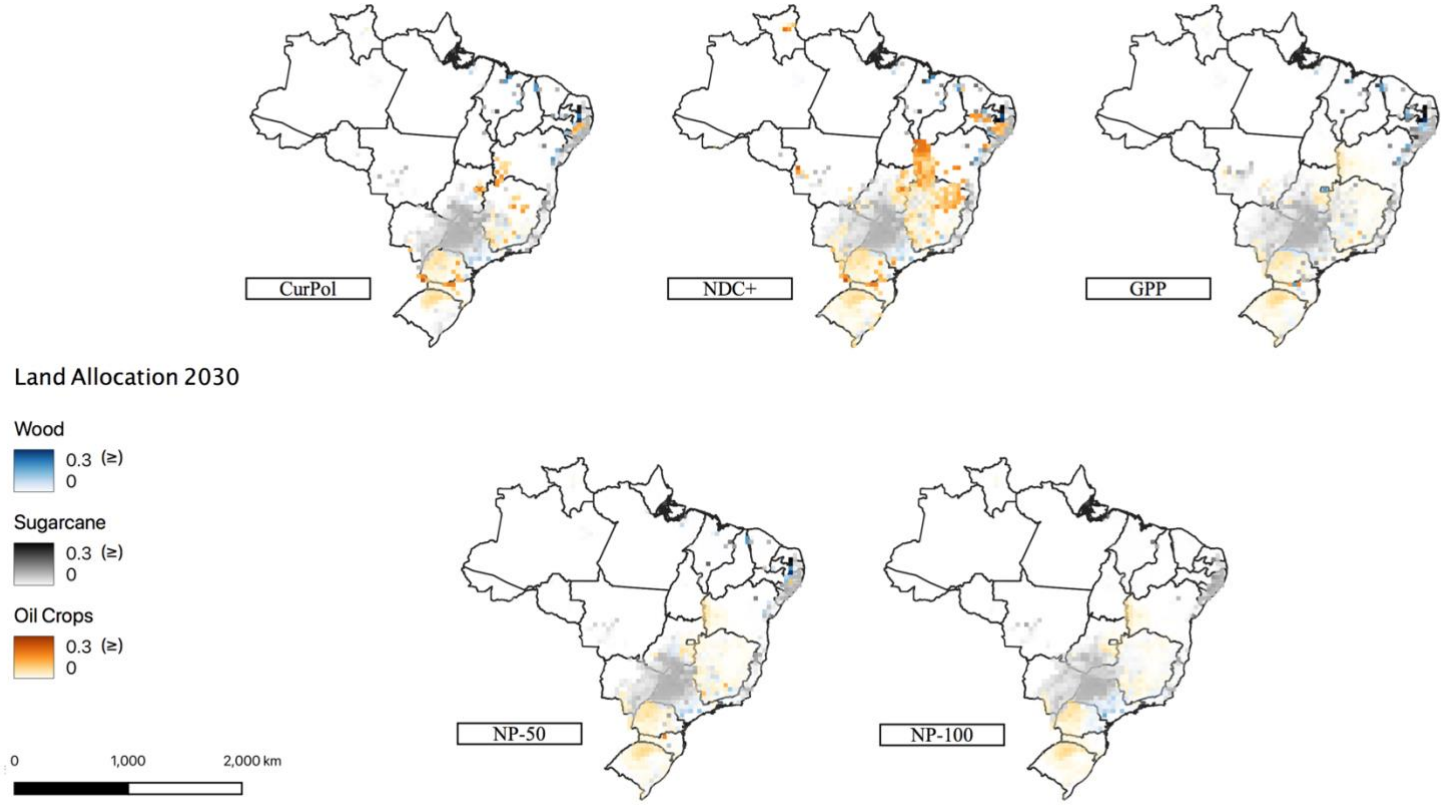

Figure 4.10. Land allocation per crop in 2030

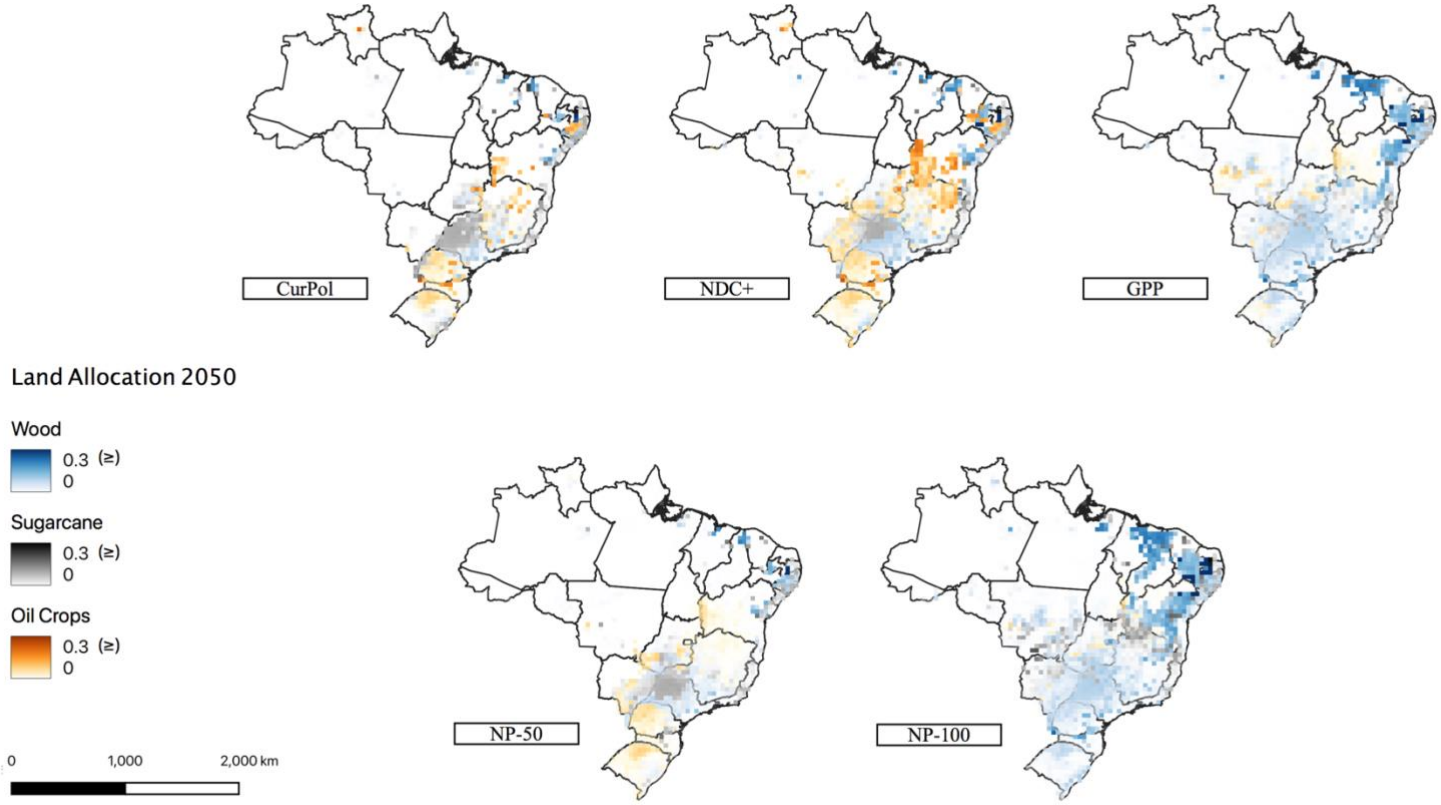

Figure 4.11. Land allocation per crop in 2050

In 2030, results indicate that sugarcane continues to be predominantly grown in the Center-South and the Northeast coastline. Dedicated wood crops appear in minor scales both in the Southeast and Northeast. Oil crops for biofuel production expand in the South, Southeast, and the axis between Southeast, Northeast and Center-West (Minas Gerais, Bahia, Goiás), especially in the NDC+ scenario, which comprehends a larger expansion of biodiesel production. Such choices for land allocation in the model are related to the location of existing capacities (i.e., installed capacities in the base year) and the logistics constraints on biomass transportation (the model prefers to use capacities already installed rather than installing new ones), as well as a combination of costs and yields.

In 2050, sugarcane production reduces in all scenarios, still mostly remaining in the Center-South. Wood crops greatly expand in both GPP and NP-100, the two scenarios with larger expansion of cellulosic biofuels, namely green diesel and biojet (or biokerosene). For these scenarios, wood crops move to the Northeast and displace part of the sugarcane production in the Center-South. Oil crops follow the 2030 trend, except for GPP and NP-100. In GPP, oil crops move more towards the Center-West, while in NP-100, the reduced biodiesel production is seen mostly in the Center-South. By 2050, the existing capacities are decommissioned. Therefore, land allocation is driven by a combination of costs and yields, as well as the logistics of bioenergy supply and the location of demand centers.

Figure 4.12 shows the cumulative direct land use change and direct land use change emissions related to the production of bioenergy crops, for all scenarios, for the period between 2020 and 2050. For NP-50, roughly, 3 million ha of “other land” are displaced for the production of mostly sugarcane (48%) and wood (50%), indicating the lowest cumulative direct land use change observed among all of the analyzed scenarios. For CurPol, around 5 million ha of “other land” are displaced for biomass production, evenly divided between sugarcane, oil crops and wood. For NDC+, approximately 10 million ha of “other land” are displaced, most of it for the production of oil crops (46%) and wood (33%). This result is coherent with the expansion of biodiesel production seen in this scenario. Finally, GPP and NP-100 are the scenarios with highest observed direct land use change (11 million ha of “other land” for GPP and 15 million ha for NP-100), most of which related to wood production for cellulosic biofuels: 74% and 77%,

respectively. Cumulative direct land use change emissions follow the direct land use change trends.

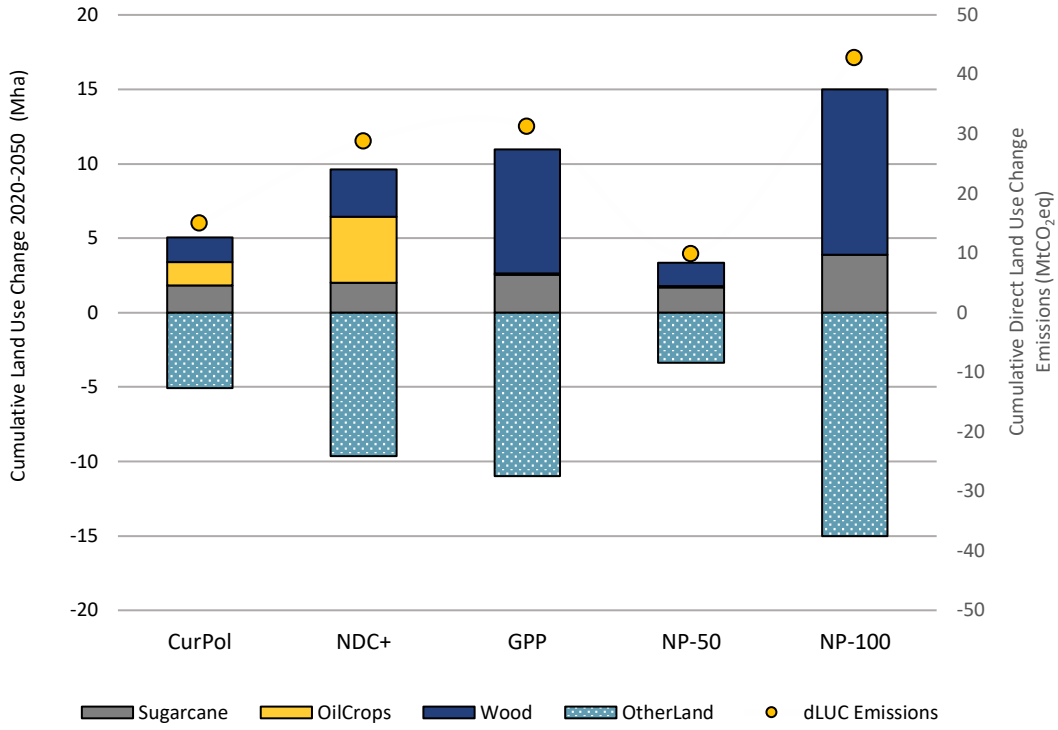

Figure 4.12. Cumulative (2020-2050) land use change and land use change emissions

Note that "other land" includes savannahs, scrublands, grasslands.

To put these numbers into context, current agricultural area in Brazil is of approximately 76 million ha, of which 10 million ha are dedicated to sugarcane and 36 million ha to soybeans (IBGE, 2019). Overall, the results are coherent with the level of ambition of each scenario. GPP and NP-100 are the most ambitious scenarios in terms of bioenergy expansion, leading to higher levels of direct land use change. However, the least ambitious scenario, CurPol, is not the one leading to lower cumulative direct land use change. This can be explained by the absence of carbon prices in CurPol, such that the carbon prices in a slightly more ambitious scenario such as NP-50 lead to a lower expansion of bioenergy into other lands (savannahs, scrublands). This result arises since the carbon price is also applied on direct land use change emissions, thus in the presence of a carbon price there is a preference to reduce direct land use change emissions, thus moving towards higher yielding lands, reducing the overall land footprint.

4.3.3 System's Expansion and Location of Conversion Plants

The regional shares of installed capacities in use, for 2030 and 2050, are presented in Figure 4.13. For all scenarios, the Southeast is the most important region for bioenergy production. This result is coherent with the current geographical distribution of existing capacities for bioenergy production in the country and their lifetime and expected year of retirement, as well as their proximity to the demand centers. On the other hand, the North is the least important one, mostly because of the lower demands and the strict land constraints due to the protection of forest areas, largely located in this region.

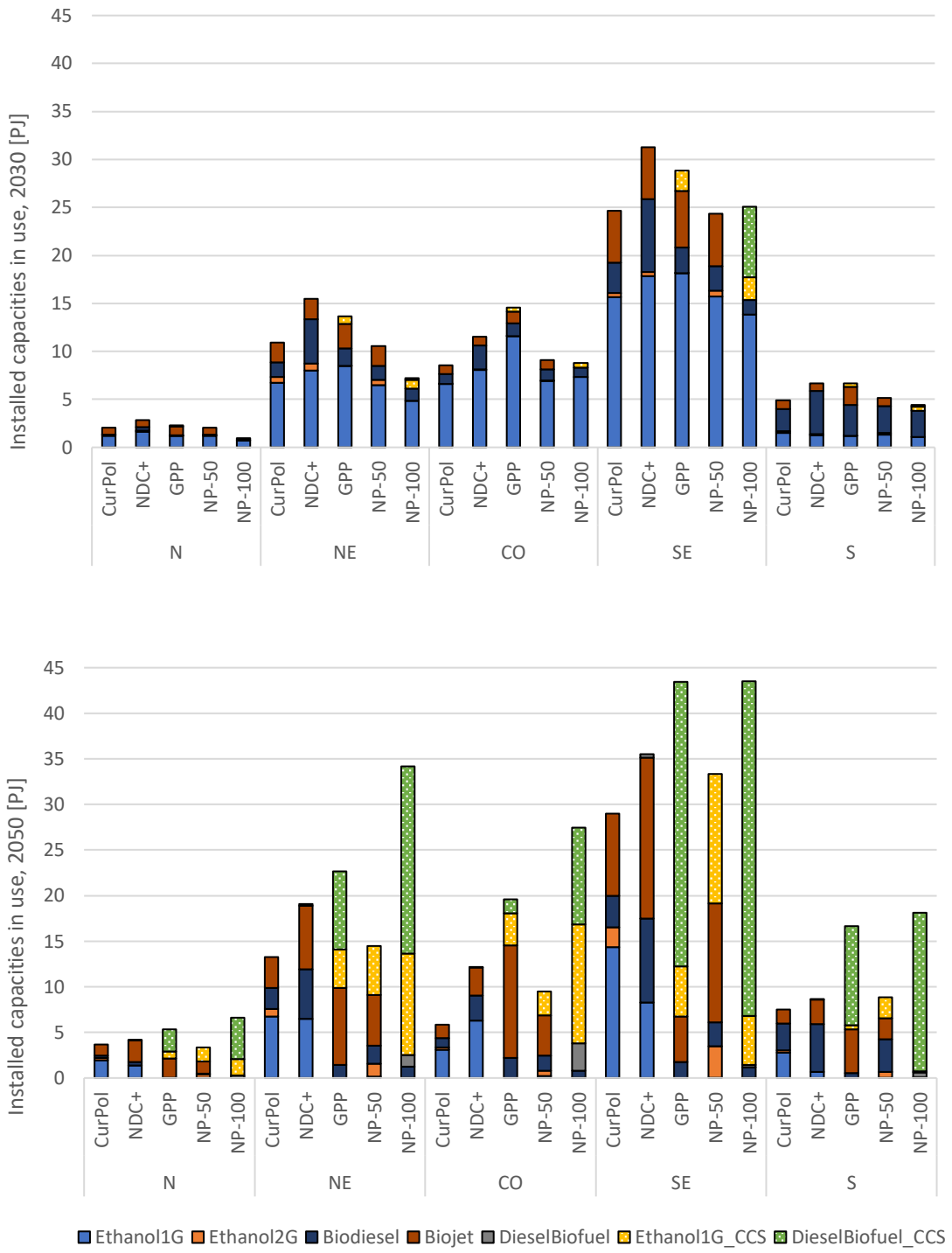

Figure 4.13. Regional share of installed capacities in use (2030, 2050)

For CurPol, bioenergy production expands from 2030 to 2050 in all regions, except for the Center-West. The retraction in this region is pulled by a reduction in ethanol production. Biodiesel expands modestly in the Southeast, South and Northeast, while the production of cellulosic biofuels, in this case biojet, expands in the Southeast and Northeast regions. Figure 4.14 displays in more detail the expansions/retractions in installed capacities between 2030, for the CurPol scenario.

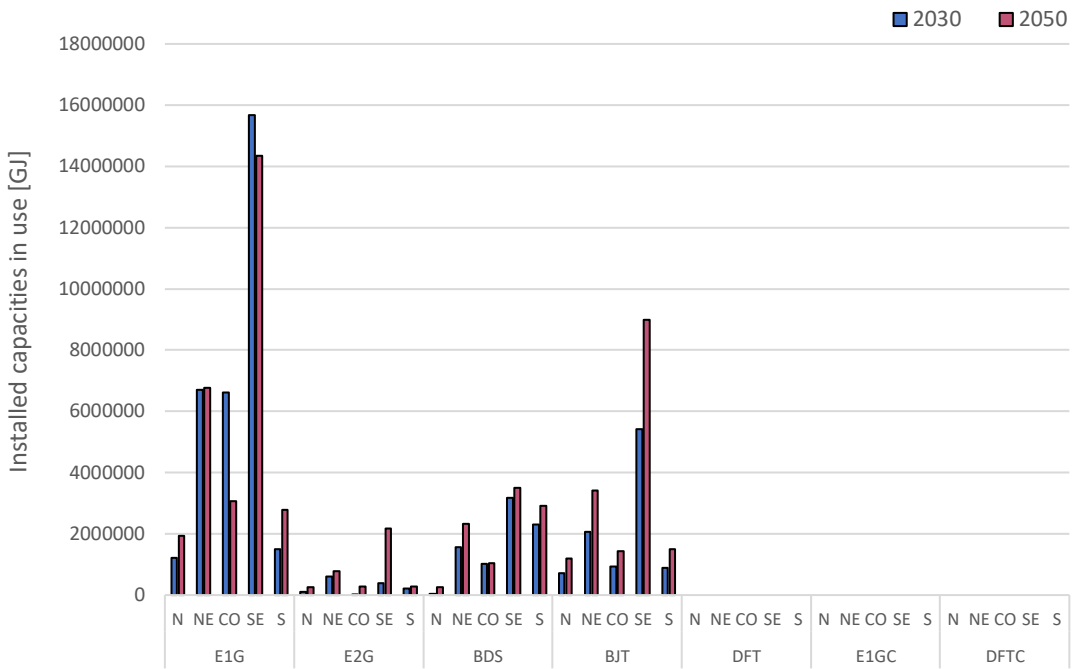

Figure 4.14. Installed capacities per technology, per region – CurPol

For NDC+, bioenergy production expands from 2030 to 2050 in all regions. The production of biodiesel expands in the Southeast, Northeast and Center-West. The production of cellulosic biofuels, in this case biojet, expands in all regions, notably the Southeast and Northeast regions. Interestingly, in the Southeast there is a shift from ethanol first generation to biojet, with E1G capacities retiring while BJT capacities are installed by 2050. Figure 4.15 displays in more detail the expansions/retractions in installed capacities between 2030, for the NDC+ scenario.

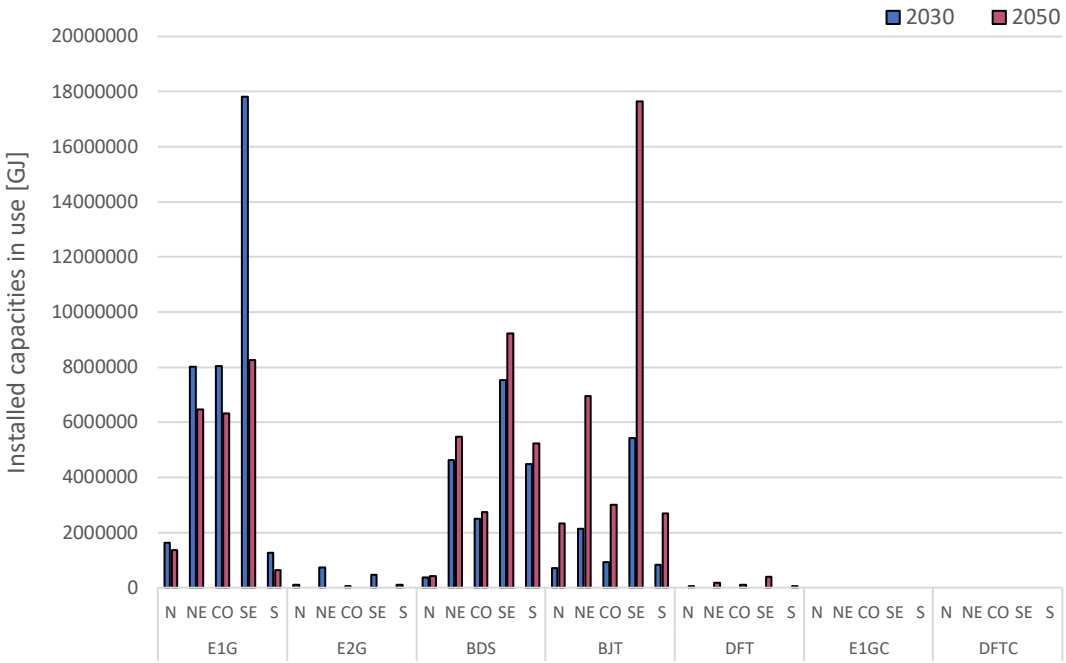

Figure 4.15. Installed capacities per technology, per region – NDC+

For GPP, there is a clear shift in the portfolio of technologies from 2030 to 2050, where the remaining production of ethanol first generation adds on carbon capture systems, while the system moves towards the production of cellulosic biofuels, with and without carbon capture (green diesel with and biojet without carbon capture)[39]. In this context, the model projects the remaining production of ethanol first generation in the Center-South and Northeast regions. Cellulosic biofuels expand in all regions, with biojet more prominently in the Center-West and Northeast, and green diesel with carbon capture in Southeast and South. The model's choice of allocation in this case is driven by the costs for transporting the CO_2 captured in the production of green diesel. Therefore, such facilities are installed closer to the storage sites, in the Southeast and South. Figure 4.16 displays in more detail the expansions/retractions in installed capacities between 2030, for the GPP scenario.

[39] The bioenergy production levels, as well as the technology portfolio, are results from BLUES, which are communicated to BLOEM. The geographic allocation and regional shares of capacities, and correspondent land allocation for biomass production, are a result from BLOEM.

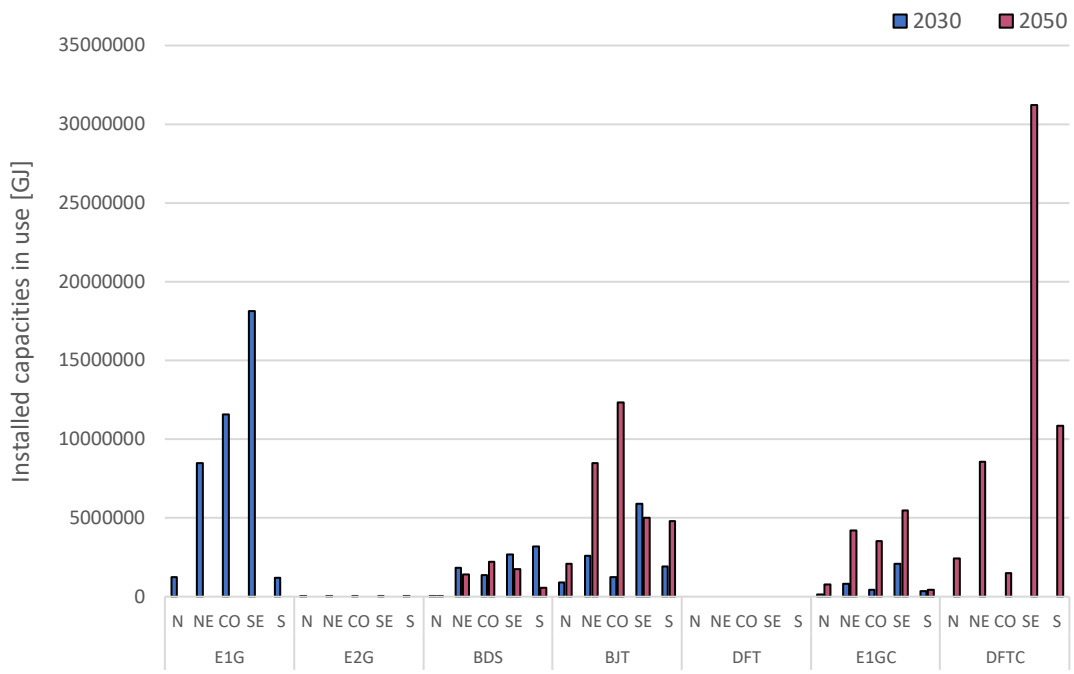

Figure 4.16. Installed capacities per technology, per region – GPP

For NP-50, ethanol first generation is no longer commissioned without carbon capture. In this context, the production of ethanol first generation (now with carbon capture) and ethanol second generation remain concentrated in the Center-South and Northeast. The production of biodiesel slightly increases in all regions, except for the North. The production of biojet expands in all regions, most notably the Southeast. As previously discussed, the concentration of bioenergy production in the Center-South and the Northeast is highly influenced by the logistic costs of distribution and the proximity to the demand centers. In the cases including carbon capture and transportation, the model preferably allocates such technologies closer to the potential storage sites, which are mostly offshore (one onshore, but at the coastline). Figure 4.17 displays in more detail the expansions/retractions in installed capacities between 2030, for the NP-50 scenario.

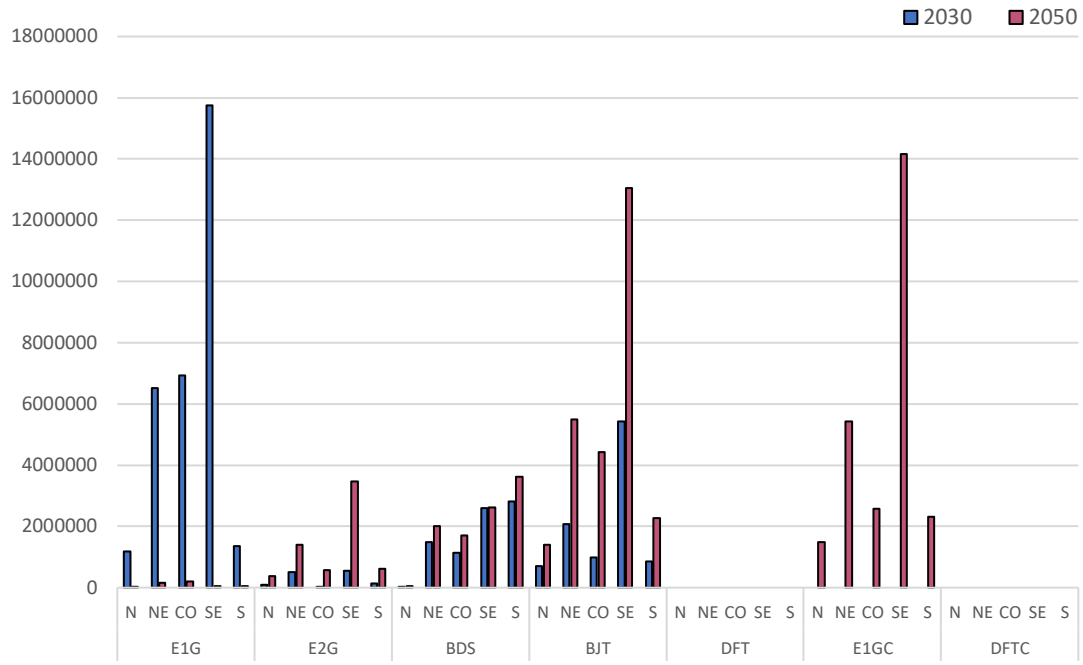

Figure 4.17. Installed capacities per technology, per region – NP-50

For NP-100, conventional biofuels (i.e., ethanol first generation without carbon capture and biodiesel) are decommissioned in all regions, being substituted by ethanol first generation with carbon capture and green diesel, with and without carbon capture. In this context, ethanol production shifts from the Southeast to the Center-West, which can be also observed in the displacement previously seen in land allocation between wood crops and sugarcane (Figure 2.10). The production of green diesel, with and without carbon capture, largely dominates all other regions. Once again, technologies with carbon capture are preferably located in the Center-South and Northeast in order to reduce the costs of CO_2 transportation, while also staying in the vicinity of the demand centers countrywide. Figure 4.18 displays in more detail the expansions and/or retractions in installed capacities between 2030, for the NP-100 scenario.

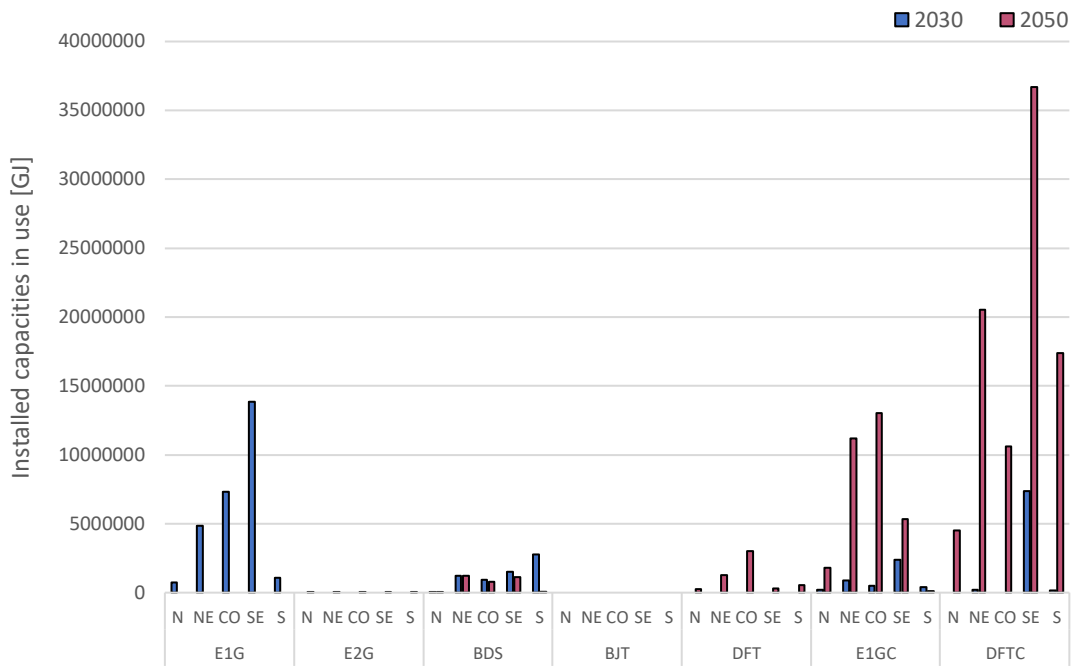

Figure 4.18. Installed capacities per technology, per region – NP-100

Finally, Figures 4.19-4.20 present the regional shares of total installed capacities (in 2030 and 2050, respectively) and Figures 4.21-4.25 present the geographic location of conversion plants per technology, per scenario, for 2030 and 2050. Conversion capacities are placed in the centroid of the grid cell where they are located. These figures need to be evaluated in combination with previous Figures 4.14-4.18, for a better understanding of location and magnitude of installed capacities. Just looking at the geographic location of capacities without taking into account their order of magnitude can be misleading. For example, most notably for GPP (Figure 4.23) and NP-100 (Figure 4.25), the geographically explicit results indicate that in 2050 green diesel with carbon capture installs capacities in the North and in the Center-West. However, when evaluating the order of magnitude, results indicate that those are smaller capacities to attend the demand centers in those regions, where there is trade-off between the costs of transportation of the CO_2 captured (since the locations are further away from the storage sites) and the logistics costs for the distribution of biofuels (from conversion to demand).

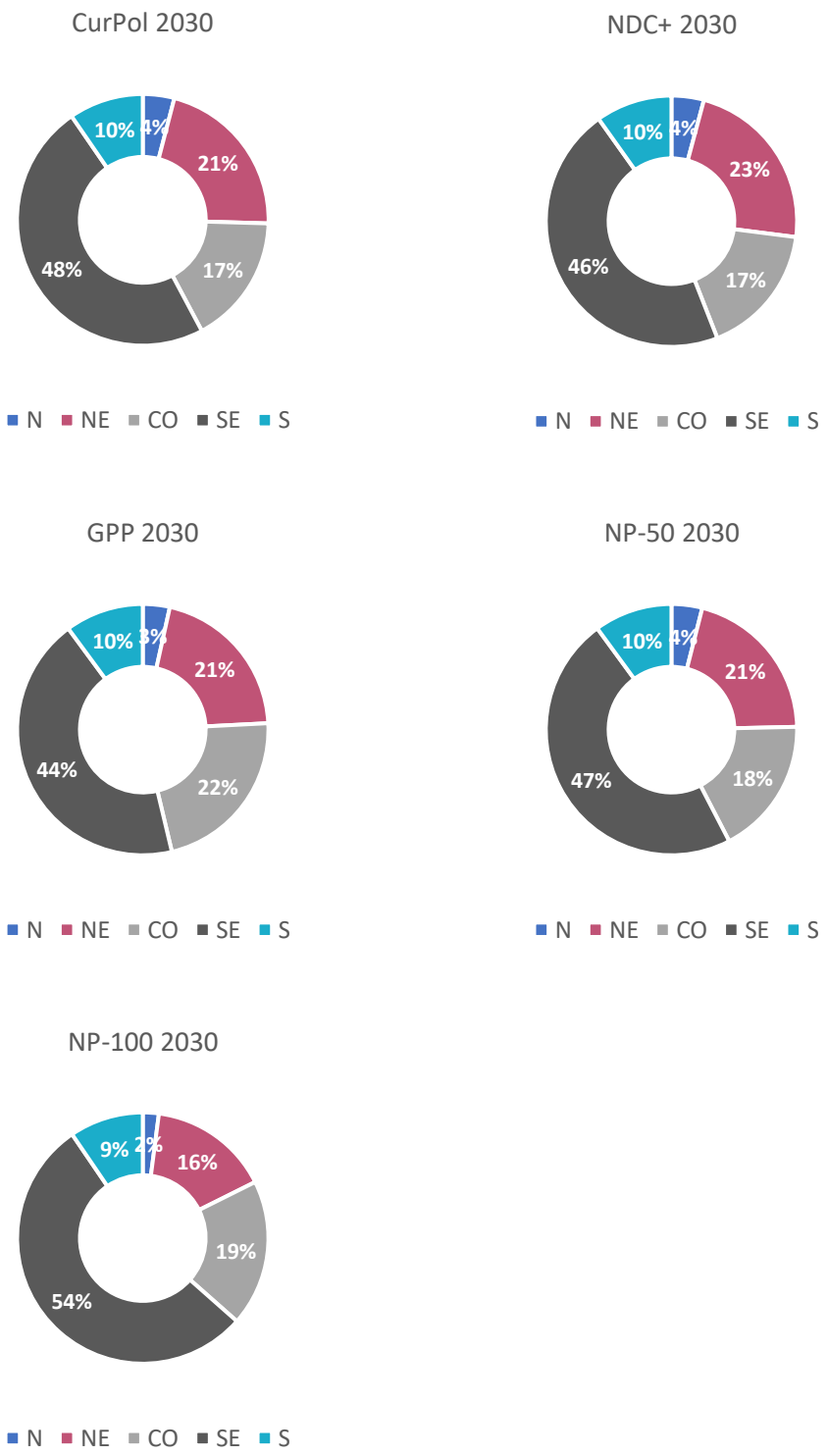

Figure 4.19. Regional shares of total installed capacities in 2030

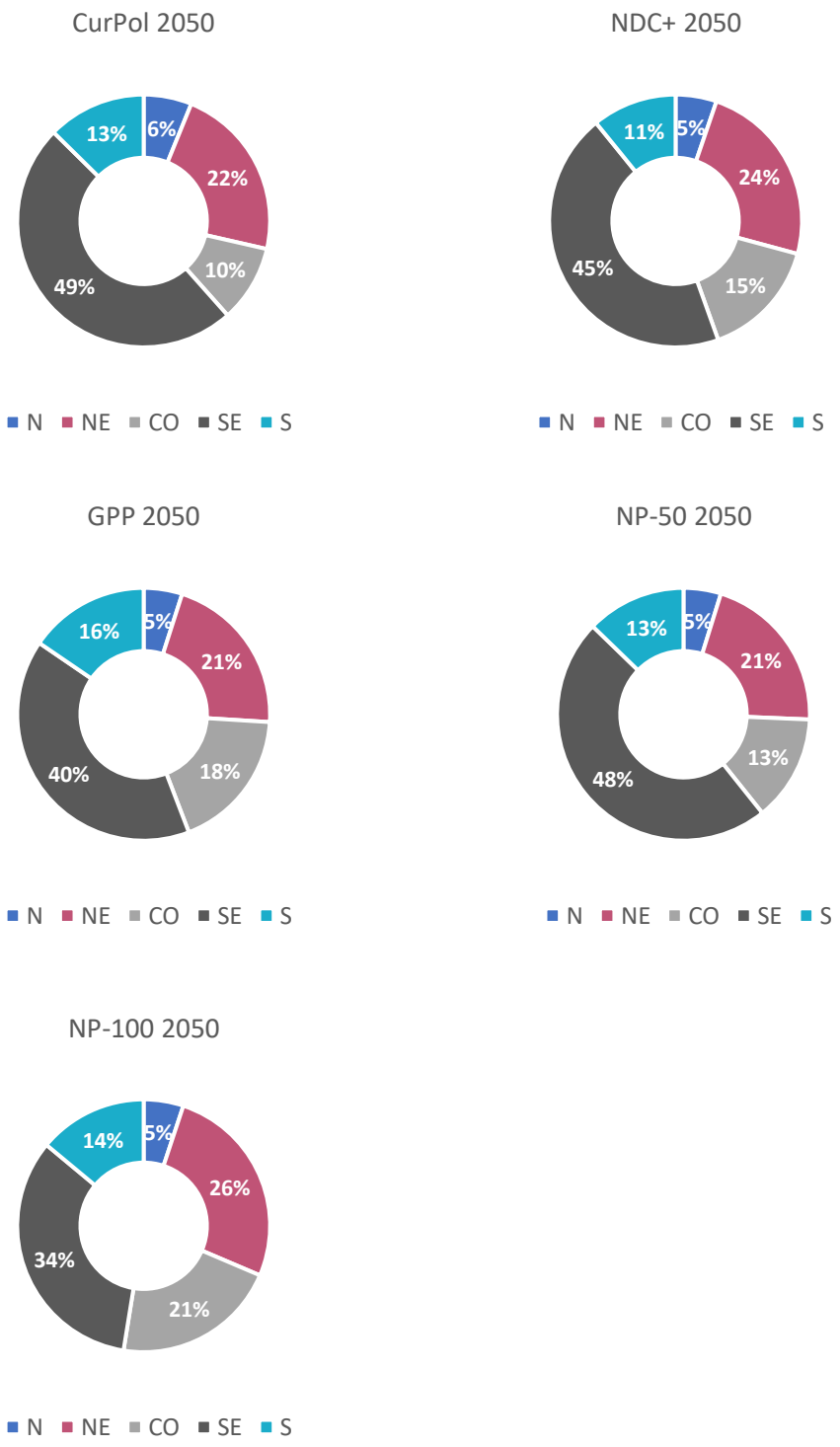

Figure 4.20. Regional shares of total installed capacities in 2050

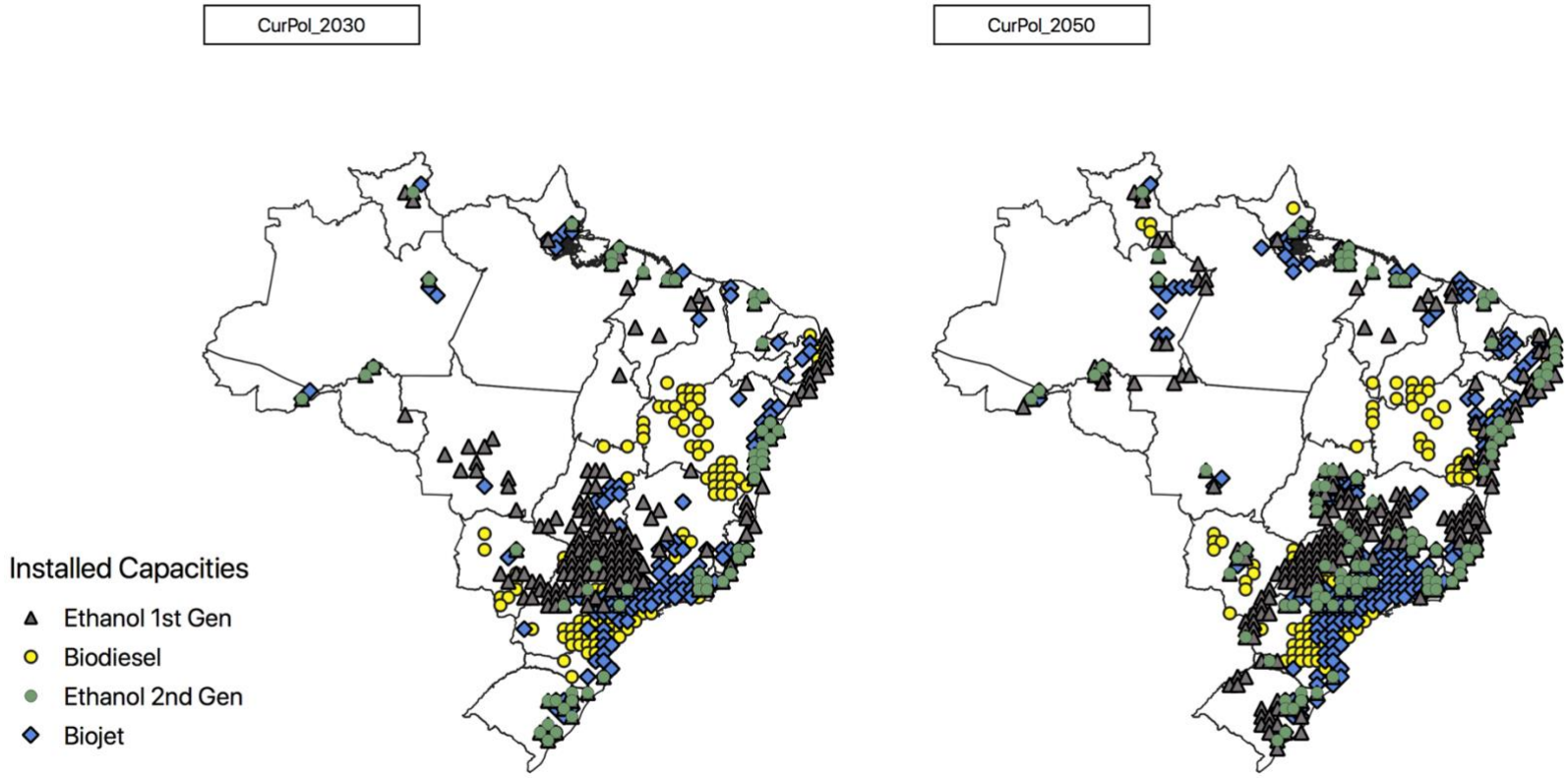

Figure 4.21. Installed capacities – CurPol

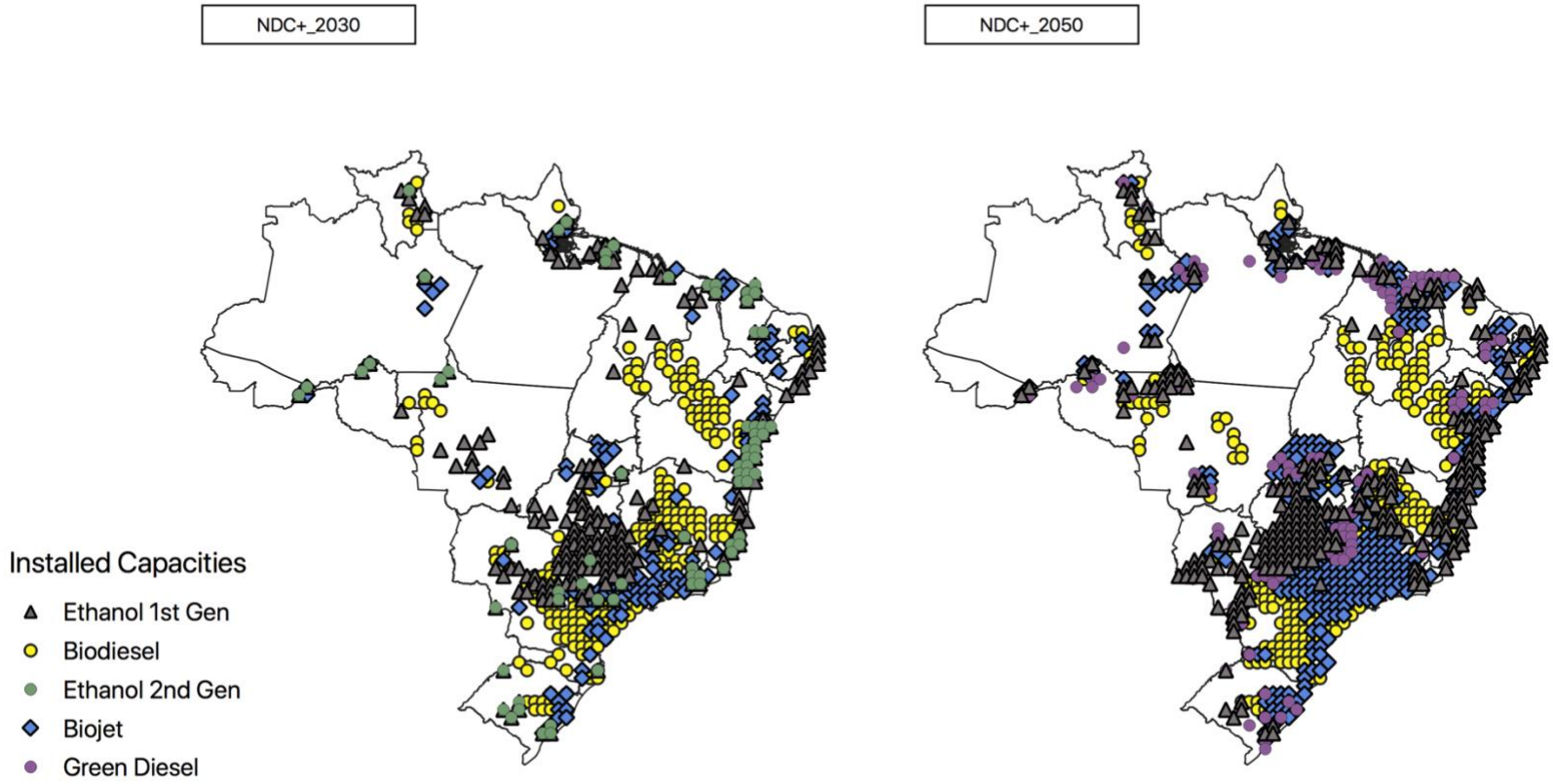

Figure 4.22. Installed capacities – NDC+

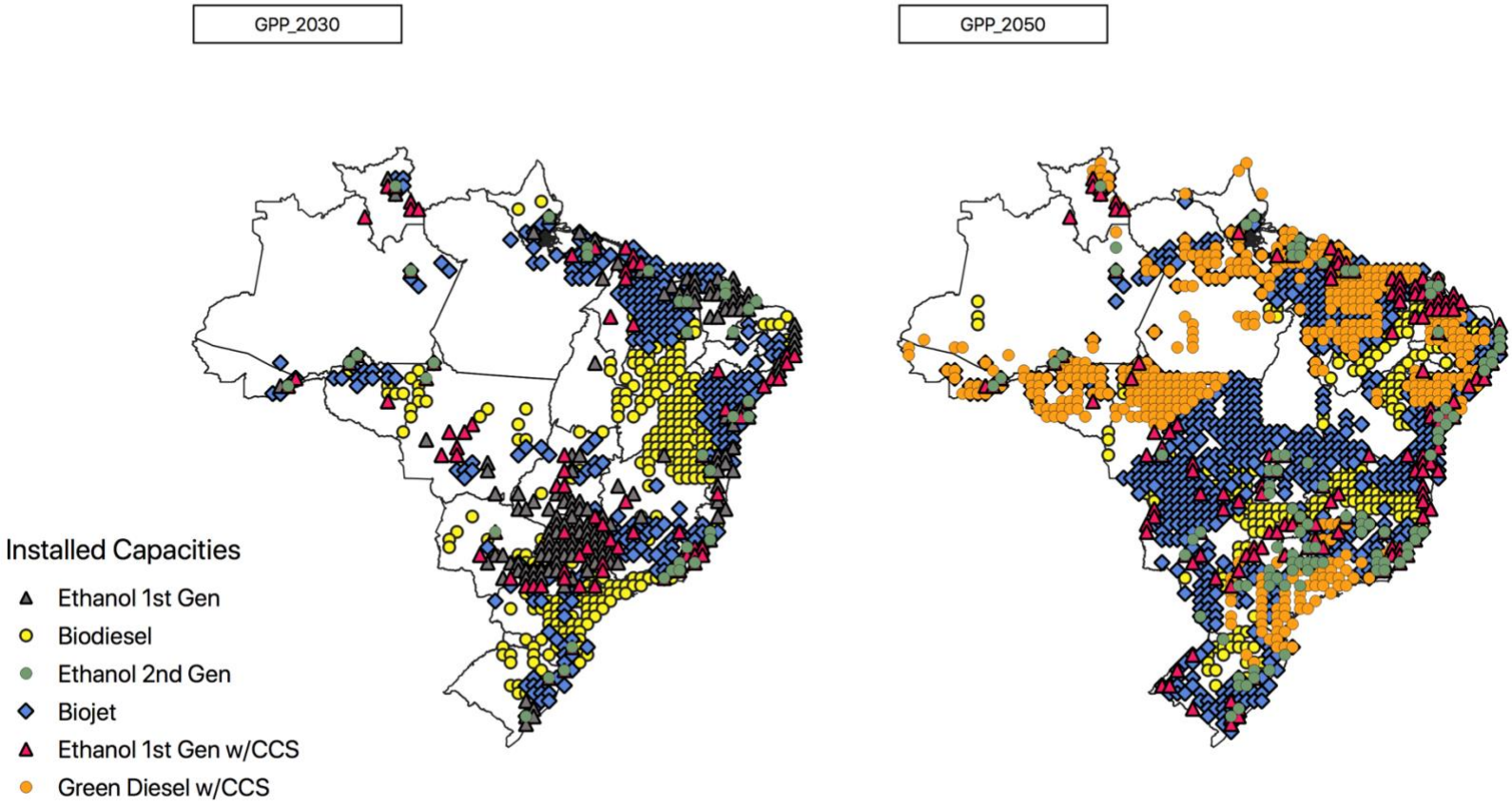

Figure 4.23. Installed capacities – GPP

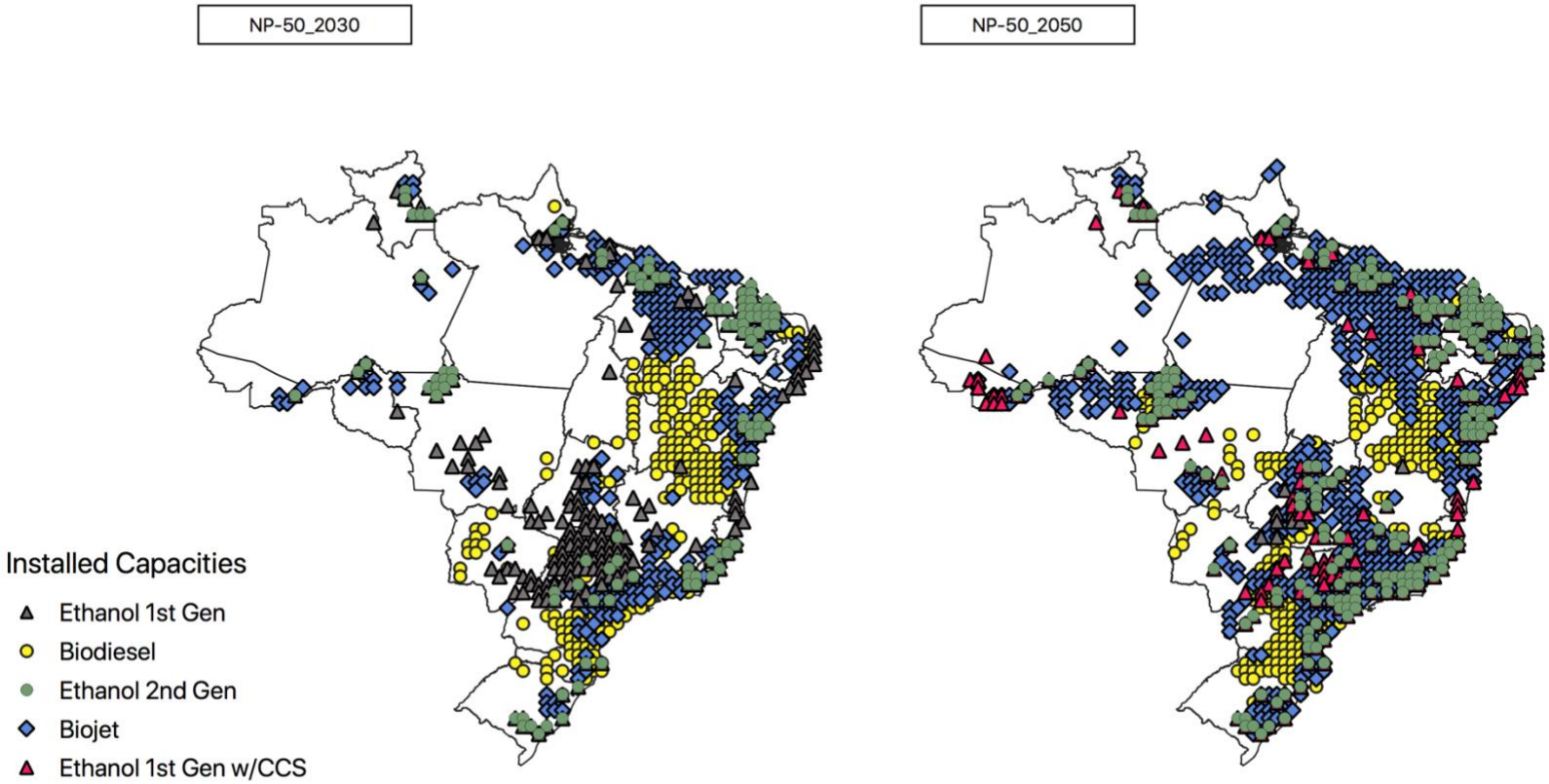

Figure 4.24. Installed capacities – NP-50

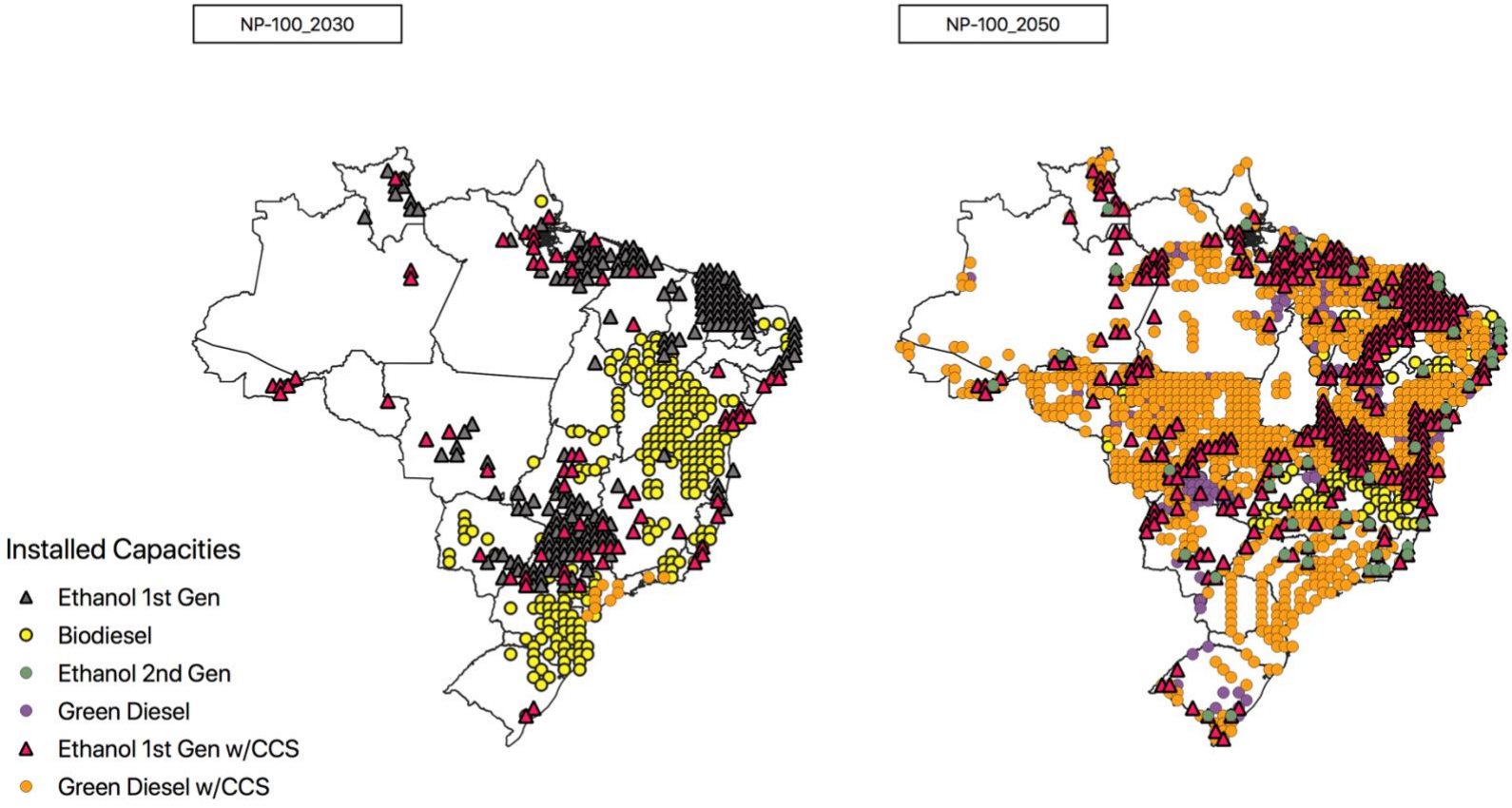

Figure 4.25. Installed capacities – NP-100

4.3.4 CO_2 Transportation and Storage

Three of the five selected scenarios include technologies with carbon capture, transportation and storage: GPP, NP-50 and NP-100.

NP-50 has a less extensive deployment of BECCS, starting in 2040. Most of the CO_2 captured is stored offshore, in the Campos and Santos basins, in the Southeast, as can be seen in Figure 4.26.

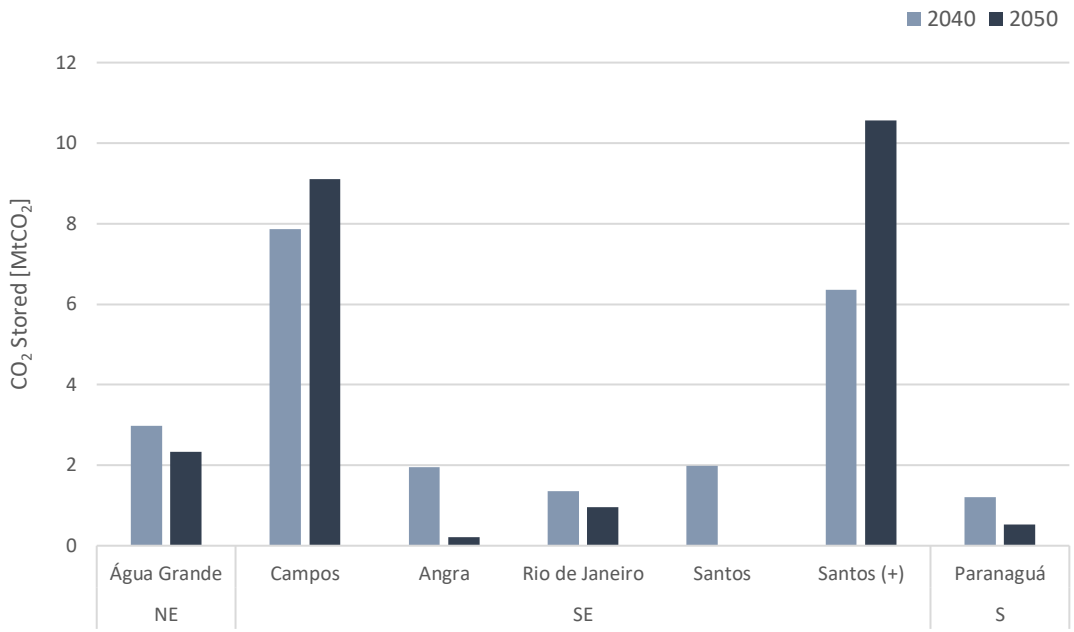

Figure 4.26. CO_2 storage – NP-50

GPP and NP-100 are intensive in BECCS deployment, but each scenario presents a different profile for CO_2 storage allocation across storage sites and across time, as can be seen on Figures 4.27 and 4.28.

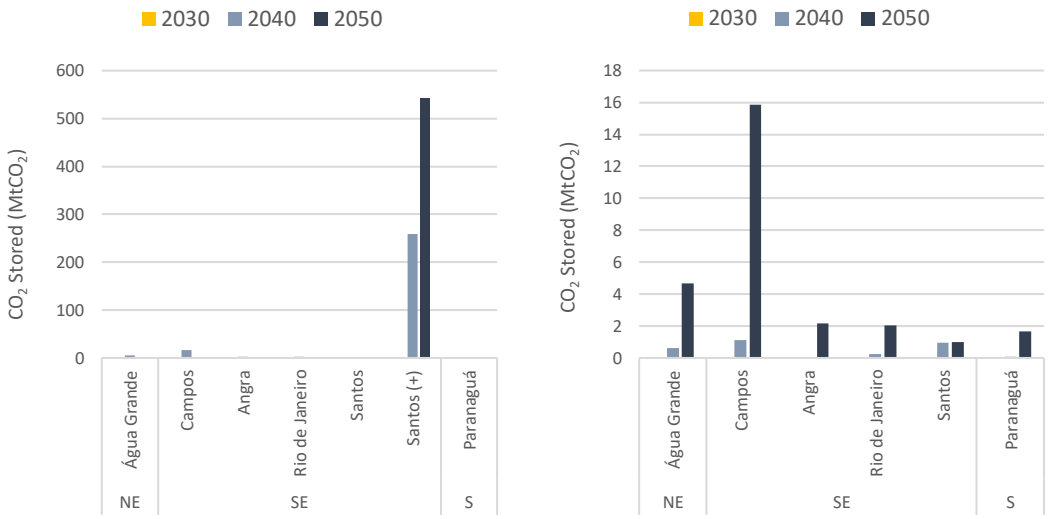

Figure 4.27. CO_2 storage: with Santos+ (left), without Santos+ (Right) – GPP. Note the different scales.

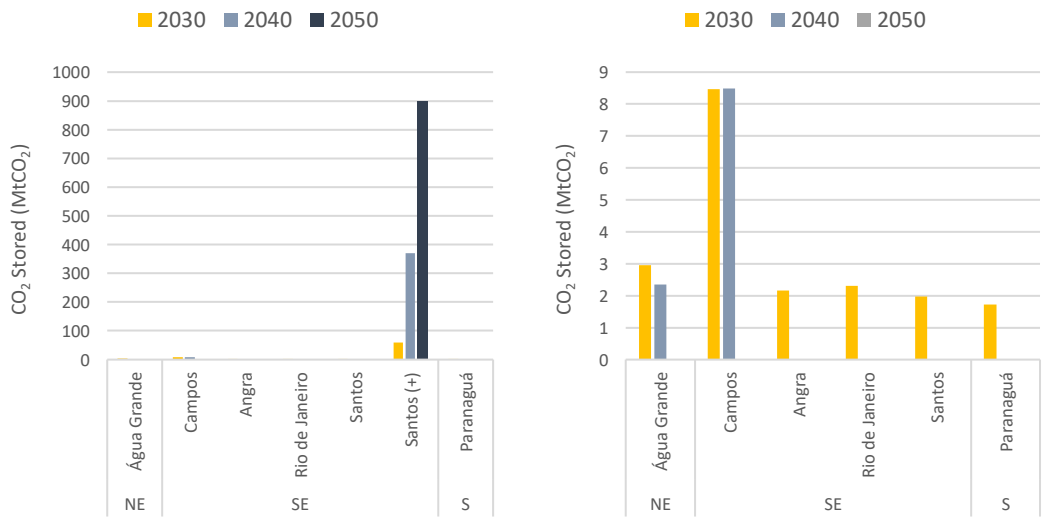

Figure 4.28. CO_2 storage: with Santos+ (left), without Santos+ (Right) – NP-100. Note the different scales.

For GPP, the lower cost storage options capacities are filled by 2050, with the remaining storage need being filled by the higher cost option (Santos+, for which no revenues from EOR are considered). For NP-100, some lower cost storage options capacities are filled already by 2030, with only Água Grande (onshore, Northeast) and

Campos (offshore, Southeast) still available in 2040. By 2050, only the higher cost option (Santos+) still has available capacity.

4.3.5 System Costs

The breakdown of costs for each scenario is presented in Figure 4.29. The least cost scenario is CurPol (which is also the least ambitious in terms of bioenergy production and climate goals), while GPP has the highest overall costs. The net-zero scenario (NP-100) high costs are largely compensated by the revenues from negative emissions. If such revenues were not accounted for, the costliest scenarios would be NP-100 and GPP, the two scenarios with larger deployments of BECCS, with carbon transportation costs alone corresponding to 24% and 13% of total costs, respectively. For NP-50, positive emissions offset negative emissions, balancing out the revenues from CO_2 capture and storage.

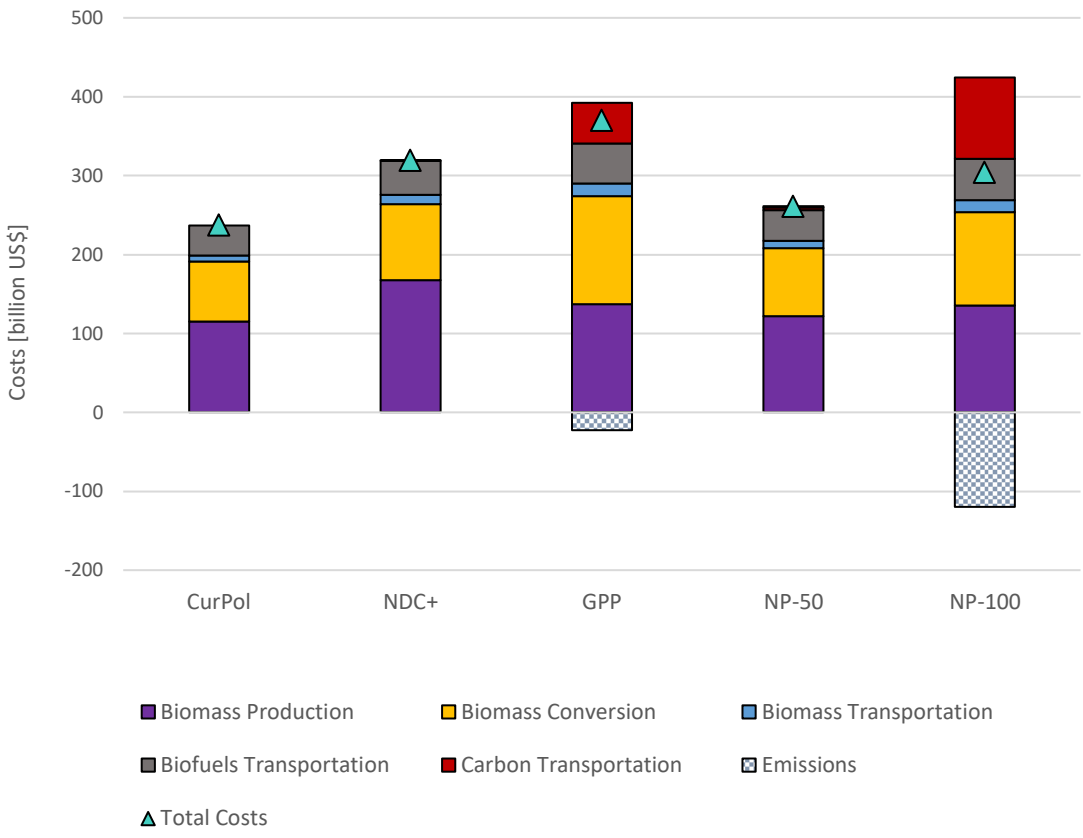

Figure 4.29. System costs breakdown

Biomass production and conversion are the biggest contributors to total costs. Biomass production shares are largest for NDC+, reaching 53% of total costs. NDC+ is a scenario which shows an expansion in the production of biodiesel, and as previously seen in the cost-supply curves, oil crops have the highest supply costs. On the other hand, biomass conversion shares of costs are larger for the scenarios with higher participation of cellulosic biofuels, which implies higher investments. Finally, biomass transportation contributes the least in the costs breakdown, representing less than 5% of total costs in all scenarios, which corroborates similar findings in the literature (Samsatli et al., 2015, Tagomori et al., 2018).

4.3.6 GHG Emissions

The cumulative GHG emissions related to the bioenergy value chain in Brazil, from 2020 to 2050, for all scenarios are presented in Figure 4.30.

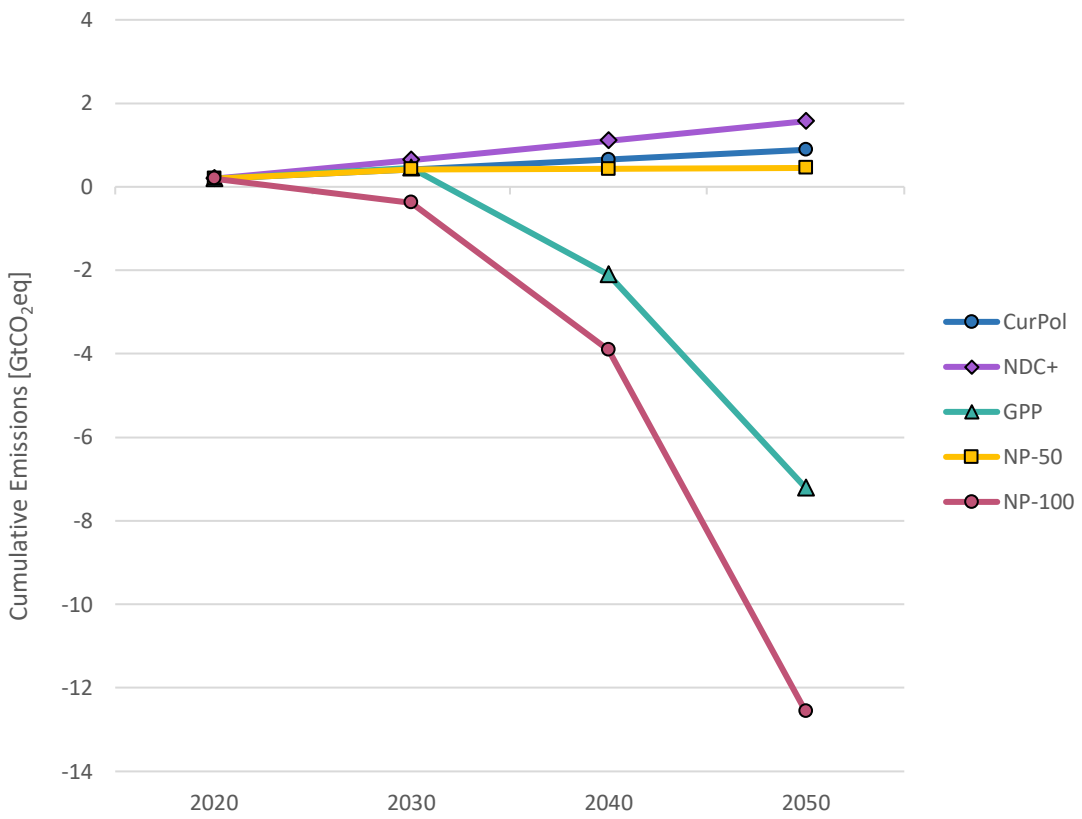

Figure 4.30. Cumulative emissions (2020-2050) related to the bioenergy value chain in Brazil

As can be seen in Figure 4.30, the scenario with highest emissions related to the bioenergy value chain is NDC+, reaching 1.6 $GtCO_2eq$ by 2050. This can be explained by the significant expansion of biodiesel from oil crops production in this scenario. Oil crops have higher factors of emissions regarding production (higher consumption of fuel for farming, fertilizer use, collection), which results in much larger emissions related to biomass production, as can also be seen in the breakdown of emissions, in both Figures 4.31 and 4.32.

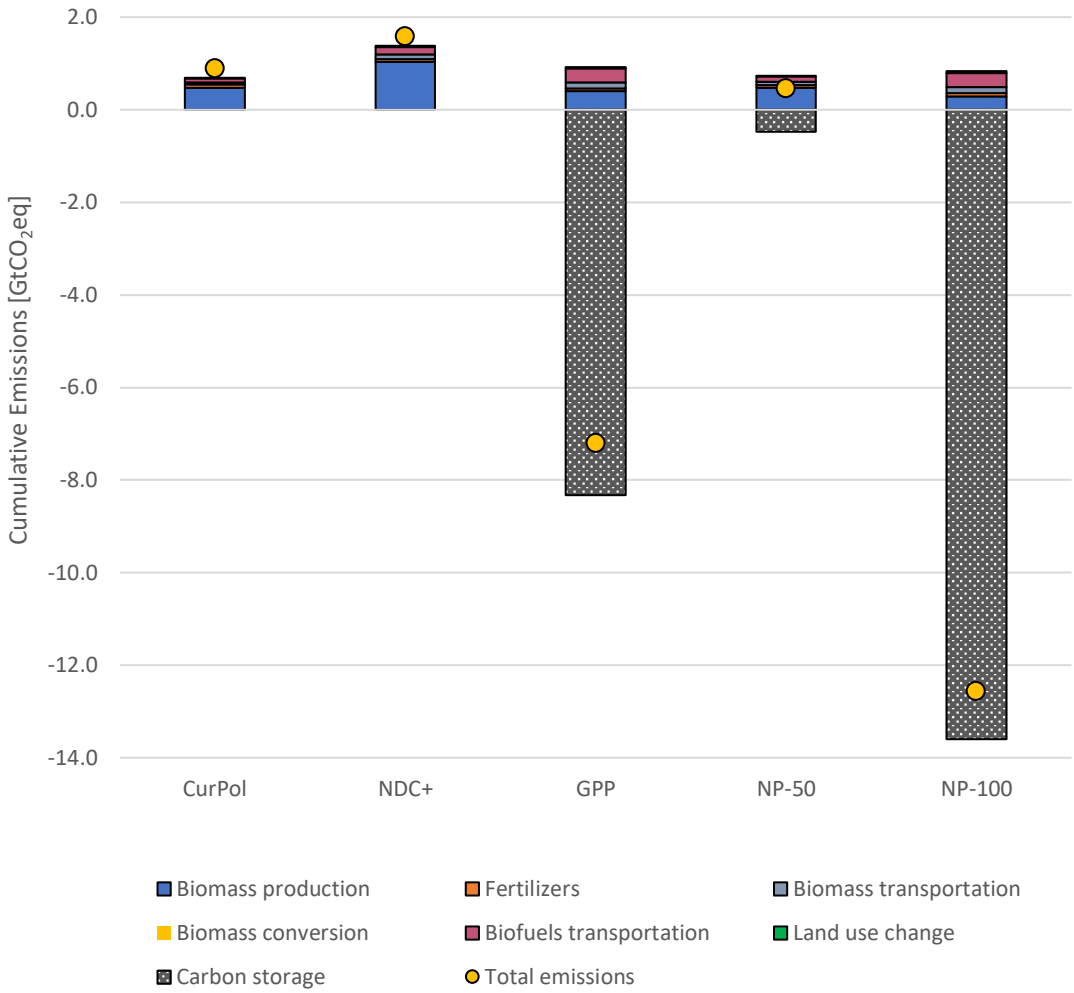

Figure 4.31. Breakdown of cumulative emissions (2020-2050), including negative emissions

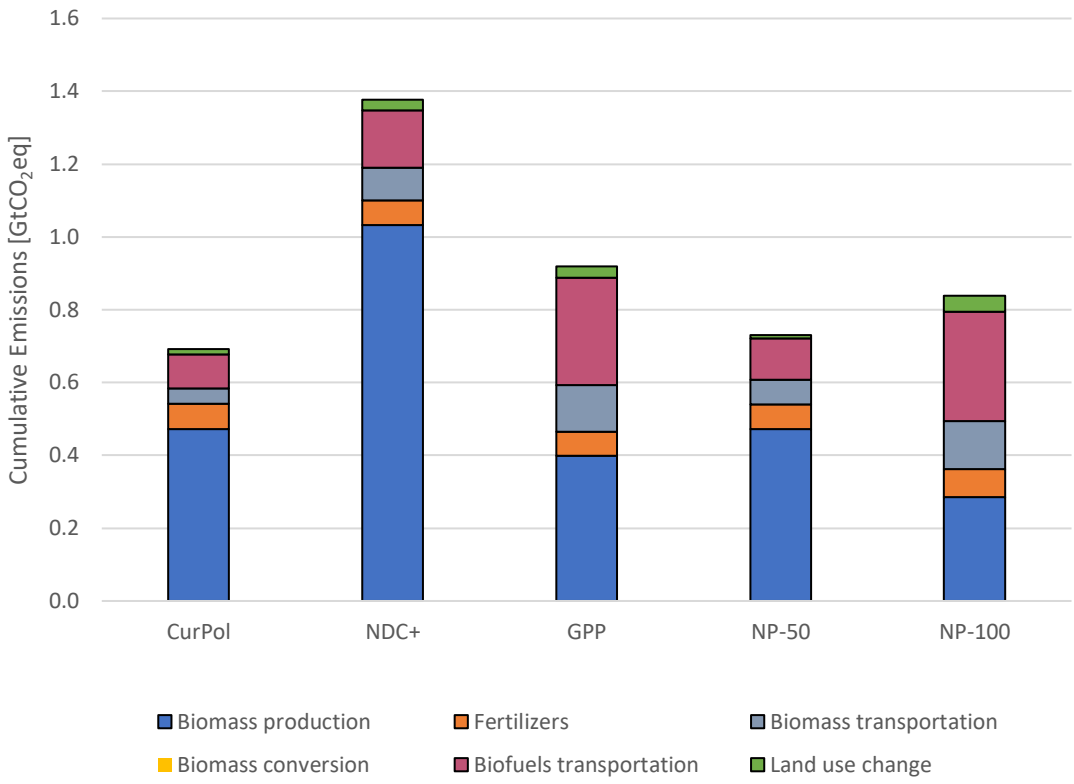

Figure 4.32. Breakdown of cumulative emissions (2020-2050), excluding negative emissions

Results indicate that up to 2030, cumulative emissions for CurPol, GPP and NP-50 follow similar trends. From 2030 on, CurPol has slightly higher emissions when compared to NP-50 (0.9 $GtCO_2eq$ and 0.5 $GtCO_2eq$, in 2050, respectively), while GPP diverges, going net negative and reaching -7.2 $GtCO_2eq$ in 2050. Even though NP-50 also includes carbon capture and storage technologies in its portfolio, the amount of CO_2 sequestration is not enough to offset the cumulative emissions before 2050. NP-100 is the scenario is the lowest cumulative emissions reaching -12.6 $GtCO_2eq$ by 2050, going net-negative early on in the projections.

As can be seen in Figure 4.32, for most scenarios, biomass production is the main contributor to GHG emissions. For CurPol, biomass production accounts for 53% of total emissions, followed by biofuels transportation (10%), fertilizer use (8%), biomass transportation (5%) and direct land use change (2%). For NDC+, biomass production corresponds to 66% of total emissions, followed by biofuels transportation (10%), biomass transportation (6%), fertilizer use (4%) and direct land use change (2%). For NP-50, excluding negative emissions, biomass production accounts for 51% of emissions,

followed by biofuels transportation (12%), biomass transportation and fertilizer use (both with 7% each), and direct land use change (1%).

For GPP, emissions shares are more balanced, with biomass production and biofuels transportation sharing respectively 36% and 26% of total emissions, excluding negative emissions, followed by biomass transportation (12%), fertilizer use (6%) and direct land use change (3%). Finally, for NP-100, biofuels transportation takes the lead with 29% of emissions, excluding negative emissions. Biomass production closely follows with 28%, while biomass transportation, fertilizer use and direct land use change account for 13%, 7% and 4% of emissions, respectively. In all scenarios, emissions from biomass conversion are negligible.

For both GPP and NP-100, results indicate that the expansion of the production of cellulosic biofuels imply in higher costs for transportation of both biomass (from the where the biomass is grown to where it is converted) and biofuels (from conversion to the consumer centers), which is evidence of the importance of encompassing logistics aspects to a more robust bioenergy value chain analysis. Furthermore, the results also point out to a trade-off between direct land use change emissions and the large deployment of carbon sequestration (BECCS technologies). While NP-100 and GPP are the scenarios with the largest observed direct land use change, they are also the scenarios with the most significant amount of carbon captured and stored, that highly offsets the positive emissions in the value chain.

5. Final Remarks

This chapter describes the findings and contributions of this thesis and addresses the limitations while providing suggestions for improvements and future work developments.

5.1 Findings, Contributions and Policy Implications

There are many challenges for the deployment of bioenergy and BECCS systems. This is relevant due to the role such systems are expected to play in many climate mitigation scenarios, heavily relying on negative emissions. Therefore, it is of the utmost importance the development of modelling frameworks capable of fully incorporating the various and diverse aspects of bioenergy systems. From this perspective, the main contribution from this study relies on the systemic approach of its methodological proposal, and the attempt to simultaneously embrace as many variables as possible, investigating how the whole system is organized and can be optimized.

While considering both the spatial and temporal dynamics of bioenergy systems, assessing the availability and demand for resources, properly allocating available land, and stablishing the necessary logistic interconnections, the model aims to provide a more robust evaluation of the role bioenergy and BECCS can actually fulfill, in terms of energy supply and climate mitigation, as well as offering support for policy making in sustainable bioenergy expansion. This is especially relevant for Brazil, given the importance of biomass and bioenergy for the current energy matrix and its expected role in the future, but can also be a powerful tool for other regions where the biomass potential could be relevant.

In this context, this thesis described the mathematical formulation of a spatially explicit, least-cost optimization model, called Bioenergy and Land Optimization spatially Explicit Model (BLOEM), and its application to the Brazilian context. This application of the model represents the Brazilian bioenergy system at a considerable level of detail, i.e., on a grid basis with 2912 grid cells of approximately 50 km per 50 km. Model validation was based on the comparison of current land allocation and system distribution for the base year, i.e., 2020, to which the results indicate that the model provides a good fit.

IAMs projections usually make use of stylized assumptions about resource costs and logistical constraints for large regions. Using BLOEM, the feasibility of IAMs projections can be downscaled while accounting for logistical constraints, such as transportation of feedstocks and final products, CO_2 transportation and storage, conversion capital, hotspots for system expansion, location of conversion facilities and their connection to distribution and consumer centers. In this thesis, results for five scenarios from BLUES were downscaled (CurPol, NDC+, GPP, NP-50 and NP-100). For all scenarios, with different levels of ambition, the model was able to provide insights on total system costs, geographically detailing the system distribution and expansion, and the corresponding level of emissions.

In comparing the different levels of ambition, results indicate an important trade-off between direct land use change and negative emissions: the scenarios where the stringent climate goals lead to a substantial amount of negative emissions were the ones with the highest observed direct land use changes. In such cases, the negative emissions largely offset the positive emissions from the rest of the system. Another important trade-off involves costs and emissions related to the transportation of biofuels from conversion units to demand centers and the transportation of the CO_2 captured (when applicable).

Sugarcane has the highest production potentials (19.8 EJ/year, in 2050) and the lowest production costs (below 8 US$/GJ throughout the 2020-2050 period). Biomass production (mostly related to fuel use for farming) and biomass and biofuel transportation (from conversion site to demand centers) are the major contributors to the bioenergy value chain emissions. However, for this case study, emission factors are deemed constant and assume that the fleets (tractors and trucks) will remain fueled by fossil diesel. Therefore, a potential future electrification of the fleet or a shift towards biofuels or less carbon intensive fuels could substantially reduce these emissions, resulting in much lower emissions for the value chain.

Only the land categories of bioenergy land and other land (which includes savannahs, grasslands, scrublands and others) are deemed available for the expansion of bioenergy crops. Forests, pastures and agricultural areas are off-limits. Overall, results indicate that there is enough land for bioenergy expansion without impacts on forests and other protected areas or direct threats to food security and agricultural areas (the model follows a food-first principle), even in scenarios with large production of biofuels. An even more stringent land availability was tested, running the large cellulosic biofuels

scenarios (GPP, with over 3 EJ of cellulosic biofuels in 2050, and NP-100, with approximately 4 EJ of cellulosic biofuels in 2050) where only IMAGE projected bioenergy land was deemed available for bioenergy crops (excluding savannahs, grasslands, scrublands). The model has proven infeasible in such cases, which indicates that such levels of bioenergy production cannot be met without direct land use change.

Finally, a major contribution of this thesis and the development of BLOEM lies on the spatial results it provides. Crop allocation and the logistics dynamics between production, conversion, demand and, in some cases, negative emissions and carbon storage, provide valuable insights for regional and national policy design, making this a useful tool for mapping bioenergy value chain pathways. Furthermore, the interaction with global/national IAMs results, downscaling them to a spatially explicit level and taking into account the local context, in order to develop a more robust regional assessment of climate mitigation strategies. For instance, in the results of this study the more ambitious scenarios for bioenergy production show a significant expansion of wood production in the Northeast and the Center-South, which could have severe implications for water management in the already water scarce regions, and for the biodiversity of the Caatinga and the Cerrado ecosystems, which reinforces the need to protect already highly degraded forests and natural land areas such as the Atlantic Forest and Cerrado.

5.2 Current Limitations and Future Work Recommendations

Being a mathematical cost-optimal model representing a real non-optimal world, BLOEM has intrinsic uncertainties and limitations. Moreover, BLOEM is a spatially explicit model, with typical limitations regarding data availability, increased computational effort and model complexity. In this sense, the formulation of the model as well as the solution methods applied (e.g., the choice for a linear model while avoiding the use of binary variables in a mixed-integer approach) were carefully considered to deal with the trade-off between computational effort and model complexity.

In modelling logistics, BLOEM assumes that all grid cells are connected by their centroids and does not take into account existing roads, transport networks, or potential natural barriers. The incorporation of geographically referenced information on roads connections and other factors (e.g., road quality, time of travel) could improve the logistics module in the model, but the trade-off between increasing complexity and computational effort needs to be taken into account. Furthermore, in dealing with the

distribution of biofuels, conversion units are directly connected to the demand centers, not accounting for an intermediate step with distribution centers and hubs. However, even with these limitations, the case study shows that logistics plays an important role in the optimization decisions, leading to a better calibration of the model's results.

In terms of data availability, storage sites options for CO_2 storage in this study were limited to depleted oil and gas fields due to the lack of robust knowledge about other options, e.g., saline aquifers (onshore and offshore), regarding costs, injection patterns, geological characteristics, stability, risks of leakage and safety of storage. The inclusion of these options in the model could significantly reduce the costs related to carbon transportation, shifting the system configuration as well as its expected expansion across regions.

BLOEM currently does not include the dynamics between energy crops and food crops, nor the related indirect land use change effects and resulting indirect land use change emissions. Such dynamics, as well as the carbon stocks flows for changes in land use and land cover, are exogenously applied based on IMAGE projections. By applying a food-first principle, the model assumes that food crops have preference over energy crops in land allocation, and thus indirect land use change is not modelled (or relevant). This assumption is not necessarily true in the real non-cost-optimal world, where for various reasons, from the social and economic to the political spheres, large scale deployments of bioenergy might induce shifts in agricultural areas, resulting in indirect land use changes, and endangering protected biomes and biodiversity due to illegal deforestation. This is a limitation of BLOEM, at the moment. Improvements in this regard are expected in future developments.

Current developments and work in progress include a study on the Brazilian NDC, in which different land availability scenarios are applied in order to evaluate the recovery of degraded pastures for bioenergy production and the role of carbon prices in land allocation and the preservation of protected areas. Other future work recommendations and suggestions for model improvements include:

(i) incorporating the competition with food crops, in order to address indirect land use changes and their emissions,

(ii) adding a season dimension to the model, to account for the seasonality of crops and the complementarity between them,

(iii) adding the options of double crops (which also relates to the seasonality above mentioned) and of integrated crop-livestock-forestry systems,

(iv) adding feedstocks, most importantly agricultural and forestry residues,

(v) adding conversion routes, such as alcohol-to-jet and routes to produce biofuels for maritime transportation, as well as the option of co-processing of biomass (in e.g., existing oil refineries),

(vi) better representing the transport networks, improving the logistics modules for biomass and biofuels,

(vii) adding water constraints, since up until now all bioenergy crops are considered to be rainfed, and the availability of land does not account for the exclusion of areas which are classified as arid or water scarce,

(viii) including impacts on biodiversity, to ensure that biodiversity losses are taken into account in the model decisions.

References

Akgul et al., 2011. Optimization-based approaches for bioethanol supply chains. *Industrial & Engineering Chemistry Research*, 50, 4927-4938.

Akgul et al., 2014. A mixed integer nonlinear programming (MINLP) supply chain optimisation framework for carbon negative electricity generation using biomass to energy with CCS (BECCS) in the UK. *International Journal of Greenhouse Gas Control*, 28, 189-202.

Angelkorte G., 2019. Modelagem do setor agropecuário dentro de modelo de análise integrada brasileiro. MSc Dissertation. *Universidade Federal do Rio de Janeiro* (COPPE/UFRJ). Rio de Janeiro, Brazil.

ANP, 2020. Oil, Natural Gas and Biofuels Statistical Yearbook 2020. Agência Nacional do Petróleo, Gás Natural e Biocombustíveis – Rio de Janeiro: ANP, 2020.

ANP, 2021. RenovaBio. Available at: https://www.gov.br/anp/pt-br/assuntos/renovabio.

Brasil, 2020. Brazil's Nationally Determined Contribution (NDC). Ministério do Meio Ambiente. Brasília, Brazil.

Brasil, 2021. Brazil's Updated Nationally Determined Contribution (NDC). Ministério do Meio Ambiente. Brasília, Brazil.

Calvin et al., 2021. Bioenergy for climate change mitigation: Scale and sustainability. *GCB Bioenergy*, 13, 1346-1371.

Clarke et al., 2014. Assessing transformation pathways. *Climate Change 2014: Mitigation of Climate Change. Contribution of Working Group III to the Fifth Assessment Report of the Intergovernmental Panel on Climate Change*, Cambridge, Cambridge University Press.

CNPEM, 2017. Barreiras regulatórias para comercialização de eletricidade por usinas sucroalcooleiras. Centro Nacional de Pesquisa em Energia e Materiais – São Paulo: CNPEM, 2017.

Creutzig et al., 2013. Integrating place-specific livelihood and equity outcomes into global assessments of bioenergy deployment. *Environmental Research Letters*, 8, 035047.

Creutzig F., 2016. Economic and ecological views on climate change mitigation with bioenergy and negative emissions. *GCB Bioenergy,* 8, 4-10.

Daioglou et al., 2017. Greenhouse gas emission curves for advanced biofuel supply chains. *Nature Climate Change,* 7, 920-924.

Daioglou et al., 2019. Integrated assessment of biomass supply and demand in climate change mitigation scenarios. *Global Environmental Change,* 54, 88-101.

Daioglou et al., 2020. Bioenergy technologies in long-run climate change mitigation: results from the EMF-33 study. *Climatic Change,* 163, 1603-1620.

Doelman et al., 2020. Afforestation for climate change mitigation: Potentials, risks and trade-offs. *Global Change Biology,* 26, 1576-1591.

Dooley J., 2013. Estimating the supply and demand for deep geologic CO_2 storage capacity over the course of the 21st century: a meta-analysis of the literature. *Energy Procedia,* 37, 5141-5150.

Duden et al., 2017. Modeling the impacts of wood pellet demand on forest dynamics in southeastern United States. *Biofuels, Bioproducts and Biorefining,* 11, 1007-1029.

EPE, 2012. Brazilian Energy Balance 2012 Year 2011. Empresa de Pesquisa Energética – Rio de Janeiro: EPE, 2012.

EPE, 2016. Energia Renovável – Hidráulica, Biomassa, Eólica, Solar e Geotérmica. Empresa de Pesquisa Energética – Rio de Janeiro: EPE, 2016.

EPE, 2021a. Brazilian Energy Balance 2021 Year 2020. Empresa de Pesquisa Energética – Rio de Janeiro: EPE, 2021.

EPE, 2021b. WEBMAP EPE. Energy Research Office (EPE). Rio de Janeiro. Available at: https://www.epe.gov.br/en/publications/publications/webmap-epe

Fajardy et al., 2018. Investigating the BECCS resource nexus: delivering sustainable negative emissions. *Energy and Environmental Science,* 11, 3408-3430.

Fajardy M., 2020. Developing a framework for the optimal deployment of negative emissions technologies. PhD Thesis. Centre for Environmental Policy and Centre for Process Systems Engineering, Imperial College London. London, UK.

FAO, 2018. Oilseeds and oilseed products. OECD-FAO Agricultural Outlook 2018-2027. Food and Agriculture Organization of the United Nations (FAO).

Fuss et al., 2018. Negative emissions – Part 2: Costs, potentials and side effects. *Environmental Research Letters*, 13, 063002.

Garcia et al., 2018. Increasing biomass demand enlarges negative forest nutrient budget areas in wood export regions. *Scientific Reports*, 8, 5280.

Gough C. and Upham P., 2011. Biomass energy with carbon capture and storage (BECCS or Bio-CCS). *Greenhouse Gases Science and Technology*, 1, 324-334.

Gough et al., 2018. Challenges to the use of BECCS as a keystone technology in pursuit of 1.5°C. *Global Sustainability*, 1, 1-9.

Hanssen et al., 2019. Biomass residues as twenty-first century bioenergy feedstock – a comparison of eight integrated assessment models. *Climatic Change*, 163, 1569-1586.

Hanssen et al., 2020. The climate change mitigation potential of bioenergy with carbon capture and storage. *Nature Climate Change*, 10, 1023-1029.

Hasegawa et al., 2020. Food security under high bioenergy demand toward long-term climate goals. *Climatic Change*, 163, 1587-1601.

van der Hilst et al., 2014. Integrated spatiotemporal modelling of bioenergy production potentials, agricultural land use, and related GHG balances; demonstrated for Ukraine. *Biofuels, Bioproducts and Biorefining*, 8, 391-411.

Humpenöder et al., 2018. Large-scale bioenergy production: how to resolve sustainability trade-offs? *Environmental Research Letters*, 13, 024011.

IAMC, 2021a. COFFEE-TEA. Model Documentation. Integrated Assessment Modelling Consortium – IAMC wiki. Available at: https://www.iamcdocumentation.eu/

IAMC, 2021b. IMAGE. Model Documentation. Integrated Assessment Modelling Consortium – IAMC wiki. Available at: https://www.iamcdocumentation.eu/

IAMC, 2021c. MESSAGE-GLOBIOM. Model Documentation. Integrated Assessment Modelling Consortium – IAMC wiki. Available at: https://www.iamcdocumentation.eu/

IAMC, 2021d. REMIND-MAgPIE. Model Documentation. Integrated Assessment Modelling Consortium – IAMC wiki. Available at: https://www.iamcdocumentation.eu/

IAMC, 2021e. AIM-Hub. Model Documentation. Integrated Assessment Modelling Consortium – IAMC wiki. Available at: https://www.iamcdocumentation.eu/

IBGE, 2020a. Population Estimates – Year 2020. Brazilian Institute of Geography and Statistics. Available at: https://www.ibge.gov.br/en/statistics/social/population/18448-estimates-of-resident-population-for-municipalities-and-federation-units.html?edicao=28688&t=resultados

IBGE, 2020b. PAM – Municipal Agricultural Production. Brazilian Institute Geography and Statistics. Available at: https://www.ibge.gov.br/en/statistics/economic/agriculture-forestry-and-fishing/16773-municipal-agricultural-production-temporary-and-permanent-crops.html?=&t=o-que-e

IEA, 2020. Fuels and Technology: Bioenergy. Available at: https://www.iea.org/fuels-and-technologies/bioenergy.

IEA, 2021. Net Zero by 2050. A Roadmap for the Global Energy Sector. Special Report. International Energy Agency. October 2021.

IEA Bioenergy, 2021. Commercializing conventional and advanced transport biofuels from biomass and other renewable feedstocks. IEA Bioenergy, Task 39. November 2021. Available at: https://task39.ieabioenergy.com/about/definitions/.

IIASA, 2021. BeWhere. International Institute for Applied Systems Analysis. Available at: https://iiasa.ac.at/web/home/research/researchPrograms/EcosystemsServicesandManagement/BEWHERE/BEWHERE.en.html

IPCC, 2006. 2006 IPCC Guidelines for National Greenhouse Gas Inventories, Prepared by the National Greenhouse Gas Inventories Programme, Eggleston H.S., Buendia L., Miwa K., Ngara T. and Tanabe K. (eds). Published: IGES, Japan.

IPCC, 2014. *Climate Change 2014: Mitigation of Climate Change. Contribution of Working Group III to the Fifth Assessment Report of the Intergovernmental Panel on Climate Change*, Cambridge, Cambridge University Press.

IRENA, 2021. Bioenergy. International Renewable Energy Agency. November 2021. Available at: https://www.irena.org/bioenergy.

JGCRI, 2021. Global Change Analysis Model. Joint Global Change Research Institute. Available at: http://www.globalchange.umd.edu/gcam/

Jia et al., 2019. Land–climate interactions. Climate Change and Land: an IPCC special report on climate change, desertification, land degradation, sustainable land management, food security, and greenhouse gas fluxes in terrestrial ecosystems. IPCC.

Kalt et al., 2020. Greenhouse gas implications of mobilizing agricultural biomass for energy: a reassessment of global potentials in 2050 under different food-system pathways. *Environmental Research Letters,* 15, 034066.

Kemper, J., 2015. Biomass and carbon dioxide capture and storage: A review. *International Journal of Greenhouse Gas Control*, 40, 401-430.

Koberle et al., 2021. Can global models provide insights into regional mitigation strategies? A diagnostic model comparison study of bioenergy in Brazil. *Climatic Change,* In Review.

Khan et al., 2009. Biomass combustion in fluidized bed boilers: Potential problems and remedies. *Fuel Processing Technology,* 90, 21-50.

Khatiwada et al., 2016. Optimizing ethanol and bioelectricity production in sugarcane biorefineries in Brazil. *Renewable Energy,* 85, 371-386.

Kriegler et al., 2013. Is atmospheric carbon dioxide removal a game changer for climate change mitigation? *Climatic Change,* 118, 45-57.

Kriegler et al., 2017. Fossil-fueled development (SSP5): An energy and resource intensive scenario for the 21st century. *Global Environmental Change,* 42, 297-315.

Krook-Riekkola et al., 2017. Challenges in top-down and bottom-up soft-linking: Lessons from linking a Swedish energy system model with a CGE model. *Energy*, 141, 803-817.

Lin et al., 2014. Integrated strategic and tactical biomass–biofuel supply chain optimization. *Bioresource Technology,* 156, 256-266.

Marvin et al., 2012. Economic optimization of a lignocellulosic biomass-to-ethanol supply chain. *Chemical Engineering Science,* 67, 68-79.

Minx et al., 2018. Negative emissions – Part 1: Research landscape and synthesis. *Environmental Research Letters*, 13, 063001.

Nemet et al., 2018. Negative emissions – Part 3: Innovation and upscaling. *Environmental Research Letters*, 13, 063003.

Nogueira T., 2020. Avaliação de alternativas de transporte offshore de CO_2 no Brasil. MSc Dissertation. *Universidade Federal do Rio de Janeiro* (COPPE/UFRJ). Rio de Janeiro, Brazil.

Oliveira C., 2020. Biomass-to-chemicals in energy transition scenarios: The case of Brazil. DSc Thesis. *Universidade Federal do Rio de Janeiro* (COPPE/UFRJ). Rio de Janeiro, Brazil.

Oliveira et al., 2020. CO_2 injection of ethanol distilleries in mature northeastern fields. Rio Oil & Gas 2020: Technical Papers. IBP – Rio de Janeiro, Brazil.

Pinder C., 2014. Moving below zero: Understanding bioenergy with carbon capture and storage. The Climate Institute. Sydney, Australia.

Riahi et al., 2021. Long-term economic benefits of stabilizing warming without overshoot – the ENGAGE model intercomparison. *Nature Portfolio,* In Review.

Rochedo P.R.R., 2016. Development of a global integrated energy model to evaluate the Brazilian role in climate mitigation scenarios. DSc Thesis. *Universidade Federal do Rio de Janeiro* (COPPE/UFRJ). Rio de Janeiro, Brazil.

Rochedo et al., 2018. The threat of political bargaining to climate mitigation in Brazil. *Nature Climate Change,* 8, 695-698.

Rogelj et al., 2016. Differences between carbon budget estimates unraveled. *Nature Climate Change*, 6, 245-252.

Rogelj et al., 2018. Scenarios towards limiting climate change below 1.5°C. *Nature Climate Change,* 8, 325-332.

Rose et al., 2020. An overview of the Energy Modelling Forum 33rd study: assessing large-scale global bioenergy deployment for managing climate change. *Climatic Change,* 163, 1539-1551.

Samsatli et al., 2015. BVCM: A comprehensive and flexible toolkit for whole system biomass value chain analysis and optimisation – Mathematical formulation. *Applied Energy,* 147, 131-160.

da Silva et al., 2018. CO_2 capture in ethanol distilleries in Brazil: Designing the optimum carbon transportation network by integrating hubs, pipelines and trucks. *International Journal of Greenhouse Gas Control,* 71, 168-183.

Smith et al., 2014. Agriculture, forestry and other land use. *Climate Change: Mitigation of Climate Change. Contribution of Working Group III to the Fifth Assessment Report of*

the Intergovernmental Panel on Climate Change, IPCC, Cambridge, Cambridge University Press.

Smith et al., 2016. Biophysical and economic limits to negative CO_2 emissions. *Nature Climate Change*, 6, 42-50.

Speight J., 2019. Chapter 13 – Upgrading by Gasification. Heavy Oil Recovery and Upgrading, 559-614. Gulf Professional Publishing. Laramie, WY, United States.

Stenzel et al., 2020. Global scenarios of irrigation water use for bioenergy production: a systematic review. *Hydrology and Earth System Sciences*, Discussions, EGU.

Tagomori I., 2017. Potencial técnico e econômico para a produção de Fischer-Tropsch diesel a partir de biomassa (FT-BTL) associada à captura de carbono no Brasil. MSc Dissertation. *Universidade Federal do Rio de Janeiro* (COPPE/UFRJ). Rio de Janeiro, Brazil.

Tagomori et al., 2018. Designing an optimum carbon capture and transportation network by integrating ethanol distilleries with fossil-fuel processing plants in Brazil. *International Journal of Greenhouse Gas Control*, 68, 112-127.

Tagomori et al., 2019. Techno-economic and georeferenced analysis of forestry residues-based Fischer-Tropsch diesel with carbon capture in Brazil. *Biomass and Bioenergy*, 123, 134-148.

UNICA, 2020. Production data: Sugarcane Planted Area. Observatório da Cana. Available at: https://observatoriodacana.com.br/sub.php?menu=producao

Vera et al., 2020. Spatial variation in environmental impacts of sugarcane expansion in Brazil. *Land*, 9, 397.

Verstegen et al., 2012. Spatio-temporal uncertainty in Spatial Decision Support Systems: A case study of changing land availability for bioenergy crops in Mozambique. *Computers, Environment and Urban Systems*, 36, 30-42.

Verstegen et al., 2015. What can and can't we say about indirect land-use change in Brazil using an integrated economic – land-use change model? *GCB Bioenergy*, 8, 561-578.

Verstegen et al., 2019. Recent and projected impacts of land use and land cover changes on carbon stocks and biodiversity in East Kalimantan, Indonesia. *Ecological Indicators*, 103, 563-575.

van Vuuren et al., 2013. The role of negative CO_2 emissions for reaching 2°C – insights from integrated assessment modelling. *Climatic Change,* 118, 15-27.

Wu et al., 2019. Global advanced bioenergy potential under environmental protection policies and societal transformation measures. *GCB Bioenergy,* 11, 1041-1055.

You et al., 2011. Optimal design of sustainable cellulosic biofuel supply chains: Multiobjective optimization coupled with life cycle assessment and input-output analysis. *The American Institute of Chemical Engineers (AIChE) Journal,* 58, 1157-1180.

Zhang et al., 2020. Unlocking the potential of BECCS with indigenous sources of biomass at a national scale. *Sustainable Energy & Fuels,* 4, 226-253.

Annex I

Figure AI.1. Brazilian Regions

Annex II

Table AII.1: Parameters

Parameter	Description
LdAv (l,c,t)	Fraction of land available for bioenergy
Co^{BP} (r,c,t)	Biomass production costs [US$/GJ]
Ga (c)	Grid cell area [km^2]
Y (r,c,t)	Biomass yields [GJ/km^2]
ef (r,l,c)	Emission factor for direct land use change [tCO_2/GJ]
ef^i (r,c)	Emission factor for instantaneous land use change [tCO_2/km^2]
ef^g (r,c,q)	Emission factor for gradual land use change [tCO_2/km^2]
k^* (t)	Carbon price [US$/$tCO_2$]
df (t)	Discount factor
TCI (j,c,t)	Total capital investments [US$/GJ] [US$/kW]
FOM (j,c,t)	Fixed O&M costs [US$/GJ] [US$/kW]
VOM (j,c,t)	Variable O&M costs [US$/GJ/year] [US$/kW/year]
w (j)	Technology discount factor
v	Discount rate
p	Period in lifetime of a technology facility
l (j)	Lifetime of a technology facility
CE (j,c,t)	Existing capacity in time t_1 [GJ] [kW]
CRE (j,c,t)	Retirement of existing capacities [GJ] [kW]
rf (j,t`,t)	Retirement factor
cf (j,t)	Capacity factor
ß (r,j)	Conversion efficiencies (ratio of consumption or production)
γ (j)	CO_2 capture efficiency [tCO_2/GJ]
TrCo (r)	Transportation costs [US$/GJ/km]
MX (c,c`)	Distance between grid cells [km]

Table AI.1: (Cont.) Parameters

Parameter	Description
τ (c)	Tortuosity factor
OnCo (c,c`)	Onshore costs of CO_2 transportation [US$/t$CO_2$]
OfCo (c)	Offshore costs of CO_2 transportation [US$/t$CO_2$]
MaxSt (c)	Maximum storage capacity of a storage site [tCO_2]
fp (r)	Fuel consumption for biomass production [l/GJ]
fd	Fuel emission factor (conventional diesel fuel) [tCO_2/l]
eff (r)	Emission factor for fertilizer use [tN_2O/km^2]
nf	Conversion factor tCO_2/tN_2O
eft (r)	Emission factor for biomass transportation [tCO_2/GJ/km]
efw (r)	Emission factor for bioenergy product transportation [tCO_2/GJ/km]
efc (r)	Emission factor for biomass conversion [tCO_2/GJ]
Pb (r,c,t)	Bioenergy production target [GJ] [kW]
Ex (r,c,t)	Bioenergy export target [GJ] [kW]
FCo (r,c,t)	Farm gate costs [US$/km^2]
LRt (c,t)	Land rent [US$/km^2]
TpCo (r)	Biomass collection costs (within the grid cell) [US$/GJ]
FlagBT (c,c`)	Flag to determine logistic interconnections [binary]
PopDen (c)	Population density

Annex III

Table AIII.1: Variables

Variable	Description
Z	Total system cost [US$]
I_t^{BP}	Impact of biomass production in time t [US$]
I_t^{BT}	Impact of biomass transportation in time t [US$]
I_t^{BC}	Impact of biomass conversion in time t [US$]
I_t^{ET}	Impact of bioenergy product transportation in time t [US$]
I_t^{CC}	Impact of carbon transportation and storage in time t [US$]
I_t^{TG}	Impact of GHG emissions in time t [US$]
I_t^{TCI}	Impact of total capital investments [US$]
I_t^{TOM}	Impact of O&M costs [US$]
A (r,l,c,t)	Fraction of grid cell allocated to bioenergy production
B (r,l,c,t)	Biomass production in grid cell c in time t [GJ]
CJ (j,c,t)	Installed capacity [GJ] [kW]
CA (j,c,t)	Added capacity [GJ] [kW]
CR (j,c,t)	Retired capacity [GJ] [kW]
CP (j,c,t)	Rate of operation of technologies [GJ/year] [kW/year]
E (r,c,t)	Bioenergy production [GJ] [kW]
I (r,c,t)	Intermediate products production [GJ] [kW]
S (r,c,t)	Co-products production [GJ] [t]
HB (r,c,t)	Biomass local consumption [GJ]
HE (r,c,t)	Bioenergy products local consumption [GJ] [kW]
Bn (r,c,c‘,t)	Flow of biomass between grid cells [GJ]
En (r,c,c‘,t)	Flow of bioenergy products between grid cells [GJ]
Vcap (c,t)	CO_2 captured [tCO_2]
Vseq (c,t)	CO_2 sequestrated [tCO_2]

Table AII.2: (Cont.) Variables

Variable	Description
Vn (c,c‘,t)	Flow of CO_2 between grid cells [tCO_2]
GG (t)	GHG emissions [tCO_2eq]
Gbp (t)	Emissions from biomass production [tCO_2eq]
Gfr (t)	Emissions from fertilizer use [tCO_2eq]
Gbt (t)	Emissions from biomass transportation [tCO_2eq]
Gbc (t)	Emissions from biomass conversion [tCO_2eq]
Get (t)	Emissions from bioenergy products transportation [tCO_2eq]
Glc^{i}_{t} (t)	Instantaneous emissions from direct land use change [tCO_2eq]
Glc^{g}_{t} (t)	Gradual emissions from direct land use change [tCO_2eq]
Po^{BP} (r,c,t)	Biomass supply potential [GJ]
Co^{BP} (r,c,t)	Biomass supply cost [US$/GJ]

Annex IV

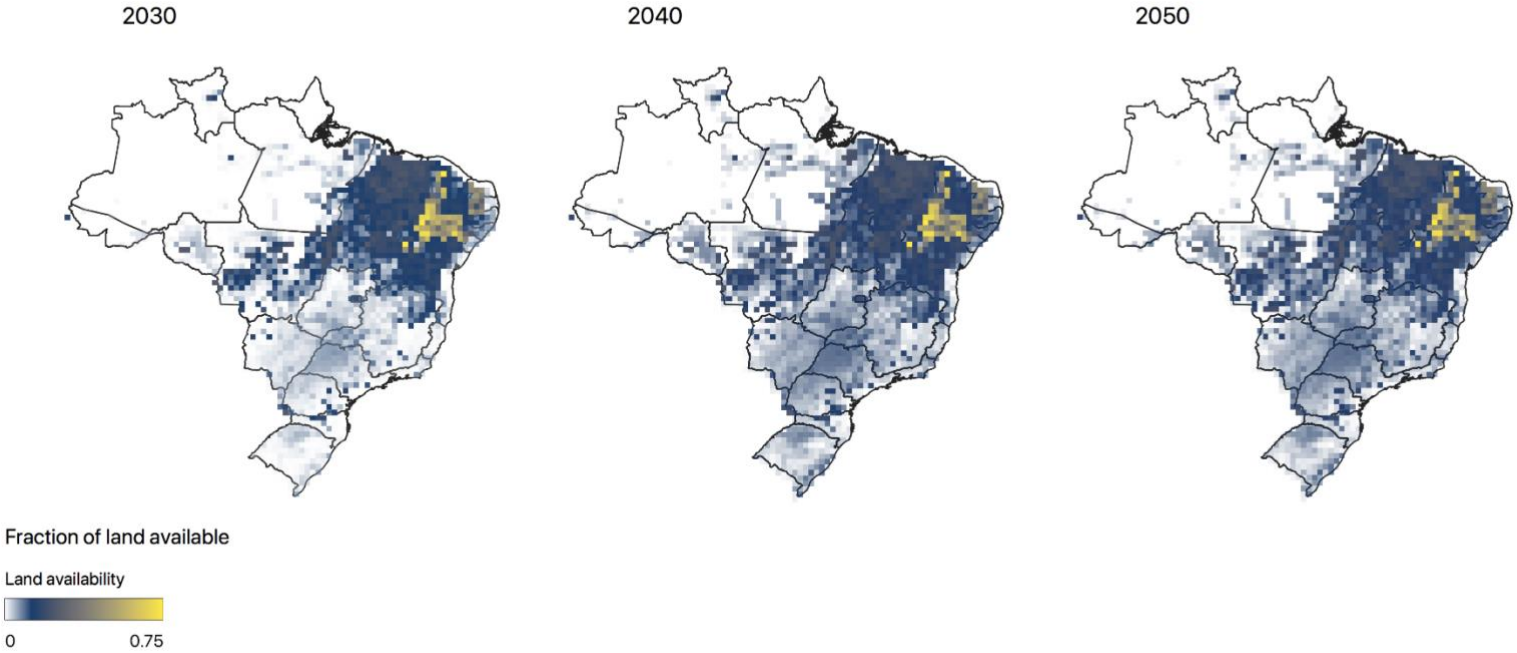

Figure AIV.1. Land Availability (2030-2050)

Annex V

Table AV.1: Management factors and water content

Crop / Decade		Management Factor	Water Content
Sugarcane	2020	1.278855	0.725
	2030	1.307314	
	2040	1.320934	
	2050	1.341298	
Oil Crops	2020	0.832788	0.010
	2030	0.907526	
	2040	0.997520	
	2050	1.093181	
Woody	2020	2.240444	0.080
	2030	1.686034	
	2040	1.552032	
	2050	1.483401	
Grassy	2020	0.640723	0.100
	2030	0.714920	
	2040	0.788991	
	2050	0.854272	
Maize	2020	4.542897	0.700
	2030	4.975124	
	2040	5.421125	
	2050	5.962096	

Annex VI

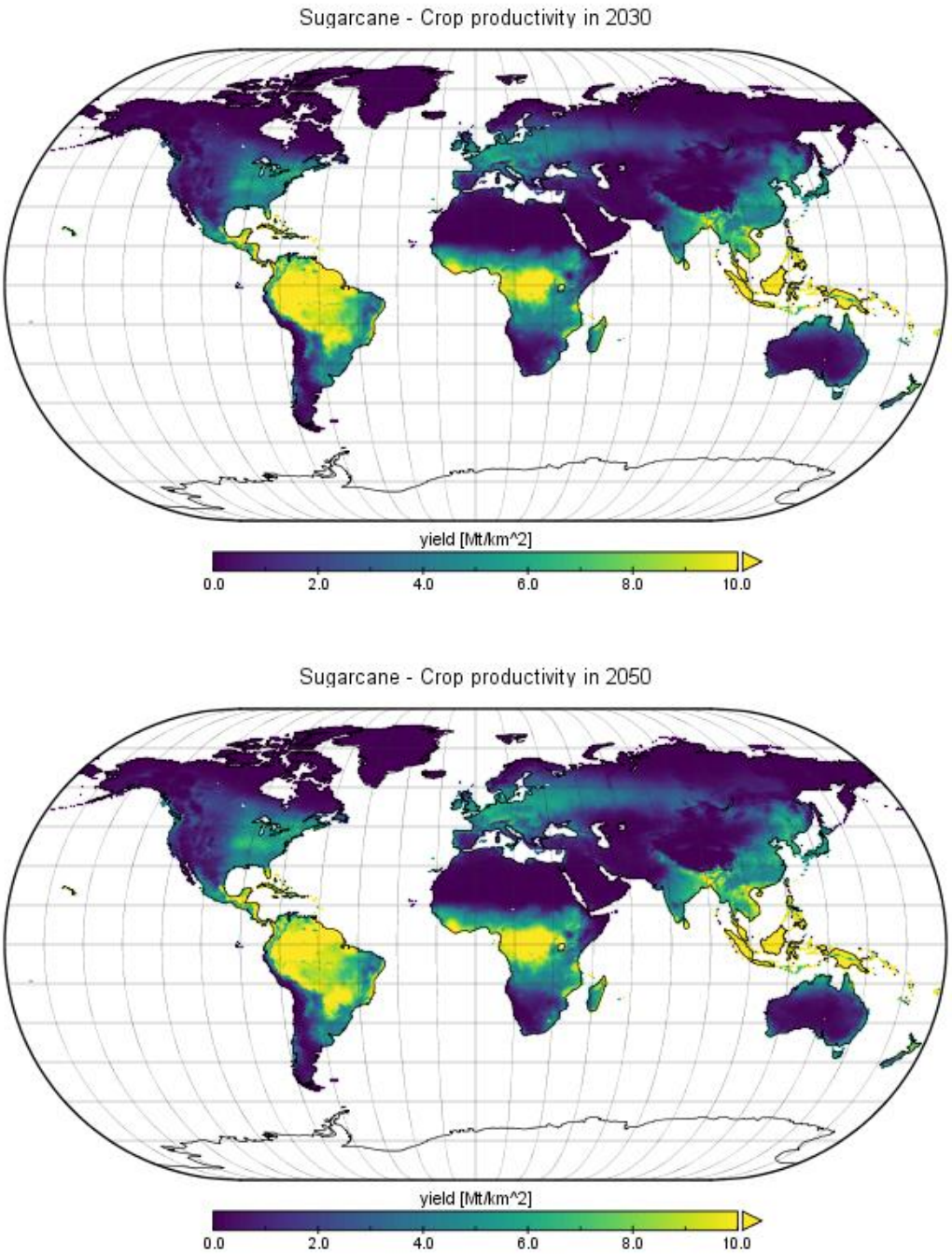

Figure AVI.1. Sugarcane – Crop Productivity (2030;2050)

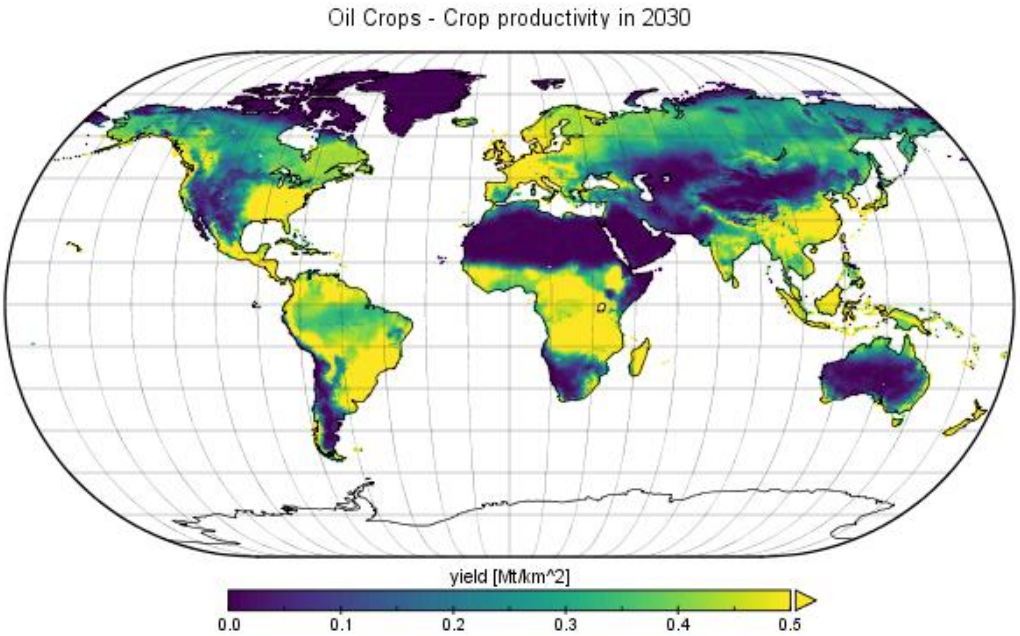

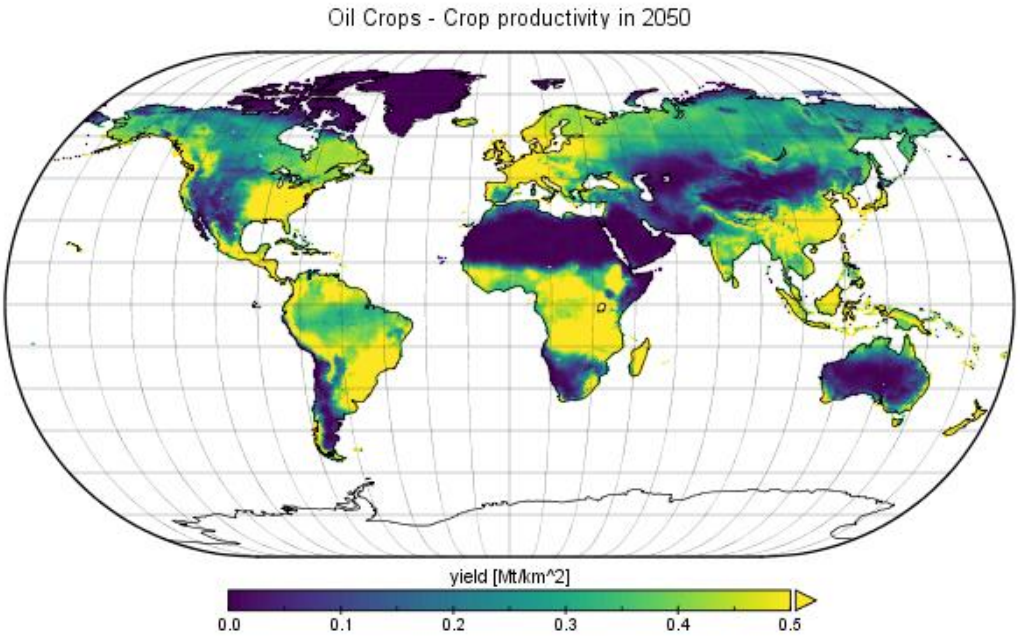

Figure AVI.2. Oil Crops – Crop Productivity (2030;2050)

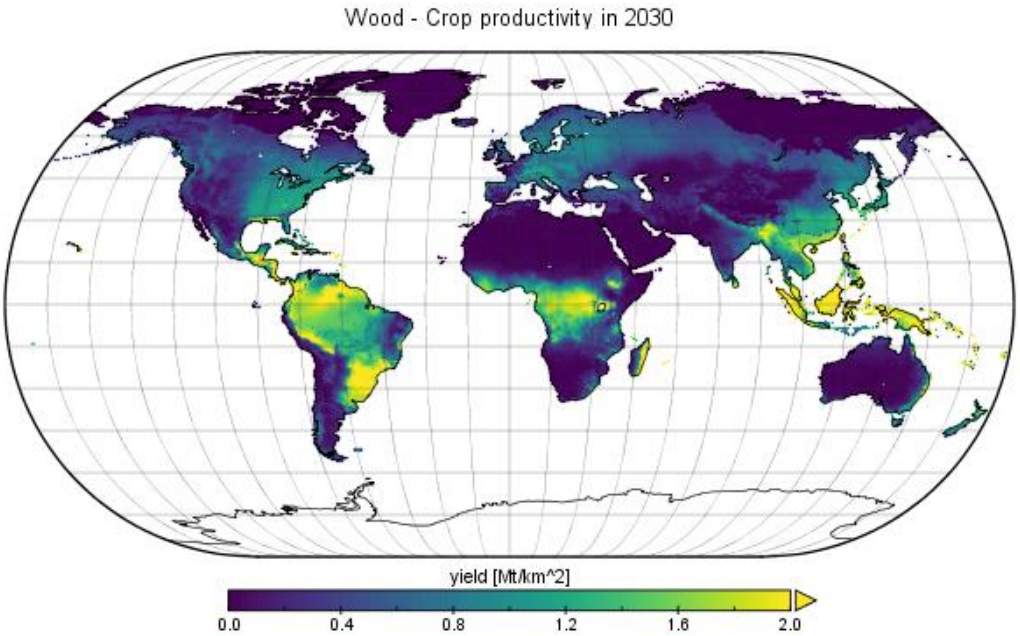

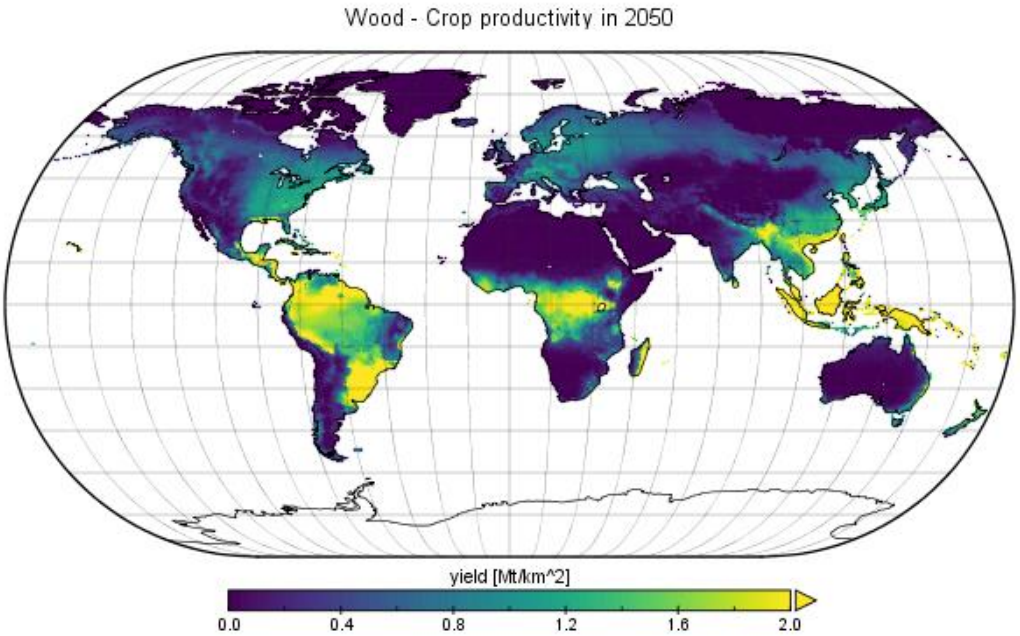

Figure AVI.3. Wood – Crop Productivity (2030;2050)

Annex VII

Table AVII.1: Farm gate costs and collection costs

Crop / Region		Farm Gate Costs (US$/ha)	Collection Costs (US$/GJ)
Sugarcane	North	659.80	0.73
	Northeast	531.93	
	Center-West	578.56	
	Southeast	559.28	
	South	440.98	
Oil Crops	North	1,995.79	0.24
	Northeast	1,972.42	
	Center-West	2,040.01	
	Southeast	1,968.93	
	South	1,844.44	
Woody	North	248.68	0.36
	Northeast	204.02	
	Center-West	213.50	
	Southeast	194.10	
	South	176.40	
Grassy	North	1,199.17	0.58
	Northeast	1,115.01	
	Center-West	1,135.54	
	Southeast	1,079.54	
	South	1,096.91	
Maize	North	848.95	0.26
	Northeast	752.48	
	Center-West	1,633.52	
	Southeast	1,548.15	
	South	1,427.73	

Based on Angelkorte (2019)

Annex VIII

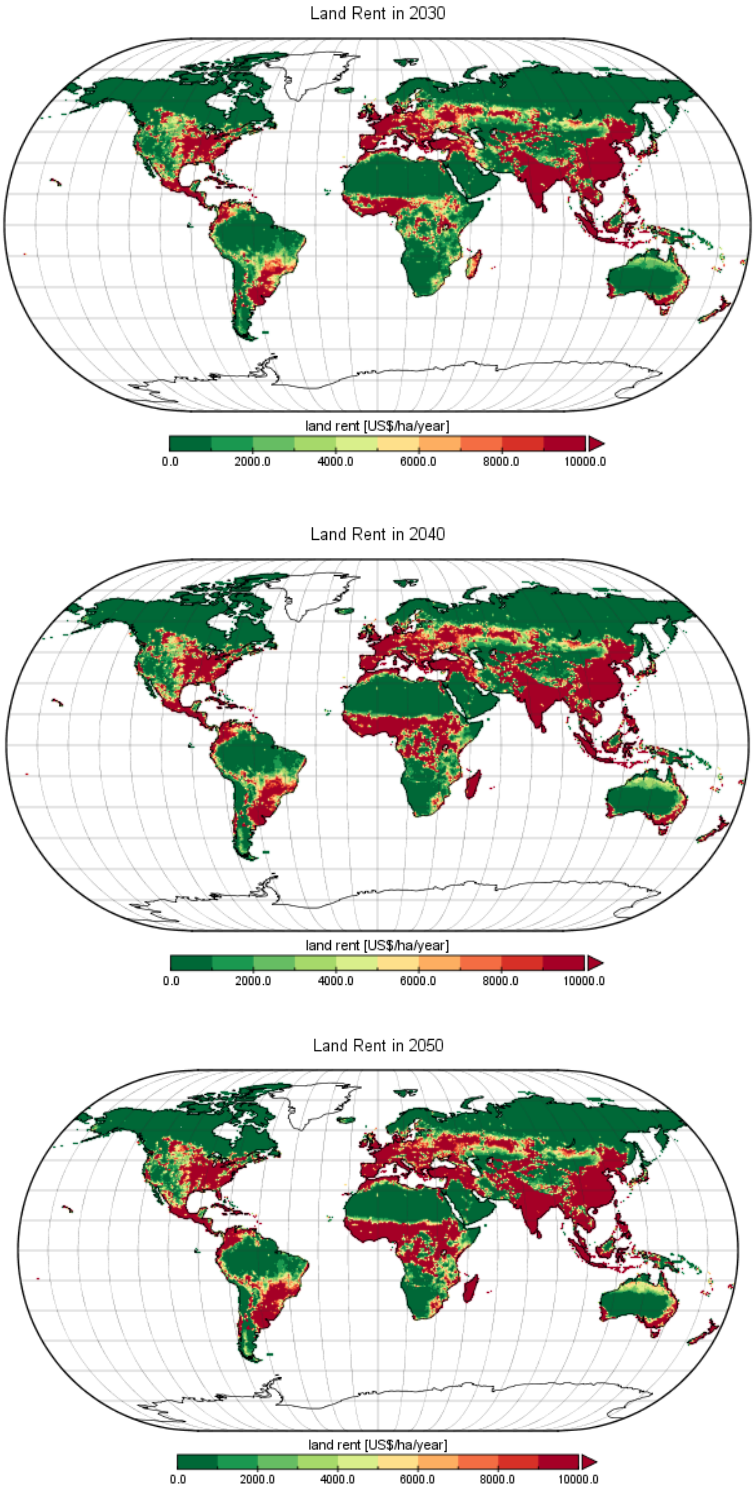

Figure AVIII.1. Land Rent (2030-2050)

Annex IX

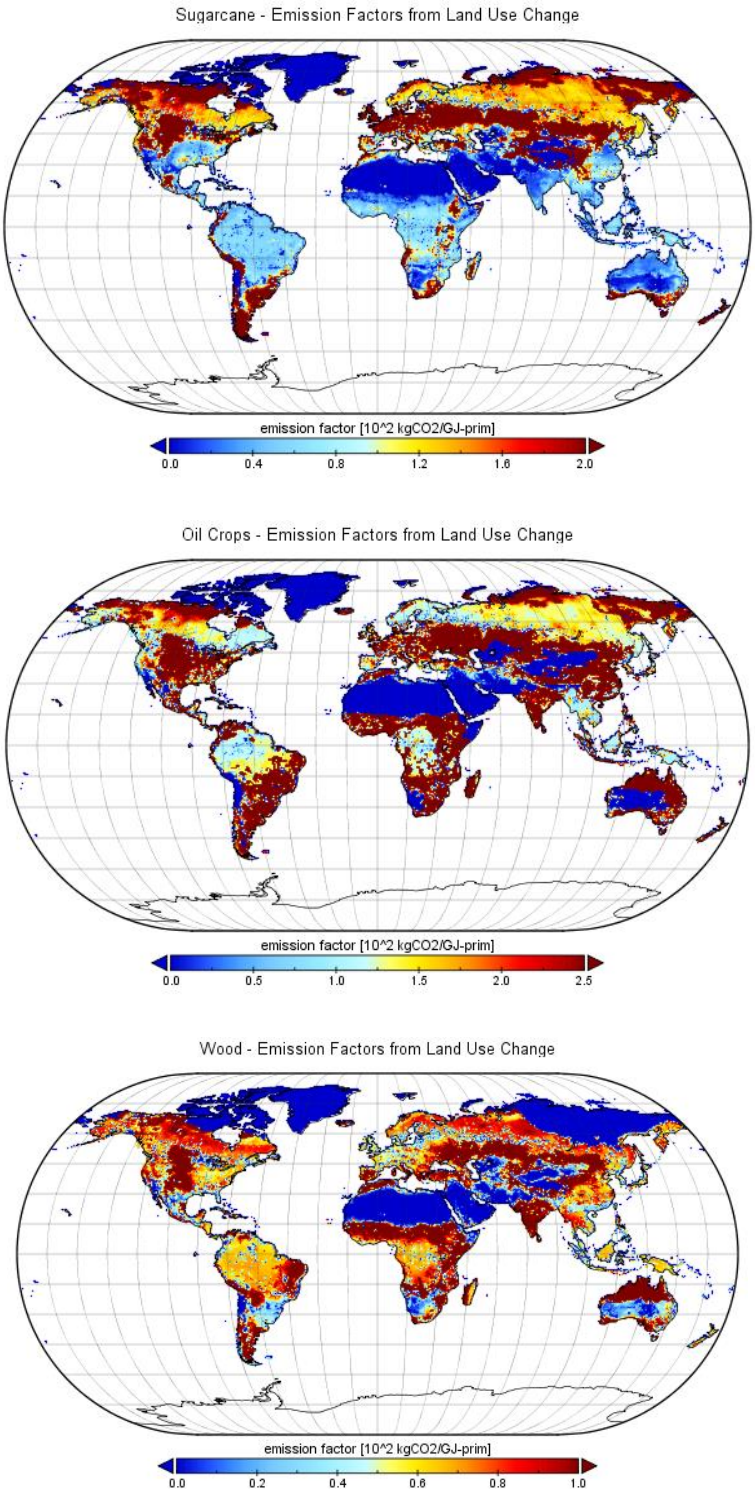

Figure AIX.1. Emission Factors from Land Use Change. Note the different scales.

Based on Daioglou et al. (2017)

Annex X

Table AXI.1: Emission factors for fertilizer use

Crop / Region		**Emission Factor (kgN_2O/km^2)**
Sugarcane	North	139.09
	Northeast	139.09
	Center-West	149.32
	Southeast	163.64
	South	159.55
Oil Crops	North	-
	Northeast	-
	Center-West	-
	Southeast	-
	South	-
Wood	North	10.00
	Northeast	7.39
	Center-West	10.00
	Southeast	10.00
	South	6.48
Grass	North	599.32
	Northeast	550.23
	Center-West	599.32
	Southeast	599.32
	South	499.09
Maize	North	79.77
	Northeast	61.36
	Center-West	216.82
	Southeast	196.36
	South	180.00

Based on Angelkorte (2019)

Annex XI

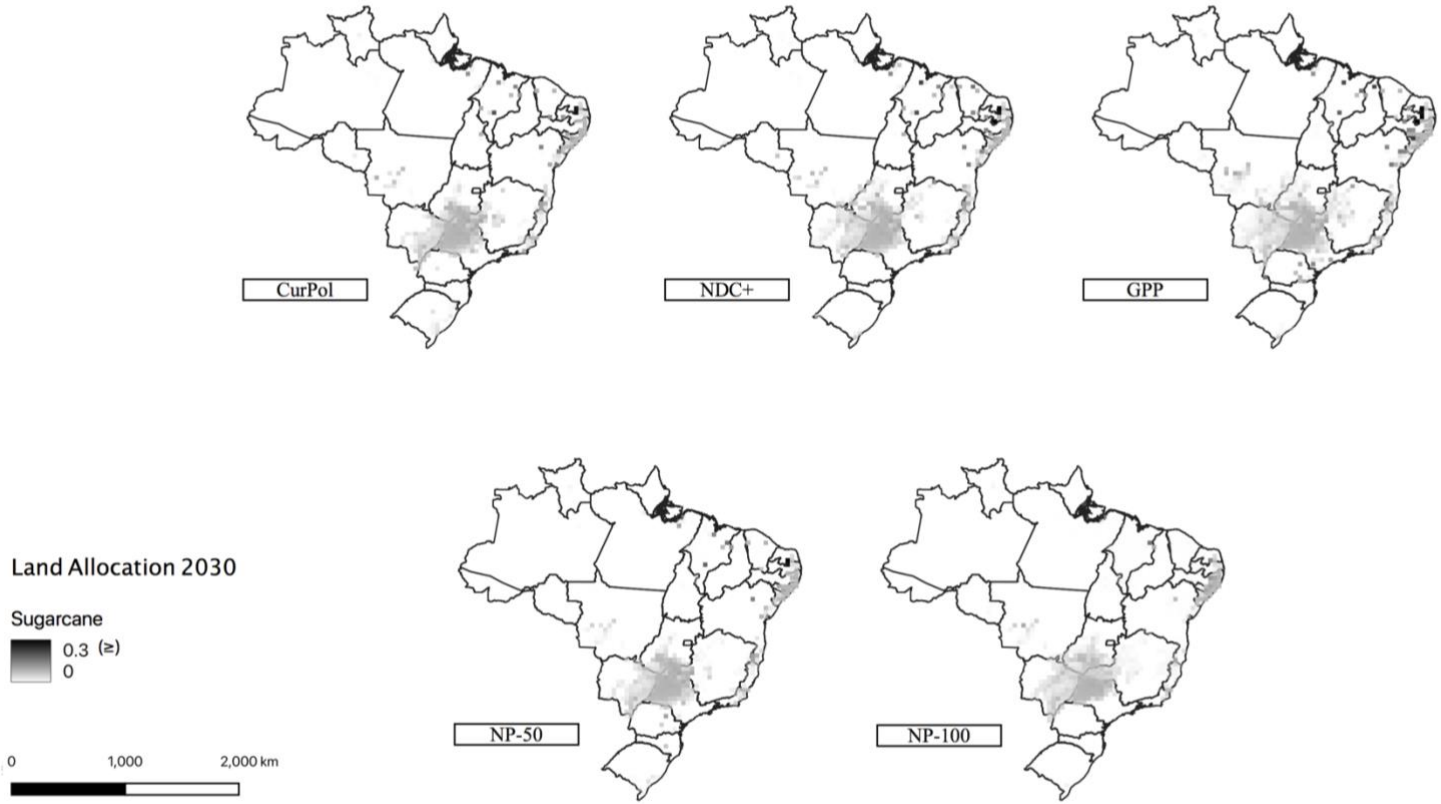

Figure AXII.1. Land Allocation, Sugarcane (2030)

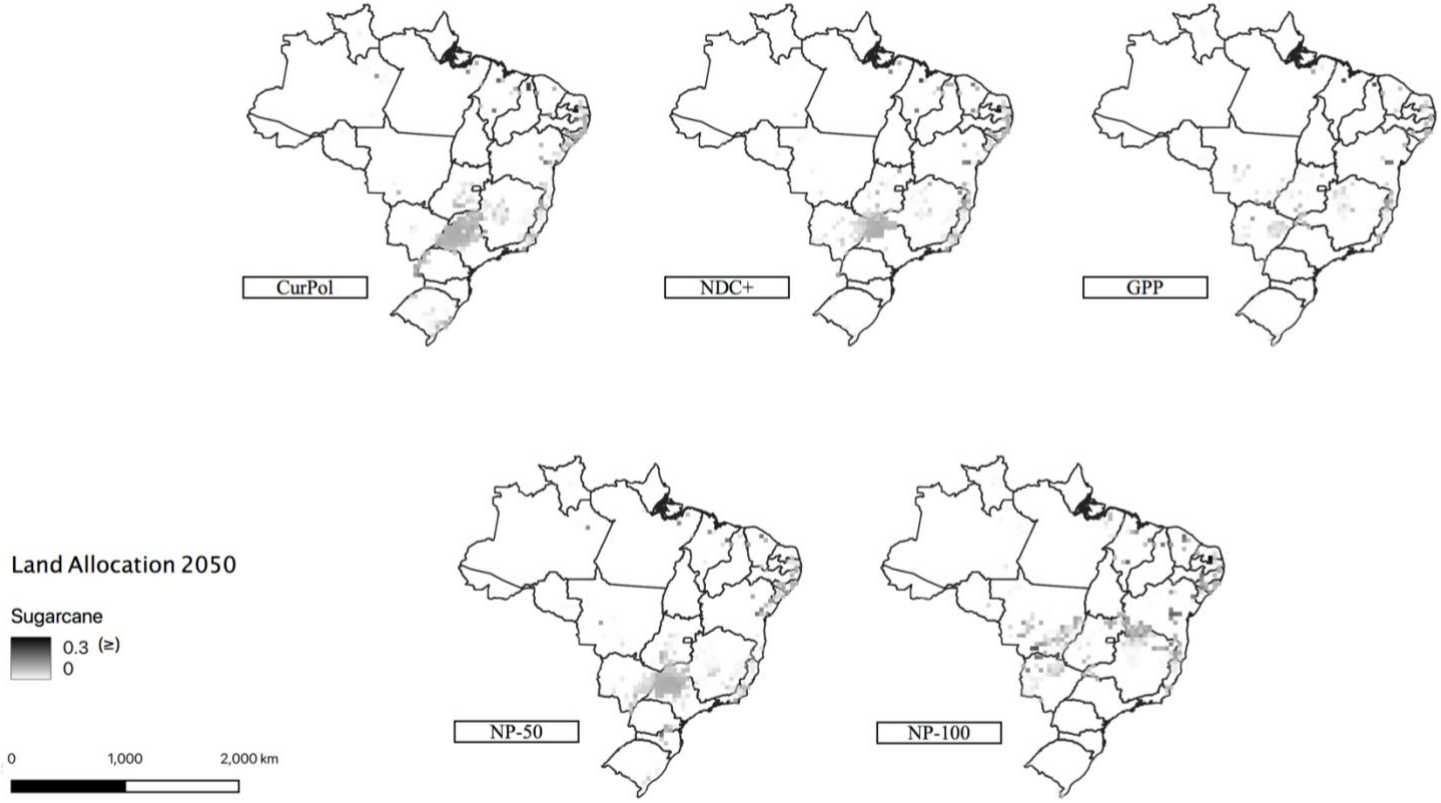

Figure AXII.2. Land Allocation, Sugarcane (2050)

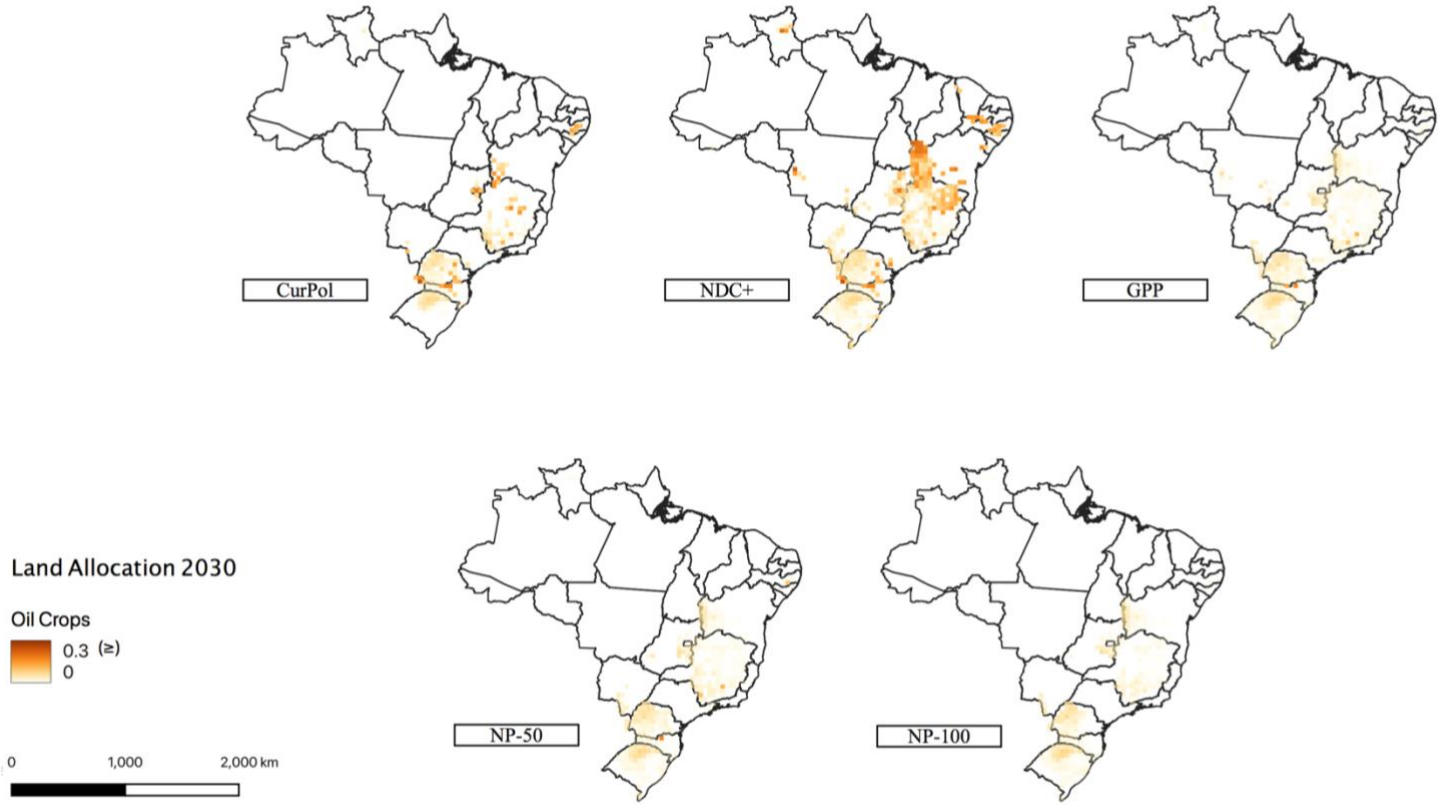

Figure AXII.3. Land Allocation, Oil Crops (2030)

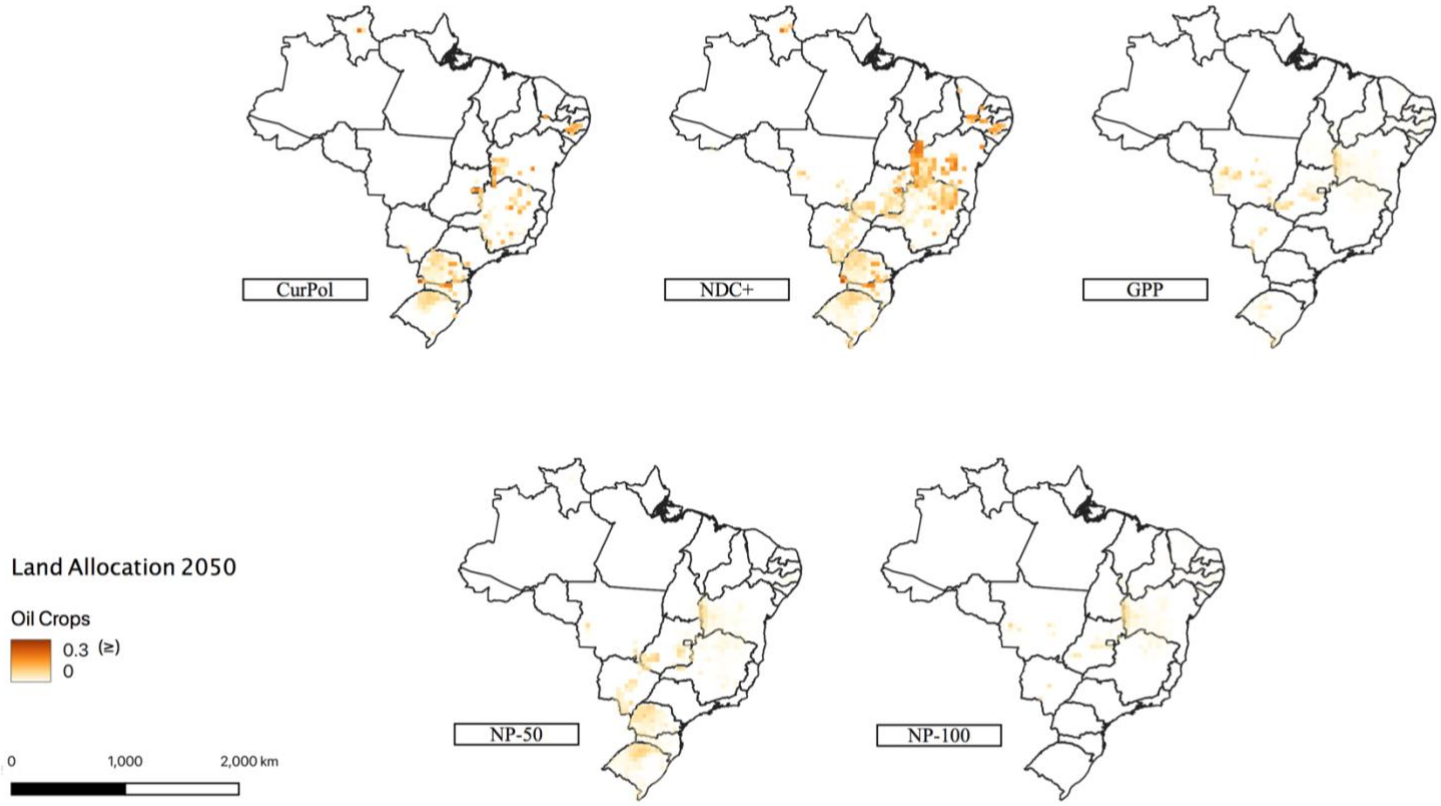

Figure AXII.4. Land Allocation, Oil Crops (2050)

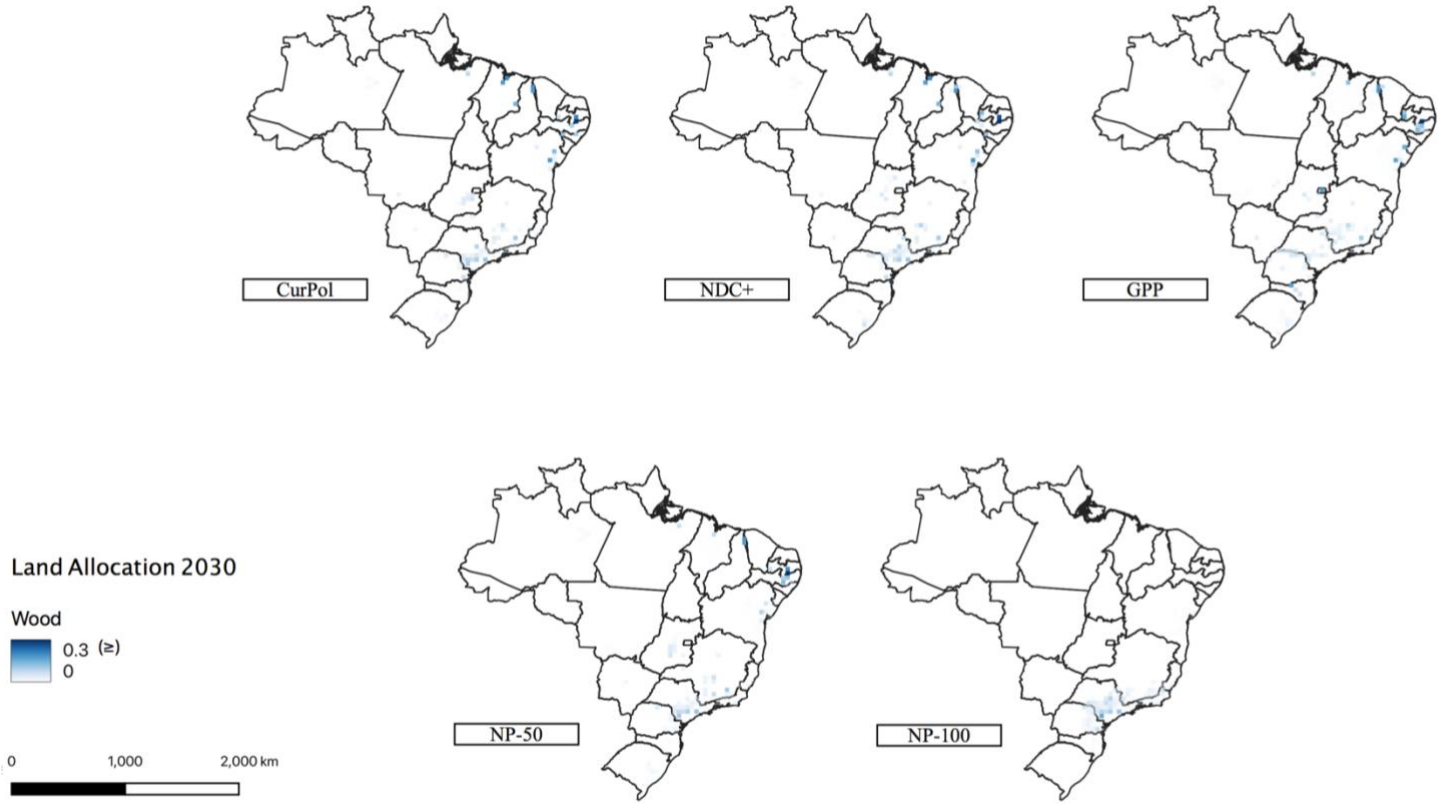

Figure AXII.5. Land Allocation, Wood (2030)

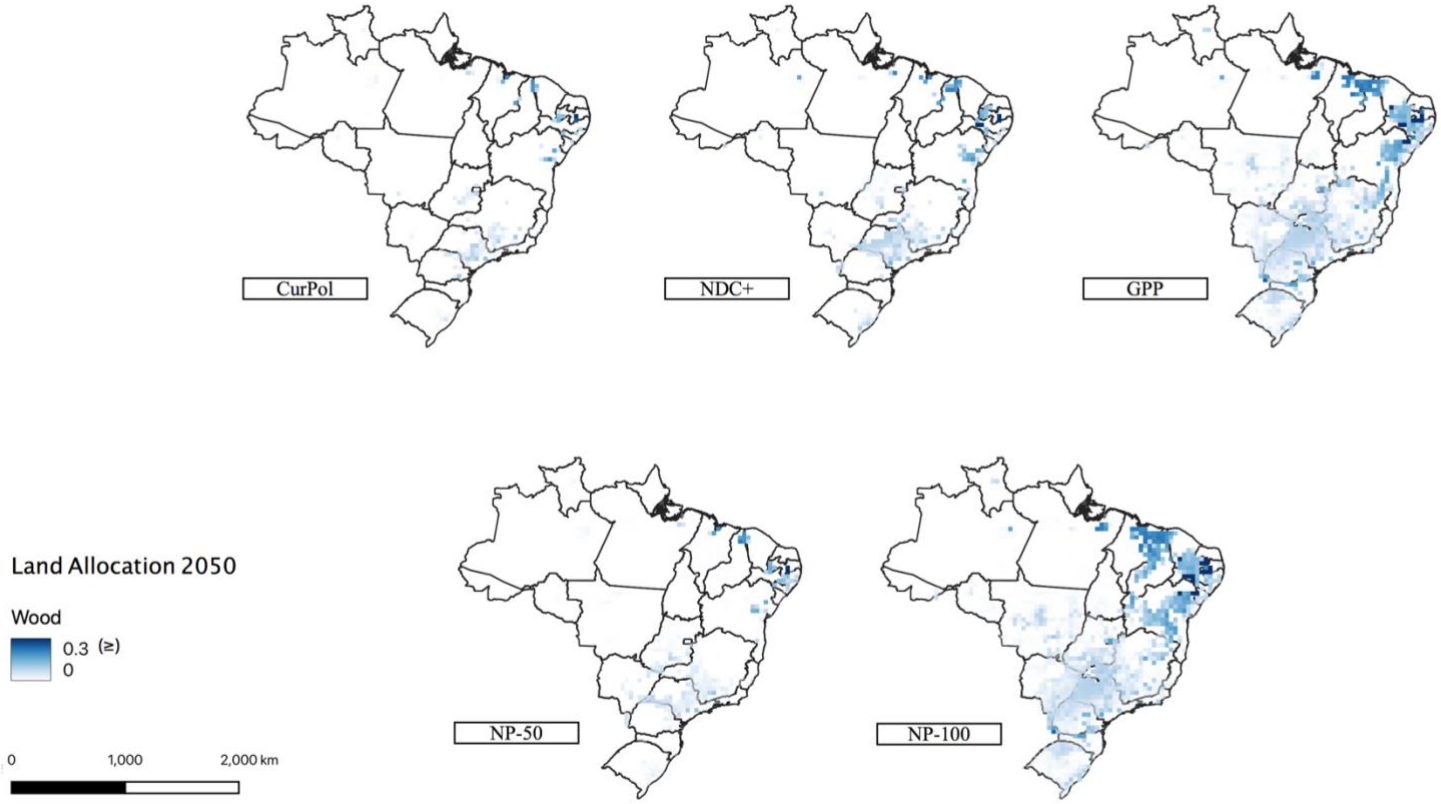

Figure AXII.6. Land Allocation, Wood (2050)